

Cleavage of IPS-1 in cells infected with human rhinovirus

Jennifer Drahos and Vincent R. Racaniello*

Department Microbiology

College of Physicians & Surgeons of Columbia University

701 W. 168th St.

New York, New York 10032

*Corresponding author:

212-305-5707

212-305-5106 (fax)

vrr1@columbia.edu (email)

Running title: Rhinovirus and IPS-1 cleavage

Abstract word count: 227

Text word count: 4433

Abstract

1
2 Rhinoviruses are prevalent human pathogens that are associated with life threatening
3 acute asthma exacerbations. The innate immune response to rhinovirus infection, which
4 may play an important role in virus-induced asthma induction, has not been
5 comprehensively investigated. We examined the innate immune response in cells infected
6 with human rhinovirus 1a (HRV1a). IFN- β mRNA was induced in HRV1a-infected cells
7 at levels significantly lower than in cells infected with Sendai virus (SeV). To understand
8 the basis for this observation, we determined whether components of the pathway leading
9 to IFN- β induction were altered during infection. Dimerization of the transcription factor
10 IRF-3, which is required for synthesis of IFN- β mRNA, is not observed in cells infected
11 with HRV1a. Beginning at 7 hr post-infection, IPS-1, a protein that is essential for
12 cytosolic sensing of viral RNA, is degraded in HRV1a-infected cells. Induction of
13 apoptosis by puromycin led to the cleavage of IPS-1, but treatment of HRV1a-infected
14 cells with the pan-caspase inhibitor, zVAD, did not block cleavage of IPS-1. IPS-1 is
15 cleaved in vitro by caspase-3 and by the picornaviral proteinases 2A^{pro} and 3C^{pro}.
16 Expression of HRV1a and polioviral 2A^{pro} and 3C^{pro} lead to degradation of IPS-1 in cells.
17 These results suggest that IPS-1 is cleaved during HRV1a infection by three different
18 proteases. Cleavage of IPS-1 may be a mechanism for evasion of the type I interferon
19 response, leading to a more robust infection.

20

Introduction

21 Human rhinoviruses, positive-stranded RNA viruses of the *Picornaviridae* family,
22 account for greater than 50% of all upper respiratory tract infections (28). Although
23 usually mild and self-limiting, viral upper respiratory tract infections are one of the most
24 common illnesses in humans, with 500 million cases and an economic burden estimated
25 at \$40 billion annually in the United States (8). Furthermore, rhinovirus is implicated in
26 causing severe exacerbation of other diseases including chronic bronchitis, sinusitis, and
27 asthma (22).

28 The innate immune response to rhinovirus infection may play an important role in
29 rhinovirus-induced asthma induction. Viral infection leads to a signaling cascade that
30 stimulates the antiviral innate immune response, limiting viral replication and initiating
31 the adaptive immune system (14). Two sensors for viral RNA have been described,
32 retinoic acid-inducible gene (RIG-I) and melanoma differentiation associated gene-5
33 (MDA-5) (12, 17, 37). Each RNA sensor comprises a DExD/H box RNA helicase
34 domain and a caspase recruitment and activation domain (CARD) (36). MDA-5 and RIG-
35 I appear to sense infections by different viruses. RIG-I, which detects double-stranded
36 RNA or single-stranded RNA with a 5'-triphosphate, is responsible for IFN α / β induction
37 by paramyxoviruses, flaviviruses, influenza viruses, and Japanese encephalitis virus
38 including Newcastle disease virus and Sendai virus (11, 31, 35-37). MDA-5 recognizes
39 double-stranded RNA, and is the critical sensor of infection by encephalomyocarditis
40 virus and mengovirus, two members of the picornavirus family (10, 13).

41 Both MDA-5 and RIG-I interact with the CARD-containing adaptor protein, IFN- β
42 promoter stimulator 1 (IPS-1) (also known as MAVS, VISA, or Cardiff) (15, 24, 26, 32).

43 IPS-1 is localized to the outer mitochondrial matrix and activates the kinases IKK ϵ
44 (inhibitor of nuclear factor kappaB kinase) and TBK1 (TANK-binding kinase), which are
45 required for the phosphorylation of IFN regulatory factor 3 (IRF-3) (9). Phosphorylated
46 IRF-3 dimerizes and translocates to the nucleus where it recruits p300/CREB binding
47 protein (CBP) (20, 33). IRF-3 cooperatively binds with the transcription factors NF- κ B
48 and AFT-2/c-Jun to form an enhancesome on the IFN- β promoter (23). This complex
49 leads to the activation of the IFN- β gene and synthesis of type I IFNs.

50 Numerous mechanisms for circumvention of the innate immune response pathway
51 have been revealed in virus-infected cells. The study of these strategies has illuminated
52 the function of innate sensing pathways (reviewed in ref. (21)). For example, the
53 proteases of hepatitis C, GB, and A viruses cleave IPS-1 (6, 34), and both MDA-5 and
54 RIG-I are degraded in cells infected with picornaviruses (2, 3).

55 The innate response to rhinovirus infection has not been comprehensively
56 investigated. We therefore examined induction of IFN- β during infection with HRV1a.
57 IFN- β mRNA was detected in HRV1a-infected cells at levels significantly lower than in
58 cells infected with Sendai virus (SeV). To understand the basis for this observation, we
59 determined whether components of the pathway leading to IFN- β induction were altered
60 during infection. Dimerization of the transcription factor IRF-3, which is required for
61 synthesis of IFN- β mRNA, is not observed in cells infected with HRV1a. When IRF-3
62 depleted cells were infected with SeV or HRV1a, small amounts of IFN- β mRNA were
63 produced. The level of IFN- β mRNA was similar to that observed during HRV1a
64 infection of the parental HeLa cell line. IRF-3 depletion did not affect HRV1a growth
65 kinetics. Beginning at 7 hr post-infection, IPS-1, a protein that is essential for cytosolic

66 sensing of viral RNA, was degraded in HRV1a-infected cells. Induction of apoptosis by
67 puromycin also led to the cleavage of IPS-1, but treatment of HRV1a-infected cells with
68 the pan-caspase inhibitor, zVAD, did not protect IPS-1 from cleavage. IPS-1 was cleaved
69 in vitro by caspase-3 and by the picornaviral proteinases 2A^{pro} and 3C^{pro}. Expression of
70 picornaviral proteinases 2A^{pro} and 3ABC in cell lines lead to cleavage of IPS-1. These
71 results suggest that IPS-1 is cleaved during HRV1a infection by viral proteinases 2A^{pro},
72 3C, and activated caspase-3. Cleavage of IPS-1 during HRV1a infection may be a
73 mechanism for evasion of the type I interferon response, leading to a more robust
74 infection.

75

Materials & Methods

76

Cells, viruses, and plasmids. S3 HeLa and 293T, and BSR T7/5 cells were grown in

77

Dulbecco's modified Eagle medium (Invitrogen, Carlsbad, CA), 10% fetal calf serum

78

(HyClone, Logan, UT), and 1% penicillin-streptomycin (Invitrogen). BSR T7/5 cells, a

79

BHK-derived cell line stably expressing T7 RNA polymerase, were generously provided

80

by Dr. Klaus Conzelmann, Ludwig-Maximilians-Universitat Munich, Germany (4).

81

Selection of BSR T7/5 was maintained by the addition of G418 (1 μ g/ml) at every other

82

passage. Stocks of HRV1a were obtained from the ATCC (Manassas, VA) and were

83

propagated in HeLa cells. Rhinovirus plaque assays were carried out using HeLa cells

84

grown in Dulbecco's modified Eagle medium (Specialty Media, Philipsburg, NJ), 0.05%

85

NaHCO₃, 2% heat-inactivated bovine calf serum, 1% penicillin-streptomycin, and 1%

86

Type VII low gelling agarose (Sigma-Aldrich, St. Louis, MO). Cells were incubated for

87

72 hrs and developed using 10% trichloroacetic acid and crystal violet. The Cantell strain

88

of Sendai virus (SeV) was a generous gift from Adolfo Garcia-Sastre, Mount Sinai

89

School of Medicine, New York, NY. pFLAG-IPS-1 was a generous gift from Dr. Zhijian

90

Chen, University of Texas Southwestern Medical Center, Dallas, Texas.

91

Generation of stable knockdown cell lines. Depletion of IRF-3 was achieved by

92

using retroviral vectors encoding microRNAs (miRNA) generously provided by Jeremy

93

Luban, University of Geneva, Switzerland. Virus stocks were generated in 293T cells by

94

co-transfection using Fugene 6 (Roche, Indianapolis, IN) with either pAPM-IRF-3

95

(targeting hIRF-3) or pAPM-L1221 (control miRNA targeting luciferase), psPAX2, and

96

pMD.G. Viruses were harvested 24 hrs post-transfection and filtered (0.45-mm filter,

97

Pall Corp., East Hills, NY). To generate cell lines stably expressing miRNA, HeLa cells

98 were infected with virus stocks and 48 hrs post-transduction cells were subjected to
99 puromycin selection with increasing dosages of puromycin every two days for 10 days
100 from 1 μ M to 5 μ M. Depletion of IRF-3 was confirmed by western blot analysis.

101 **Reagents.** Rabbit polyclonal IRF-3 and mouse monoclonal IRF-3 were purchased
102 from Sigma-Aldrich. The mouse monoclonal β -actin antibody was purchased from
103 Sigma-Aldrich. Rabbit anti-IPS-1 antibody, chicken anti-Sendai virus antibody and
104 mouse monoclonal anti-PABP were purchased from AbCam (Cambridge, MA). Rabbit
105 polyclonal anti-PARP was purchased from Cell Signaling Technology, Danvers, MA.
106 The general caspase inhibitor benzyloxycarbonyl-Val-Ala-Asp-(OMe)
107 fluoromethylketone (Z-VAD-FMK) was purchased from R&D Systems, Minneapolis,
108 MN. DNA-mediated transformation of BSR T7/5 cells was performed using
109 Lipofectamine reagent (Invitrogen) according to the manufacturer's protocol. Cell
110 extracts were prepared as described below for western blot analysis.

111 **Virus replication in cultured cells.** Adherent cell monolayers were grown in 3.5 cm²
112 plates and infected with virus at a multiplicity of infection (MOI) of 10 or 0.1 PFU per
113 cell. Virus was absorbed for 45 minutes at 37°C and then 2mL of culture medium was
114 added. Cells were incubated at 33°C for the times indicated in the figure legends. Cells
115 were then scraped into the medium and subjected to two freeze-thaw cycles, and cellular
116 debris was removed by centrifugation. Virus titer was determined by plaque assay as
117 described above.

118 **Infections and western blot analysis.** Confluent monolayers of HeLa cells were
119 infected with HRV1a or SeV for the times indicated in the figure legends. Cells were
120 scraped into the culture medium and pelleted by centrifugation. The cell pellet was

121 washed once with phosphate-buffered saline (PBS), centrifuged, and lysed for 15 minutes
122 on ice in NP-40 buffer (50 mM Tris-Cl, pH8.0, 1% Nonidet P-40, 150mM NaCl)
123 containing complete protease inhibitor cocktail (Roche). Total protein was determined by
124 Bradford Assay (BioRad, Hercules, CA) and 40 µg of each sample was mixed with SDS
125 loading dye. Proteins were separated on a 10% SDS-polyacrylamide gel and
126 electrotransferred overnight at 30V onto PDVF membranes (Millipore, Billerica, MA).
127 Membranes were incubated in blocking buffer (PBS containing 0.1% Tween and 5%
128 nonfat milk) for 1 hr at room temperature and subsequently incubated overnight at 4°C
129 with indicated antibodies diluted in blocking buffer. Membranes were washed 3 times
130 for 15 minutes in PBST and incubated for 1 hour with horseradish peroxidase-conjugated
131 secondary antibody (1:1000 anti-goat and 1:3000 anti-rabbit, Dako, Carpinteria, CA).
132 Proteins were visualized using the ECL or ECL+ chemiluminescence system (Amersham
133 Biosciences, Piscataway, NJ).

134 **Native PAGE and western blot analysis** was performed as described previously
135 (25), with the following changes: 10% gels were made with ProSieve 50 Gel Solution
136 (Cambrex, Rockland, ME). 30 µg of proteins was loaded and wet transferred to PDVF
137 membrane overnight at 30V. Membranes were probed for IRF-3 overnight at 4°C with a
138 rabbit polyclonal antibody, FL-425 (Sigma-Aldrich) or mouse monoclonal SC-12
139 (Sigma-Aldrich). Membranes were developed with the ECL+ System (Amersham
140 Biosciences).

141 **Quantitative real-time PCR.** RNA was harvested from HeLa, mi-L112, or mi-IRF-
142 3 cells infected with HRV1a or SeV virus using an RNeasy mini kit (Qiagen, Valencia,
143 CA) at the times indicated in the figure legends. RNA concentrations were determined

144 by the ND-1000 spectrophotometer (NanoDrop Technologies, Wilmington, DE).
145 Contaminating genomic DNA was removed by treating 8 µg of each sample with the
146 Turbo DNA-free kit (Ambion, Austin, TX). cDNA was generated using the SuperScript
147 III First-Strand Synthesis SuperMix for qRT-PCR according to the manufacturer's
148 protocol (Invitrogen) and qPCR mix was made with 5X Fast-Start SYBR green master
149 mix containing Rox (Roche Diagnostics, Indianapolis, IN) with a final concentration of
150 400 nM of each primer. Triplicate reactions were performed on the Prism 7500 real-time
151 PCR system in a 96-well optical plate (Applied Biosystems, Foster City, CA) with a final
152 volume of 50 µL. The primers sequence for IFN-β forward: CGA CAC TGT TCG TGT
153 TGT CA; IFN-β reverse: GAA GCA CAA CAG GAG AGC AA; porphobilinogen
154 deaminase (PBDG) forward: CTG GTA ACG GCA ATG CGG CT; and PBDG reverse:
155 CGA GAT GGC TCC GAT GGT GA.

156 **In vitro translation.** Coupled transcription-translation experiments were performed
157 using the TNT quick-coupled transcription/translation system (Promega Corp, Madison,
158 WI) in the presence of [³⁵S]-methionine (Amersham BioSciences, Piscataway, NJ). One
159 microgram of DNA was added to each 50 µL reaction and the manufacturer's protocol
160 was followed. The *in vitro* translated IPS-1 was added to cleavage buffer containing
161 100mM NaCl₂, 5mM MgCl₂, and 10mM Hepes-KOH, pH 7.4 in the presence or absence
162 of poliovirus 3C^{pro} (provided by B. Semler, University of California, Irvine CA),
163 Coxsackievirus B3 2A^{pro} (provided by R. Lloyd, Baylor College of Medicine, Houston
164 TX), or activated human caspase-3 (Calbiochem La Jolla, CA). The cleavage reactions
165 were incubated at 37°C for 18 hours. The products were separated by 10% SDS-PAGE,

166 transferred to a PDVF membrane overnight at 30V, and exposed to a phosphorimager
167 plate or subjected to western blot analysis.

168

Results

169 **HRV1a infection does not induce robust IFN- β transcription.** The results of
170 previous studies have indicated that members of the *Picornaviridae* family antagonize the
171 innate immune system at multiple levels. In a previous investigation we showed that
172 MDA-5 and RIG-I, innate cytoplasmic sensors of RNA, are degraded in cells infected
173 with picornaviruses (2, 3). Furthermore, IPS-1 is cleaved in cells infected with hepatitis
174 A virus, leading to a block in IFN- β synthesis (34). Therefore, we investigated IFN- β
175 expression during HRV1a infection. HeLa cells were infected with HRV1a or SeV. We
176 used the Cantell strain of SeV, which is sensed by RIG-I and induces high levels of IFN-
177 β (27). At different times after infection, total cellular RNA was harvested, reverse
178 transcribed into cDNA, and IFN- β transcript levels were assessed by quantitative real-
179 time PCR.

180 SeV induced high levels of IFN- β mRNA as early as 1 hour after infection, peaking
181 just after 7 hours, and falling slightly by 15 hours (Figure 1A). In contrast, although
182 HRV1a did induce IFN- β compared to mock treated cells (Figure 1B), induction was
183 100-1000 fold lower than that observed during SeV infection (Figure 1A). The low level
184 of IFN- β mRNA suggests that HRV1a infection interferes with innate sensing of viral
185 RNA.

186 **Dimerization of IRF-3 is blocked during infection with HRV1a.** To provide an
187 explanation for the low levels of IFN- β mRNA observed during HRV1a infection, we
188 examined dimerization of the transcriptional activator, IRF-3, by native-PAGE. In cells
189 infected with Sendai virus, IRF-3 dimers were first detected at 3 hours post infection

190 (Figure 2). Levels of IRF-3 dimers peaked by 7 hours, and fell slightly by 15 hours. IRF-
191 3 dimers were not observed in HRV1a- infected cells.

192 **Inhibition of SeV-induced IRF-3 activation by HRV1a.** The low levels of IFN- β
193 observed during HRV1a infection may be a consequence of poor sensing of the viral
194 RNA, or virus-induced cleavage of one or more cell proteins in the sensing pathway. To
195 address these possibilities, we determined whether IRF-3 activation induced by SeV was
196 altered during HRV1a infection. HeLa cells were mock infected or infected with HRV1a
197 at an MOI of 10 for 3 or 5 hours and then superinfected with SeV. Cell lysates were
198 harvested at different times post-infection with SeV and IRF-3 dimers were examined by
199 native-PAGE gel electrophoresis. Infection with HRV1a caused a dramatic loss in the
200 ability of SeV infection to induce dimerization of IRF-3 (Figure 3). SeV proteins
201 accumulated during HRV1a infection, indicating that the inability of SeV to induce
202 dimerization of IRF-3 is not due to inhibition of viral replication by HRV1a (Figure 4).
203 These results suggest that HRV1a infection disrupts the innate immune sensing pathway.

204 **IPS-1 is degraded in HRV1a-infected cells.** The dimerization of IRF-3 requires
205 phosphorylation by the kinases TBK and TANK-1, which are selectively activated
206 through IPS-1 (9). Because IPS-1 is an essential protein of the pathway leading to IFN- β
207 induction, we determined if it was altered during rhinovirus infection. HeLa cells were
208 infected with HRV1a, and at different times after infection, IPS-1 protein was visualized
209 by western blot analysis. By 15 hours post-infection IPS-1 protein was barely detectable
210 (Figure 5A). Degradation of IPS-1 was also observed by 5 hours after infection with
211 another member of the picornavirus family, poliovirus. IPS-1 remained intact in SeV-

212 infected cells (Figure 5B), demonstrating that degradation of the protein is not a general
213 cellular response to viral infection.

214 Picornavirus infection can lead to the inhibition of host cell translation (19, 29). To
215 ensure that IPS-1 degradation was not due to aggregate cell protein shut-off, cells were
216 treated with cycloheximide (5 μ g/mL) or infected with HRV1a, and IPS-1 levels were
217 determined by western blot analysis. IPS-1 levels remained stable during treatment with
218 cycloheximide for 24 hours, whereas HRV1a infection led to the degradation of IPS-1
219 (unpublished data). This observation suggests that the decrease in IPS-1 during an
220 HRV1a infection is not a consequence of the rapid turnover of the protein.

221 **Induction of IFN- β during rhinovirus infection in cells depleted of IRF-3.** If
222 cleavage of IPS-1 accounts for the low level of IFN- β observed during HRV1a infection,
223 then infection of cells depleted for IRF-3 should exhibit similar levels of the cytokine.
224 Efficient knockdown of IRF-3 was achieved in stable cell lines that express an IRF-3
225 specific miRNA, compared with control stable cell lines expressing a luciferase specific
226 miRNA (Figure 6A). As expected, IRF-3 dimers were observed during SeV but not
227 HRV1a infection in the control cell line (Figure 6B). Absence of IRF-3 did not affect
228 replication of HRV1a at low or high MOI (Figure 7). Induction of IFN- β by SeV or
229 HRV1a in the control and parental HeLa cell lines was similar (Figures 1 and 7). Low
230 levels of IFN- β were observed after SeV and HRV1a infection of cells depleted of IRF-3
231 (Figure 6). The amounts of IFN- β mRNA resembled those observed during HRV1a
232 infection of HeLa cells (Figure 1).

233 **Cleavage of IPS-1 during apoptosis.** The genomes of HRV1a and poliovirus
234 encode two viral proteinases, 2A^{pro} and 3C^{pro} that process the viral polyprotein and also

235 degrade cellular proteins. Picornaviral proteinases are known to induce apoptosis, a
236 process that occurs in cells infected with certain rhinoviruses (5, 7, 30). Caspases are
237 activated during apoptosis, leading to cleavage of cellular proteins such as poly(ADP)-
238 ribose polymerase (PARP). In cells infected with HRV1a, PARP cleavage is observed
239 starting at 5 hr post-infection, suggesting that HRV1a induces apoptosis (Figure 9A).
240 Furthermore, activated caspase-3 was observed in cells infected with HRV1a by 5 hr
241 post-infection (unpublished data). To address whether induction of apoptosis leads to
242 cleavage of IPS-1, cells were treated with puromycin and IPS-1 was examined by western
243 blot analysis. Puromycin treatment for 3 and 5 hr induced apoptosis, as shown by
244 cleavage of PARP (Figure 9B). In the same cells IPS-1 was degraded, and a ~50kDa
245 putative cleavage product was observed (Figure 9B).

246 **Activated caspases are not necessary for the HRV1a-induced IPS-1**
247 **degradation.** If caspases are the only mediators of IPS-1 cleavage during an HRV1a
248 infection, then inhibiting activated caspases should prevent IPS-1 degradation. To test
249 this hypothesis the effect of zVAD, a pan-caspase inhibitor, on IPS-1 cleavage was
250 determined. HeLa cells were infected with HRV1a in the presence or absence of
251 inhibitor. The levels of IPS-1 at different times after infection were determined by
252 western blot analysis. Degradation of IPS-1 was not affected by zVAD (Figure 9C). As
253 expected, the inhibitor prevented PARP cleavage (Figure 9C). Furthermore, the yield of
254 HRV1a was not altered by zVAD treatment, indicating that the drug does not inhibit viral
255 proteinases 2A^{pro} or 3C^{pro} (unpublished data). Taken together these results suggest that
256 HRV1a-induced degradation of IPS-1 is mediated not only by caspases but by other
257 cellular or even viral proteases.

258 **IPS-1 is cleaved by 3C^{pro}, 2A^{pro}, and caspase-3.** We determined whether IPS-1
259 could be cleaved in vitro by purified poliovirus 3C^{pro}, coxsackievirus 2A^{pro}, or activated
260 human caspase-3. The poliovirus and coxsackievirus enzymes were used because the
261 HRV1a proteins were not available. IPS-1 was produced by in vitro translation in a
262 reticulocyte lysate in the presence of [³⁵S]-methionine, and incubated with each enzyme.
263 Both viral proteinases were active in the reticulocyte lysate, as shown by cleavage of
264 PABP (Figure 10). IPS-1 was cleaved into fragments of different sizes by all three
265 enzymes (Figure 10).

266 To determine if 2A^{pro} and 3C^{pro} proteins of HRV1a can cleave IPS-1 in cells,
267 plasmids encoding the proteins were introduced into cells by DNA mediated
268 transformation. It has been shown that the hepatitis A virus proteinase 3C^{pro} must be
269 synthesized as part of the precursor protein 3ABC to properly target the proteinase to
270 mitochondria (34). Therefore plasmids encoding epitope-tagged 3ABC of HRV1 and
271 poliovirus were produced. However we failed to detect the proteinases by western blot
272 analysis when these plasmids were introduced into different cell lines by a variety of
273 methods.

274 To increase the expression levels of the viral proteinases, plasmids were introduced
275 into a BHK cell line (BSR T7/5) which stably produces T7 RNA polymerase. BSR cells
276 were co-transformed with a plasmid encoding IPS-1 and either eGFP or a viral
277 proteinase. Twenty-four hours later cells were harvested for western blot analysis. As
278 expected, synthesis of hepatitis A virus 3ABC protein lead to cleavage of IPS-1 (Figure
279 11). Expression of 2A^{pro} and 3ABC proteins of HRV1a and poliovirus 3ABC lead to
280 degradation of IPS-1 (Figure 11). These results show that degradation of IPS-1 observed

281 during HRV1a and poliovirus infection is likely a consequence of the activity of both
282 viral proteinases and caspases.

283

Discussion

284 Human rhinovirus 1a induced expression of IFN- β mRNA in HeLa cells, but at levels
285 far lower than those observed during infection with SeV. Consistent with this
286 observation, we found that IRF-3 dimers did not form during HRV 1a infection.
287 Phosphorylation of IRF-3 is mediated by protein kinases whose activation depends upon
288 signals received from IPS-1 and, in turn, MDA-5 or RIG-I. IPS-1 is cleaved in cells
289 infected with HRV 1a, which could explain the absence of IRF-3 dimers. It also possible
290 that the kinases IKK ϵ and TBK1 are also modified during infection, but degradation of
291 IPS-1 would be sufficient to prevent dimerization of IRF-3. MDA-5 is cleaved in
292 HRV 1a-infected cells (3), but the kinetics and extent of cleavage are not consistent with
293 the complete absence of IRF-3 dimers observed here. To prove that cleavage of IPS-1 is a
294 mechanism to abrogate IFN- β synthesis will require production of IPS-1 that is not
295 cleaved in HRV 1a infected cells.

296 Our results show that cleavage of IPS-1 during HRV 1a infection may be carried out
297 by either of the two viral proteinases, 2A^{pro} or 3C^{pro}. These proteinases process the viral
298 polyprotein, and for some picornaviruses, have been shown to cleave a variety of cell
299 proteins such as eIF4G (18) (cleaved by 2A^{pro}) and PABP (19) (cleaved by both
300 proteinases). Previously it had not been demonstrated that 2A^{pro} and 3C^{pro} of HRV 1a
301 cleaved any cellular proteins. In cells infected with hepatitis A virus, IPS-1 is cleaved by
302 3C^{pro} produced from a 3ABC precursor (34).

303 Our findings also imply that cellular caspases are involved in cleavage of IPS-1
304 during HRV 1a infection. It was previously demonstrated that apoptosis is induced during
305 infection with certain rhinoviruses. HeLa cells infected with human rhinovirus 14, a

306 major group rhinovirus, exhibited typical apoptotic cellular alterations including cell
307 contraction, nuclear condensation, and activation of caspase-9 and caspase-3 (7).
308 Induction of apoptosis has also been demonstrated in cells infected with the minor group
309 rhinovirus 1B, which is highly related to the serotype used in these studies, HRV1a (30).
310 We have found that apoptosis is also induced in HRV1a- infected cells as indicated by
311 activation of caspase-3 and cleavage of PARP, a known caspase-3 substrate, within 5
312 hours of infection. Activated caspase-3 can cleave IPS-1 in vitro to yield a ~50 kDa
313 protein. Induction of apoptosis during HRV1a- infection may be a unique viral strategy to
314 cleave IPS-1 and limit IFN- β mRNA levels.

315 Induction of apoptosis by puromycin treatment of cells caused cleavage of IPS-1. The
316 ~50 kDa putative cleavage product is similar in size to the fragment produced when IPS-
317 1 is cleaved by caspase-3 in vitro. However, treating cells with the pan-caspase-inhibitor,
318 zVAD, did not block IPS-1 degradation. This observation indicates that other proteases
319 are involved in the degradation of the protein. Surprisingly, IPS-1 was cleaved in a rabbit
320 reticulocyte lysate by poliovirus 3C^{pro} and coxsackievirus B3 2A^{pro}, and specific products
321 were formed. In contrast, no cleavage products of IPS-1 are observed in HRV1a-infected
322 cells, or in cells producing 3ABC from plasmid vectors. The combined action of the viral
323 proteinases and caspase-3 on IPS-1 in vivo may make the cleavage products unstable.

324 Although IPS-1 is degraded in cells upon expression of 3ABC or 2A^{pro}, it is not
325 known if IPS-1 is a direct substrate of the viral proteinases. Synthesis of picornaviral
326 2A^{pro} or 3C^{pro} in cells induces apoptosis (5, 7, 30) which may lead to degradation of IPS-
327 1 through activated caspase-3. However, two of our observations suggest a role for the
328 viral proteinases in direct cleavage of the protein: the failure to block degradation of IPS-

329 1 by treatment of HRV1a infected cells with the caspase inhibitor zVAD and the direct
330 cleavage of IPS-1 by purified viral proteinases in vitro.

331 There are two predicted caspase-3 cleavage sites in IPS-1 protein, at amino acids 86
332 and 429. Cleavage only at amino acid 429 would produce the ~50 kDa putative cleavage
333 product observed in cells treated with puromycin, in reticulocyte lysates incubated with
334 caspase-3, and in cells expressing HRV1a and poliovirus 2A^{pro}. There are several
335 potential cleavage sites for 2A^{pro} and 3C^{pro} within IPS-1 that would, if utilized, produce
336 the putative cleavage products observed in vitro. Experiments are currently in progress to
337 identify the cleavage sites for each protease.

338 IPS-1 undergoes lysine 48-linked polyubiquitination by the E3 ubiquitin ligase
339 RNF125 and is likely subject to proteasomal degradation (1). Degradation of IPS-1
340 during HRV1a infection could be due in part to proteasome degradation. To test this
341 hypothesis, we treated cells with the proteasome inhibitor MG132 and infected cells with
342 HRV1a. IPS-1 protein levels decreased within 15 hours post-infection; however the
343 protein was partially protected from degradation when protein levels were compared to
344 cells not treated with MG132 (data not shown). These data suggests a role for the
345 proteasome in IPS-1 degradation. We also observed some inhibition of the viral
346 proteinases in cells treated with MG132, which could lead to protection of IPS-1.
347 Additional experiments are needed to determine the role of the proteasome in IPS-1
348 degradation during HRV1a infection.

349 Induction of IFN- β mRNA was examined in a stable cell line depleted of IRF-3. After
350 infection with SeV, cytokine levels were significantly reduced as expected. However,
351 during HRV1a infection, IFN- β levels were similar whether or not IRF-3 was present.

352 This observation suggests that other transcription factors, such as IRF-7 and NF- κ B, may
353 allow synthesis of IFN- β when IRF-3 is not present or inactive.

354 Infection by the major group rhinovirus HRV14 leads to very low levels of IFN- β
355 mRNA, which correlated with impairment of IRF-3 activation (16). This observation is
356 consistent with our finding that IFN- β mRNA synthesis is impaired during HRV1a
357 infection, concomitant with IPS-1 cleavage and inhibition of IRF-3 activation. Cleavage
358 of IPS-1 by both viral proteases and cellular caspase-3 may be a strategy to ensure
359 effective abrogation of the innate antiviral response.

Acknowledgements

This work was supported in part by Public Health Service Grants AI50754 and T32AI07161 from the National Institute of Allergy and Infectious Diseases.

We thank Adolfo Garcia-Sastre for the Cantell strain of Sendai virus, Richard Lloyd for the gift of 2A^{pro} and 3C^{pro}, Jeremy Luban for the lentiviral vectors, Klaus Conzelmann for BSR T7/5 cells, Dr. Zhijian Chen for pFLAG-IPS-1.

References

1. **Arimoto, K., H. Takahashi, T. Hishiki, H. Konishi, T. Fujita, and K. Shimotohno.** 2007. Negative regulation of the RIG-I signaling by the ubiquitin ligase RNF125. *Proc Natl Acad Sci U S A* **104**:7500-7505.
2. **Barral, P., D. Sarkar, P. Fisher, and V. Racaniello.** 2009. RIG-I is cleaved during picornavirus infection. *Virology* **In Press**.
3. **Barral, P. M., J. M. Morrison, J. Drahos, P. Gupta, D. Sarkar, P. B. Fisher, and V. R. Racaniello.** 2007. MDA-5 is cleaved in poliovirus-infected cells. *J Virol* **81**:3677-3684.
4. **Buchholz, U. J., S. Finke, and K. K. Conzelmann.** 1999. Generation of bovine respiratory syncytial virus (BRSV) from cDNA: BRSV NS2 is not essential for virus replication in tissue culture, and the human RSV leader region acts as a functional BRSV genome promoter. *J Virol* **73**:251-259.
5. **Calandria, C., A. Irurzun, A. Barco, and L. Carrasco.** 2004. Individual expression of poliovirus 2Apro and 3Cpro induces activation of caspase-3 and PARP cleavage in HeLa cells. *Virus Res* **104**:39-49.
6. **Chen, Z., Y. Benureau, R. Rijnbrand, J. Yi, T. Wang, L. Warter, R. E. Lanford, S. A. Weinman, S. M. Lemon, A. Martin, and K. Li.** 2007. GB virus B disrupts RIG-I signaling by NS3/4A-mediated cleavage of the adaptor protein MAVS. *J Virol* **81**:964-976.
7. **Deszcz, L., E. Gaudernak, E. Kuechler, and J. Seipelt.** 2005. Apoptotic events induced by human rhinovirus infection. *J Gen Virol* **86**:1379-1389.

8. **Fendrick, A. M., A. S. Monto, B. Nightengale, and M. Sarnes.** 2003. The economic burden of non-influenza-related viral respiratory tract infection in the United States. *Arch Intern Med* **163**:487-494.
9. **Fitzgerald, K. A., S. M. McWhirter, K. L. Faia, D. C. Rowe, E. Latz, D. T. Golenbock, A. J. Coyle, S. M. Liao, and T. Maniatis.** 2003. IKKepsilon and TBK1 are essential components of the IRF3 signaling pathway. *Nat Immunol* **4**:491-496.
10. **Gitlin, L., W. Barchet, S. Gilfillan, M. Cella, B. Beutler, R. A. Flavell, M. S. Diamond, and M. Colonna.** 2006. Essential role of mda-5 in type I IFN responses to polyriboinosinic:polyribocytidylic acid and encephalomyocarditis picornavirus. *Proc Natl Acad Sci U S A* **103**:8459-8464.
11. **Hornung, V., J. Ellegast, S. Kim, K. Brzozka, A. Jung, H. Kato, H. Poeck, S. Akira, K. K. Conzelmann, M. Schlee, S. Endres, and G. Hartmann.** 2006. 5'-Triphosphate RNA is the ligand for RIG-I. *Science* **314**:994-997.
12. **Kang, D. C., R. V. Gopalkrishnan, L. Lin, A. Randolph, K. Valerie, S. Pestka, and P. B. Fisher.** 2004. Expression analysis and genomic characterization of human melanoma differentiation associated gene-5, mda-5: a novel type I interferon-responsive apoptosis-inducing gene. *Oncogene* **23**:1789-1800.
13. **Kato, H., O. Takeuchi, S. Sato, M. Yoneyama, M. Yamamoto, K. Matsui, S. Uematsu, A. Jung, T. Kawai, K. J. Ishii, O. Yamaguchi, K. Otsu, T. Tsujimura, C. S. Koh, C. Reis e Sousa, Y. Matsuura, T. Fujita, and S. Akira.**

2006. Differential roles of MDA5 and RIG-I helicases in the recognition of RNA viruses. *Nature* **441**:101-105.
14. **Kawai, T., and S. Akira.** 2006. Innate immune recognition of viral infection. *Nat Immunol* **7**:131-137.
 15. **Kawai, T., K. Takahashi, S. Sato, C. Coban, H. Kumar, H. Kato, K. J. Ishii, O. Takeuchi, and S. Akira.** 2005. IPS-1, an adaptor triggering RIG-I- and Mda5-mediated type I interferon induction. *Nat Immunol* **6**:981-988.
 16. **Kotla, S., T. Peng, R. E. Bumgarner, and K. E. Gustin.** 2008. Attenuation of the type I interferon response in cells infected with human rhinovirus. *Virology*.
 17. **Kovacovics, M., F. Martinon, O. Micheau, J. L. Bodmer, K. Hofmann, and J. Tschopp.** 2002. Overexpression of Helicard, a CARD-containing helicase cleaved during apoptosis, accelerates DNA degradation. *Curr Biol* **12**:838-843.
 18. **Krausslich, H. G., M. J. H. Nicklin, H. Toyoda, D. Etchison, and E. Wimmer.** 1987. Poliovirus proteinase 2A induces cleavage of eukaryotic initiation factor 4F polypeptide p220. *J. Virol.* **61**:2711-2718.
 19. **Kuyumcu-Martinez, N. M., M. E. Van Eden, P. Younan, and R. E. Lloyd.** 2004. Cleavage of poly(A)-binding protein by poliovirus 3C protease inhibits host cell translation: a novel mechanism for host translation shutoff. *Mol Cell Biol* **24**:1779-1790.
 20. **Lin, R., C. Heylbroeck, P. M. Pitha, and J. Hiscott.** 1998. Virus-dependent phosphorylation of the IRF-3 transcription factor regulates nuclear translocation, transactivation potential, and proteasome-mediated degradation. *Mol Cell Biol* **18**:2986-2996.

21. **Loo, Y. M., and M. Gale, Jr.** 2007. Viral regulation and evasion of the host response. *Curr Top Microbiol Immunol* **316**:295-313.
22. **Mallia P, J. S.** 2006. How viral infections cause exacerbation of airway diseases. *Chest* **130**:1203-1210.
23. **Merika, M., and D. Thanos.** 2001. Enhanceosomes. *Curr Opin Genet Dev* **11**:205-208.
24. **Meylan, E., J. Curran, K. Hofmann, D. Moradpour, M. Binder, R. Bartschlager, and J. Tschopp.** 2005. Cardif is an adaptor protein in the RIG-I antiviral pathway and is targeted by hepatitis C virus. *Nature* **437**:1167-1172.
25. **Mori, M., M. Yoneyama, T. Ito, K. Takahashi, F. Inagaki, and T. Fujita.** 2004. Identification of Ser-386 of interferon regulatory factor 3 as critical target for inducible phosphorylation that determines activation. *J Biol Chem* **279**:9698-9702.
26. **Seth, R. B., L. Sun, C. K. Ea, and Z. J. Chen.** 2005. Identification and characterization of MAVS, a mitochondrial antiviral signaling protein that activates NF-kappaB and IRF 3. *Cell* **122**:669-682.
27. **Strahle, L., J. B. Marq, A. Brini, S. Hausmann, D. Kolakofsky, and D. Garcin.** 2007. Activation of the beta interferon promoter by unnatural Sendai virus infection requires RIG-I and is inhibited by viral C proteins. *J Virol* **81**:12227-12237.
28. **Strauss, J. H., and E. G. Strauss.** 2002. *Viruses and human disease*. Academic Press, San Diego, Calif.

29. **Svitkin, Y. V., A. Gradi, H. Imataka, S. Morino, and N. Sonenberg.** 1999. Eukaryotic initiation factor 4GII (eIF4GII), but not eIF4GI, cleavage correlates with inhibition of host cell protein synthesis after human rhinovirus infection. *J Virol* **73**:3467-3472.
30. **Taimen, P., H. Berghall, R. Vainionpaa, and M. Kallajoki.** 2004. NuMA and nuclear lamins are cleaved during viral infection--inhibition of caspase activity prevents cleavage and rescues HeLa cells from measles virus-induced but not from rhinovirus 1B-induced cell death. *Virology* **320**:85-98.
31. **Takeuchi, O., and S. Akira.** 2007. Recognition of viruses by innate immunity. *Immunol Rev* **220**:214-224.
32. **Xu, L. G., Y. Y. Wang, K. J. Han, L. Y. Li, Z. Zhai, and H. B. Shu.** 2005. VISA is an adapter protein required for virus-triggered IFN-beta signaling. *Mol Cell* **19**:727-740.
33. **Yang, H., G. Ma, C. H. Lin, M. Orr, and M. G. Wathelet.** 2004. Mechanism for transcriptional synergy between interferon regulatory factor (IRF)-3 and IRF-7 in activation of the interferon-beta gene promoter. *Eur J Biochem* **271**:3693-3703.
34. **Yang, Y., Y. Liang, L. Qu, Z. Chen, M. Yi, K. Li, and S. M. Lemon.** 2007. Disruption of innate immunity due to mitochondrial targeting of a picornaviral protease precursor. *Proc Natl Acad Sci U S A* **104**:7253-7258.
35. **Yoneyama, M., and T. Fujita.** 2007. Function of RIG-I-like receptors in antiviral innate immunity. *J Biol Chem* **282**:15315-15318.
36. **Yoneyama, M., M. Kikuchi, K. Matsumoto, T. Imaizumi, M. Miyagishi, K. Taira, E. Foy, Y. M. Loo, M. Gale, Jr., S. Akira, S. Yonehara, A. Kato, and**

- T. Fujita.** 2005. Shared and unique functions of the DExD/H-box helicases RIG-I, MDA5, and LGP2 in antiviral innate immunity. *J Immunol* **175**:2851-2858.
37. **Yoneyama, M., M. Kikuchi, T. Natsukawa, N. Shinobu, T. Imaizumi, M. Miyagishi, K. Taira, S. Akira, and T. Fujita.** 2004. The RNA helicase RIG-I has an essential function in double-stranded RNA-induced innate antiviral responses. *Nat Immunol* **5**:730-737.

Figure Legends

Figure 1. Induction of IFN- β mRNA during HRV1a infection. HeLa cells were infected with HRV1a or SeV, total cellular RNA was harvested at the times indicated, and IFN- β mRNA was detected by Sybergreen RT-qPCR. Results were normalized to PBDG mRNA copy number and displayed as fold induction to uninfected cells using the $\Delta\Delta C_T$ method. (A). Induction of IFN- β in cells infected with either HRV1a or SeV. (B) Induction of IFN- β during HRV1a infection. The HRV1a results were plotted separately (B) to highlight the induction of IFN- β mRNA synthesis.

Figure 2. HRV1a infection does not induce IRF-3 homodimers. HeLa cells were infected with either SeV or HRV1a and harvested at the times indicated. Cell extracts were prepared, fractionated by native-PAGE, and IRF-3 was detected by western blot analysis using polyclonal rabbit antiserum against IRF-3, which strongly recognizes both the monomeric and dimeric forms of the protein. Monomeric and dimeric forms of IRF-3 are labeled.

Figure 3. HRV1a infection inhibits SeV-induced homodimerization of IRF-3. HeLa cells were either mock treated or infected with HRV1a for 3 hr or 5 hr, and then super-infected with Sendai virus for the times indicated. Cell extracts were prepared, fractionated by native-PAGE, and IRF-3 was detected by western blot analysis using a mouse monoclonal antibody. Monomeric and dimeric forms of IRF-3 are labeled.

Figure 4. Accumulation of Sendai viral proteins during coinfection with HRV1a.

HeLa cells were infected with HRV1a for 8 hr (lane 1), SeV for 3, 5, 7, or 15 hr (lanes 3-5), or with HRV1a for 5 hr followed by SeV for 3 or 5 hr (lanes 7, 8). No sample was loaded in lane 6. Cell extracts were prepared, fractionated by SDS-PAGE, and SeV proteins were detected by western blot analysis using anti-Sendai virus antiserum.

Figure 5. Cleavage of IPS-1 in cells infected with HRV1a or poliovirus. Monolayers of HeLa cells were infected with HRV1a, poliovirus, or SeV. Cell extracts were prepared after infection at the times indicated, fractionated by SDS-PAGE, and IPS-1 was detected by western blot analysis. (-), mock-infected cells. A separate bottom panel shows detection of β -actin (**A**) or GAPDH (**B**) to ensure that equal amounts of protein were applied to each lane.

Figure 6. Knockdown of IRF-3 in HeLa cells. Stable cells lines were produced that produce miRNA targeting IRF-3 (mi-IRF-3) or luciferase as a control (mi-L1221). Cell extracts were prepared and analyzed for IRF-3 protein levels by SDS-PAGE and western blot analysis (**A**). Dimerization of IRF-3 was examined by native-PAGE in cells infected with HRV1a or SeV (**B**).

Figure 7. Effect of IRF-3 knockdown on HRV1a replication. HeLa, mi-IRF-3, and mi-L1221 cells were infected with HRV1a at an MOI of 0.1 or 10. At the indicated times after infection virus titers were determined by plaque assay on HeLa cell monolayers.

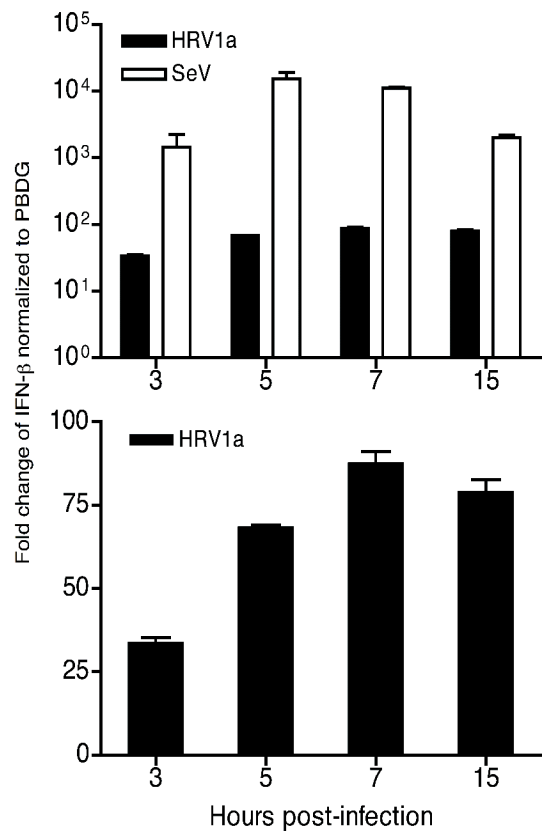
Figure 8. Induction of IFN- β mRNA during HRV1a infection in cells with reduced IRF-3. mi-L1221 or mi-IRF-3 cells were infected with HRV1a or SeV, total cellular RNA was harvested at the times indicated, and IFN- β mRNA was detected by Sybergreen RT-quantitative real-time PCR. Results were normalized to PBDG mRNA copy number and displayed as fold induction to uninfected cells using the $\Delta\Delta C_T$ method.

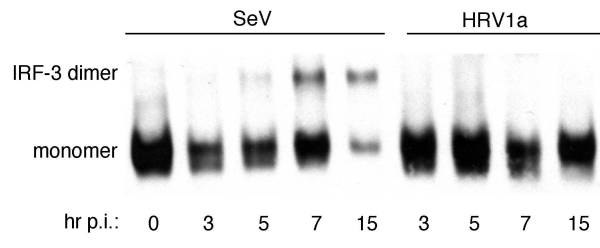
Figure 9. Cleavage of IPS-1 and PARP during apoptosis. Monolayers of HeLa cells were infected with HRV1a (MOI of 10) (A), treated with puromycin (20 μ M) (B) to induce apoptosis, or infected with HRV1a (MOI of 10) and treated with zVAD (20 μ M) (C). At different times after infection, or after addition of puromycin or zVAD to the culture medium, cell extracts were prepared, fractionated by SDS-PAGE, and PARP and IPS-1 were detected by western blot analysis. Separate bottom panels shows detection of β -actin or GAPDH to ensure that equal amounts of protein were applied to each lane.

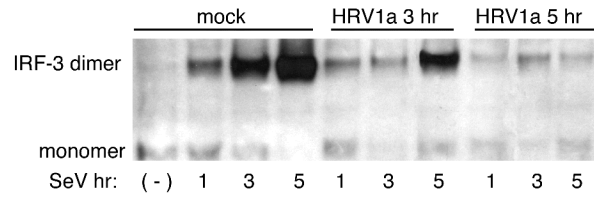
Figure 10. Effect of 3C^{pro}, 2A^{pro}, and caspase-3 on IPS-1 in vitro. IPS-1 was produced by in vitro translation in a reticulocyte lysate in the presence of [³⁵S]-methionine. The lysate was subsequently incubated with purified 3CD^{pro}, 2A^{pro}, or caspase-3, fractionated by SDS-PAGE, and [³⁵S]-methionine labeled proteins were detected by phosphorimaging. PABP (to confirm enzyme activity) and β -actin (loading control, not shown) were detected by western blot analysis. Asterisks indicate putative cleavage products of IPS-1.

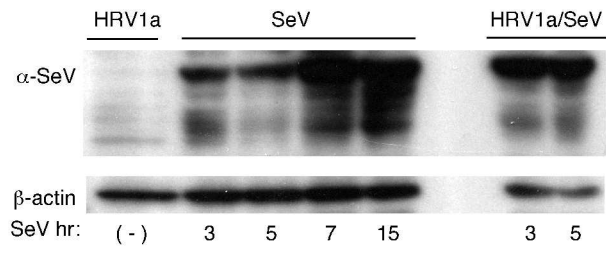
Figure 11. Expression of viral proteinases in cells. BSR T7/5 cells were co-transformed with plasmids encoding IPS-1 and either eGFP or proteinases of human

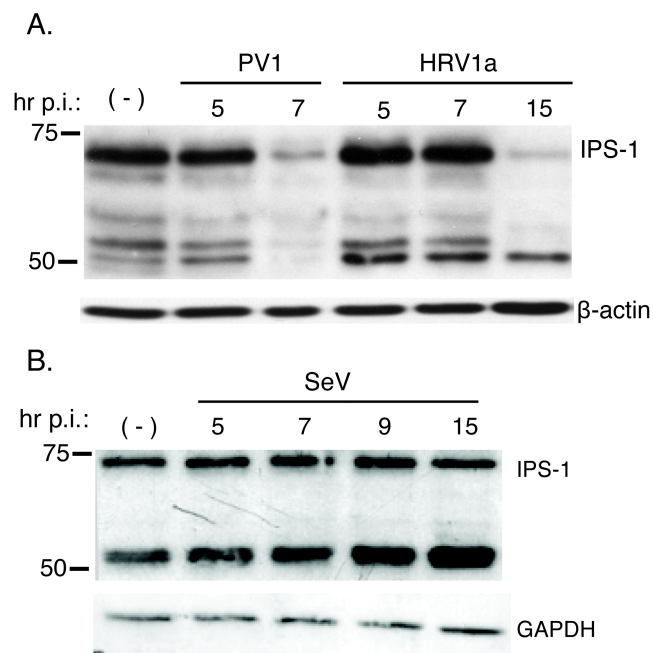
rhinovirus type 1a (HRV1a), poliovirus (PV1), or hepatitis A virus (HAV). After 24 hr cell extracts were prepared, fractionated by SDS-PAGE, and IPS-1 was detected by western blot analysis. Separate bottom panel shows detection of β -actin to ensure that equal amounts of protein were applied to each lane.

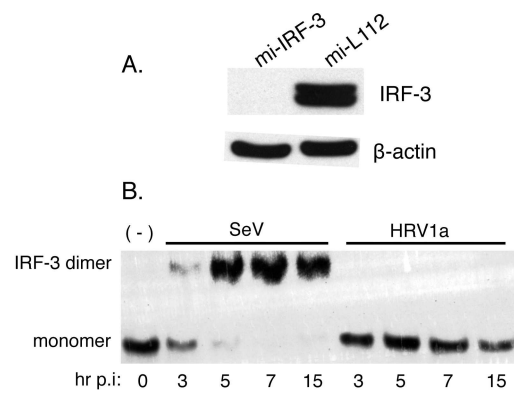


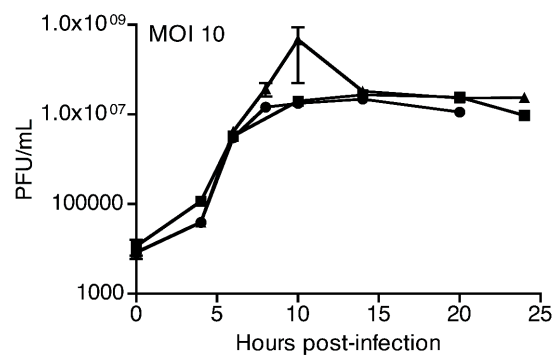
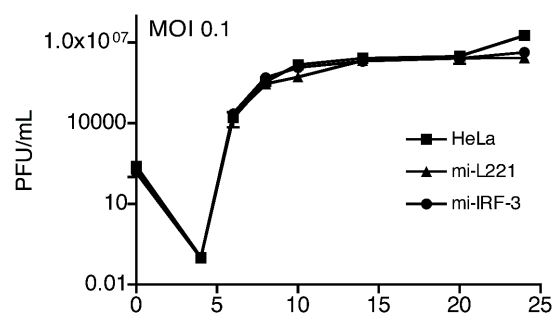


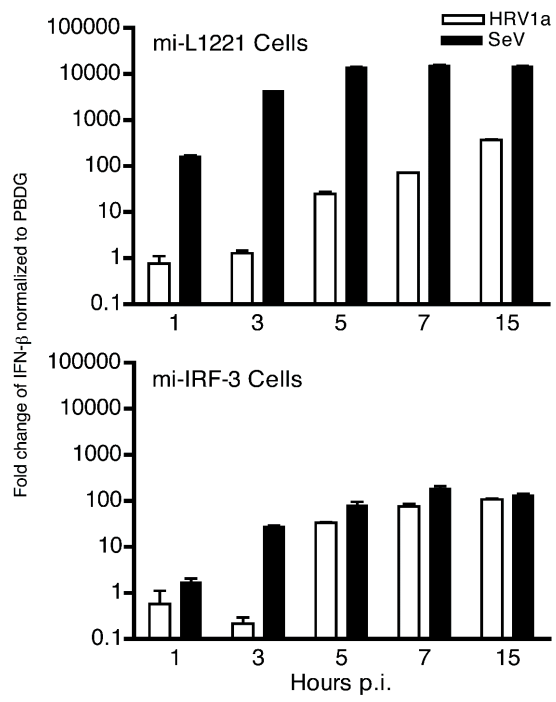


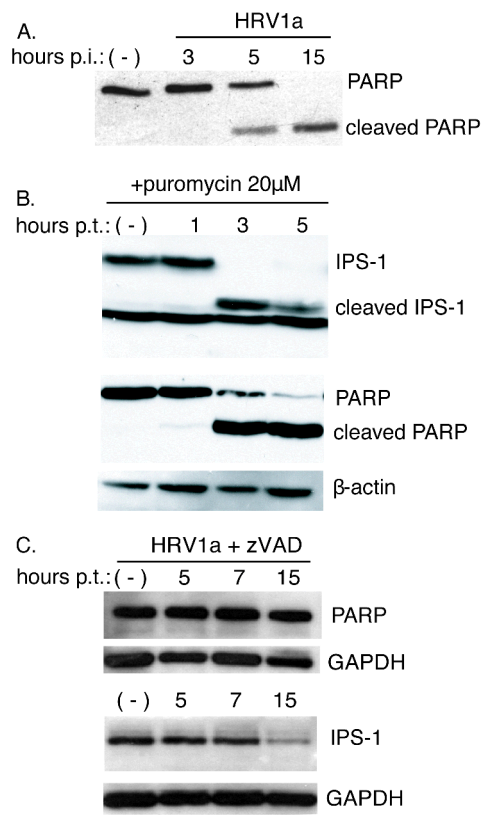


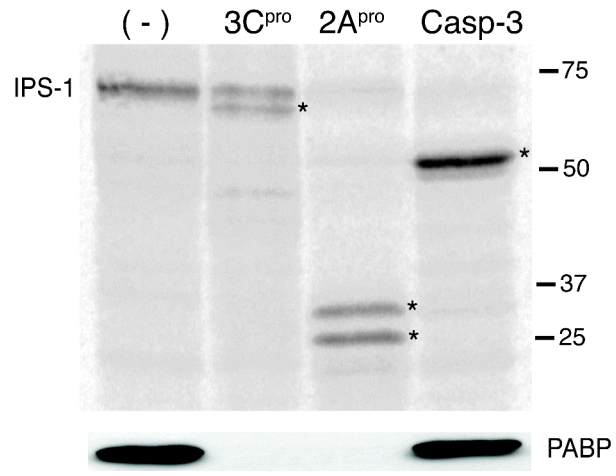


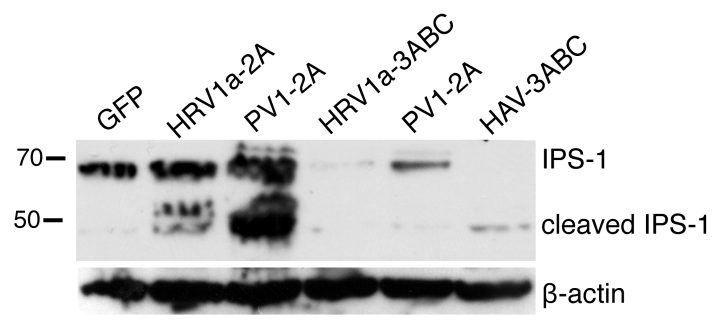












HIV-1 Nef Interferes with Host Cell Motility by Deregulation of Cofilin

Bettina Stolp,¹ Michal Reichman-Fried,⁴ Libin Abraham,^{1,2} Xiaoyu Pan,¹ Simone I. Giese,¹ Sebastian Hannemann,¹ Polyxeni Goulimari,³ Erez Raz,⁴ Robert Grosse,³ and Oliver T. Fackler^{1,*}

¹Department of Virology, Im Neuenheimer Feld 324

²The Hartmut Hoffmann-Berling International Graduate School of Molecular and Cellular Biology, Im Neuenheimer Feld 282

³Institute of Pharmacology, Im Neuenheimer Feld 366
University of Heidelberg, 69120 Heidelberg, Germany

⁴Institute for Cell Biology, University of Münster, 48149 Münster, Germany

*Correspondence: oliver.fackler@med.uni-heidelberg.de

DOI 10.1016/j.chom.2009.06.004

SUMMARY

HIV-1 Nef is a key factor in AIDS pathogenesis. Here, we report that Nef potently inhibits motility of fibroblasts and chemotaxis of HIV-1-infected primary human T lymphocytes toward the chemokines SDF-1 α , CCL-19, and CCL-21 *ex vivo*. Furthermore, Nef inhibits guided motility of zebrafish primordial germ cells toward endogenous SDF-1a *in vivo*. These migration defects result from Nef-mediated inhibition of the actin remodeling normally triggered by migratory stimuli. Nef strongly induces phosphorylation of cofilin, inactivating this evolutionarily conserved actin-depolymerizing factor that promotes cell motility when unphosphorylated. Nef-dependent cofilin deregulation requires association of Nef with the cellular kinase Pak2. Disruption of Nef-Pak2 association restores the cofilin phosphorylation levels and actin remodeling that facilitate cell motility. We conclude that HIV-1 Nef alters Pak2 function, which directly or indirectly inactivates cofilin, thereby restricting migration of infected T lymphocytes as part of a strategy to optimize immune evasion and HIV-1 replication.

INTRODUCTION

The host cell cytoskeleton plays a key role in the life cycle of viral pathogens whose propagation depends on mandatory intracellular steps. Viruses have consequently evolved strategies to modulate actin as well as microtubule filament systems to facilitate cell entry, intracellular transport, and egress of new viral progeny. Such strategies were also adopted by human retroviruses, such as the human immunodeficiency virus type 1 (HIV-1), that rely on actin remodeling for early entry and postentry steps during productive infection (Bukrinskaya et al., 1998; Jiménez-Baranda et al., 2007; McDonald et al., 2002; Yoder et al., 2008). Which cytoskeleton machineries are specifically targeted and by which mechanism HIV-1 affects host cell cytoskeleton remodeling, however, have remained unclear.

Remodeling of the cytoskeleton is also essential for directed movement of host cells themselves (Fackler and Grosse, 2008;

Pollard and Borisy, 2003). While individual cell types exhibit motility in response to different exogenous triggers and use distinct types of cell movement depending on their physiological environment, core principles of cell motility probably apply to most scenarios (Rafelski and Theriot, 2004). One central aspect of directed cell motility is polarization of the moving cell, including translocation of the microtubule organizing center (MTOC) and the Golgi apparatus toward the direction of cell movement (Nabi, 1999). Also, the actin cytoskeleton undergoes dynamic changes in response to a migratory stimulus, typically leading to pronounced actin polymerization and depolymerization events that critically determine a cell's motile capacity. Such actin remodeling is subject to tight control, primarily by *de novo* nucleation of actin filaments (Chhabra and Higgs, 2007). In addition, F-actin disassembly via depolymerization factors such as cofilin also contributes to actin remodeling by providing F-actin fragments as substrate for new filaments (Bamburg and Bernstein, 2008).

The Nef protein of HIV-1 is a 25–35 kDa myristoylated protein that is expressed abundantly already at early stages of HIV-1 infection. Importantly, Nef expression is a prerequisite for efficient HIV-1 replication in the infected host. The absence of Nef, therefore, significantly slows down or completely abolishes development of acquired immunodeficiency syndrome (AIDS) (Deacon et al., 1995; Kestler et al., 1991). Moreover, isolated Nef expression in transgenic mice is sufficient to establish AIDS-like depletion of CD4⁺ T lymphocytes (Hanna et al., 1998). While these results clearly established Nef as a critical viral factor in AIDS pathogenesis, the molecular basis for this activity still remains unclear. Nef is a versatile manipulator of host cell vesicular transport and signal transduction processes, effects that are mediated by a plethora of protein interactions with host cell factors such as components of the endocytic sorting and T cell receptor (TCR) signaling machineries (Malim and Emerman, 2008). Many of these interactions were mapped to defined protein interaction surfaces of Nef. However, which of the proposed ligands are functionally relevant remains elusive (Geyer et al., 2001). While effects of Nef in receptor transport are relatively well defined (Roeth and Collins, 2006), Nef's effects on signal transduction are not well understood. In T lymphocytes, one of the main target cell populations of HIV, Nef predominantly affects signal transduction via the TCR. While Nef generally elevates the basal state of T cell activation, multiple effects of HIV-1 Nef in response to TCR engagement leading to

selective activation or inhibition, respectively, of distinct downstream signaling events have been observed (Haller et al., 2006; lafrate et al., 1997; Schindler et al., 2006; Schragar and Marsh, 1999). By the combination of these effects, Nef may prevent premature activation-induced death of infected cells while simultaneously increasing their permissivity for HIV-1 replication (Fackler et al., 2007). In addition, Nef prevents T lymphocyte chemotaxis toward the chemoattractant SDF-1 α (Choe et al., 2002), but the mechanism and in vivo relevance of this activity are unclear.

Several protein assemblies have been described to interact with select surfaces on Nef and mediate individual downstream effects on T lymphocyte homeostasis. These include the kinase complex NAK-C, which facilitates transcription of the viral genome (Witte et al., 2004) and association of Nef with DOCK2-ELMO1, a complex implied in Nef's effect on T lymphocyte chemotaxis (Janardhan et al., 2004). In addition, Nef associates with a highly active population of the cellular kinase Pak2 in the context of a labile multiprotein complex (Nunn and Marsh, 1996; Rauch et al., 2008; Renkema et al., 1999). Pak2 is a member of the group I family of p21-activated kinases that act as downstream effectors of the activated Rho GTPases Cdc42 and Rac1 to modulate various processes such as cytoskeletal organization, transcription, and cell survival (Bokoch, 2003). In line with these functions of Pak2, Nef was suggested to modulate such cellular processes via its association with Pak2 (Haller et al., 2006; Lu et al., 1996; Wolf et al., 2001), but without establishing a direct role of Pak2 in these effects or addressing their mechanism or physiological relevance. To address these issues, we analyze here the effects of HIV-1 Nef on host cell motility. The results of these analyses unravel that the pathogenicity factor, via its Pak2 association, prevents actin remodeling to impair host cell motility in vitro and in vivo and define deregulation of cofilin as an underlying mechanism.

RESULTS

Inhibition of Fibroblast Wound Closure by Nef

To address whether Nef generally affects cell migration, we expressed the HIV protein in the hamster fibroblast cell line CHO, a cell type that supports key biological activities of Nef (Keppler et al., 2005). Stable cell lines were generated that express a control GFP or a GFP fusion protein of wild-type (WT) HIV-1_{SF2} Nef, a functional homolog of nonfusion Nef, in a doxycycline (Dox)-inducible manner. Cells were grown to confluence, and cell motility was analyzed after scratch wounding of the monolayer (Figure 1). GFP-expressing control cells rapidly migrated into the scratch wound, resulting in wound closure approximately after 15–20 hr (Figures 1A and 1B, Movie S1). In contrast, expression of WT Nef in the two independent CHO clones analyzed (WT12, used in all subsequent experiments, and WT17) caused a marked reduction in cell migration, resulting in incomplete wound closure even after 24 hr (Figures 1A and 1B, Movie S2). Kinetic analysis of the wound width over time identified the 20 hr postwounding time point as a robust parameter to quantify differences between GFP- and Nef-expressing cells (Figures 1B and 1C) and revealed a more than 8-fold reduction in motility of Nef-expressing cells as compared to control cells. This deficit was specific for the expression of Nef, as cells in

which Nef expression had not been induced (–Dox) displayed normal wound healing.

To map the molecular determinants of Nef that are responsible for the inhibition of wound closure, various inducible cell lines were generated for the expression of Nef mutants. Dox concentrations were titrated by flow cytometry to result in levels of Nef.GFP expression that in all cell clones were comparable or higher than for WT Nef.GFP (Figures S1A and S1B). All mutant Nef proteins displayed the expected subcellular localization (intracellular membranes, plasma membrane, and cytoplasm), and Nef expression had no impact on cell proliferation (Figures S1C and S1D). The LLAA Nef variant (leucine 168 and 169 mutated to alanine to disrupt Nef's interaction with the clathrin endocytosis machinery) interfered with wound healing as efficiently as WT Nef (Figures 1D and S2). In contrast, several Nef mutants were impaired in inhibiting wound-healing motility even when expressed at higher levels than WT Nef: G2A (a nonmyristoylated Nef with reduced membrane association), E4A4 (glutamic acid 66–69 mutated to alanine to disrupt association with the PACS sorting adaptor), and AxxA (proline 76 and 79 mutated to alanine to disrupt interaction with SH3 domain-containing ligands). In contrast to these mutants that are deficient in several biological properties of Nef, a single point mutation, F195A/I, which specifically interrupts the association of Nef with the cellular kinase Pak2 without affecting other Nef activities (O'Neill et al., 2006; Rauch et al., 2008), even more potently abrogated the Nef-mediated inhibition of cell motility 20 hr after wounding. Kinetic analysis revealed that Nef F195A-expressing cells exhibit an initial motility defect after scratch wounding, but then accelerate to result in wound closure indistinguishable from GFP-expressing control cells (Figure S2F).

Nef Affects Actin Turnover in Migrating Cells

To determine the mechanism by which Nef interferes with wound healing, cell polarization and cytoskeletal organization was compared in GFP- and WT Nef.GFP-expressing CHO cells. While WT Nef-expressing cells displayed a slight defect in polarization of the Golgi apparatus toward the wound (Figures S3A and S3B), analysis of Nef mutants ruled out that this phenomenon is required for the migration defect of Nef-expressing cells (data not shown). Polarization of the MTOC toward the wound was unaffected by Nef expression (Figures S3C and S3D), and organization of total as well as detyrosinated, stable microtubules, which are required for wound healing (Cook et al., 1998), was normal in the presence of Nef (Figures S3E and S3F). In contrast, analysis of F-actin organization revealed pronounced effects of Nef expression. While all cells displayed low levels of F-actin directly after wounding ($t = 0$ hr), GFP-expressing control cells showed pronounced filament assembly after 4 hr (Figures 1E and S4A). This induction of actin filaments was fully inhibited in the presence of WT Nef that, in turn, induced the formation of small punctuate F-actin aggregates in the cytoplasm instead. While Nef mutants LLAA or G2A, E4A4, and AxxA showed WT or intermediate activity in blocking filament assembly, respectively, Nef F195A was entirely deficient and allowed for pronounced formation of actin filaments (Figures 1F and S4A). Across this panel of CHO cell lines, we observed a strong correlation between inhibition of wound closure and filament assembly by Nef (Figure S4B). Since the pivotal role of

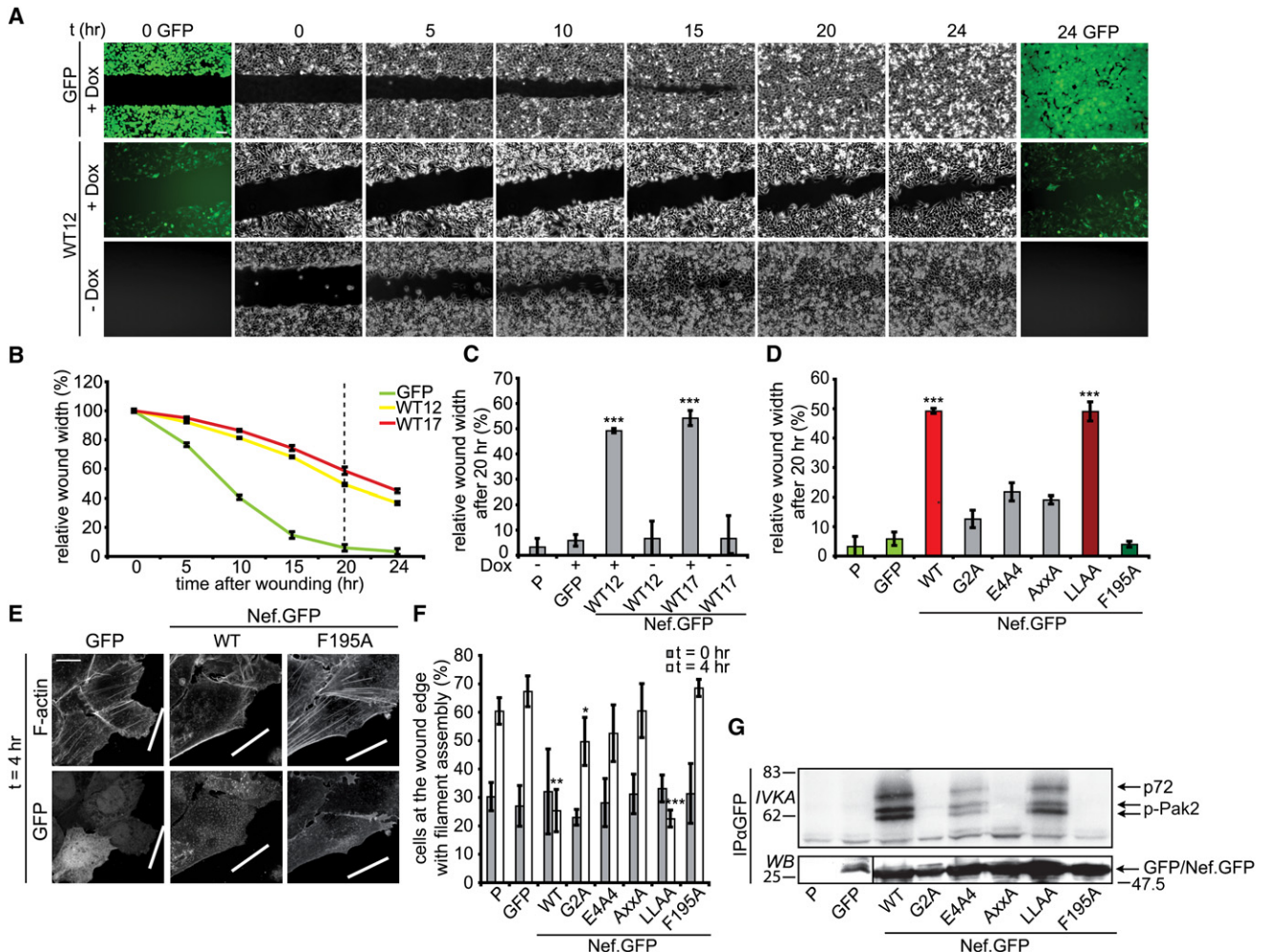


Figure 1. HIV-1 Nef Interferes with Wound Healing Cell Motility and Wound-Induced Actin Filament Assembly

(A) Representative micrographs of wound closure kinetics of the indicated cell lines. CHO cells stably transduced with expression constructs for GFP or WT Nef.GFP were induced for transgene expression (+Dox) or left untreated (–Dox) and grown to confluency. After introduction of a wound by a pipette tip, cell migration into the wound was monitored over 24 hr. Scale bar = 100 μm.

(B) Wound closure time course of GFP-expressing CHO cells versus the WT Nef.GFP-expressing CHO clones 12 and 17. Depicted are mean values ± SEM of 7–9 independent experiments.

(C and D) Quantification of relative wound width at 20 hr after wounding of the indicated cell clones (P, parental) as indicated by the dotted line in (B). Shown is the mean ± SEM of 3–9 independent experiments. P values are calculated relative to the GFP control.

(E) Representative confocal micrographs of the indicated CHO cell clones at the wound edge 4 hr after wounding. Cells were fixed and stained with phalloidin to reveal F-actin. Bold white lines indicate the trajectory of the wound. Scale bar = 10 μm. Pictures of additional Nef mutants and cells directly after wounding are shown in Figure S4A.

(F) Quantification of actin filament assembly. Shown are mean values ± SD from three independent experiments of cells displaying actin stress fibers near the wound, with at least 100 cells counted per experiment.

(G) Nef-associated Pak2 activity. CHO cells expressing the indicated GFP/Nef.GFP proteins were transfected with a Pak2 expression construct and subjected to anti-GFP immunoprecipitation and subsequent *in vitro* kinase assay (IVKA). Phosphorylated endogenous and overexpressed Pak2 (p-PAK2) or immunisolated GFP/Nef.GFP present in the IVKA were detected by autoradiography and western blotting, respectively (IVKA and WB panels). p72 designates an unidentified Pak2 substrate.

the F195 residue for Nef-Pak2 association has thus far only been investigated in human cells, we next tested whether this mutation also disrupts the interaction in CHO cells. *In vitro* kinase analysis (IVKA) of immunisolated Nef indeed revealed the specific association of WT, but not G2A, AxxA, and F195A Nef with autophosphorylated Pak2 (Figure 1G), indicating that Pak2 association might be involved in the Nef-mediated inhibition of actin remodeling and wound closure.

Nef Prevents SDF-1α-Induced T Lymphocyte Membrane Ruffling and Chemotaxis

We next asked whether Nef also interferes with actin remodeling and cell motility in natural target cells of HIV-1 infection such as T lymphocytes. Chemotaxis was used as an experimental system, since incubation of T lymphocytes with chemoattractants such as SDF-1α results in pronounced actin remodeling that is required for directional movement toward chemokine gradients

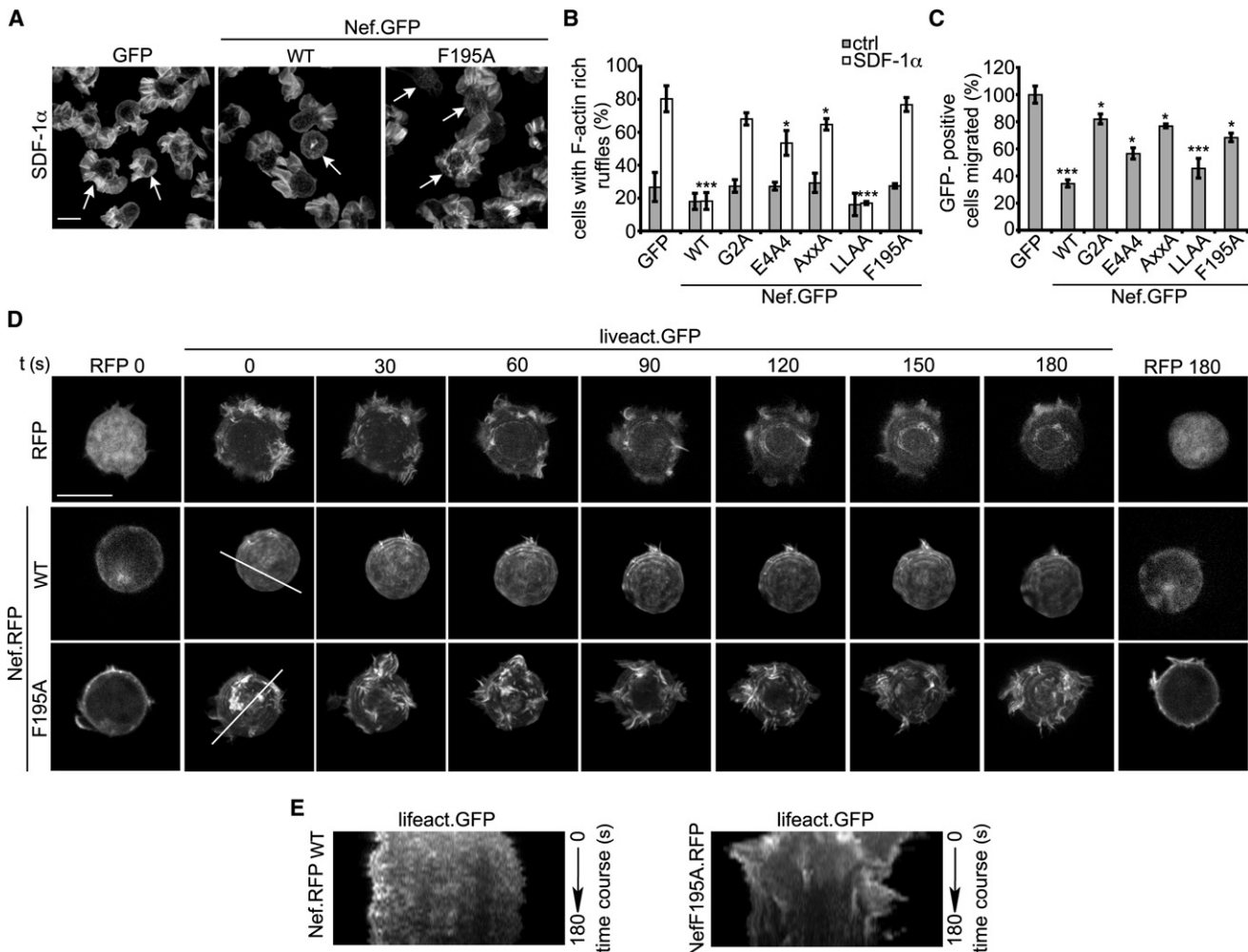


Figure 2. Nef Inhibits SDF-1 α -Induced Actin Ruffling and Chemotaxis in T Lymphocytes

(A) Representative maximum projections of confocal Z stacks of Jurkat T lymphocytes (Jurkat TAG) transiently expressing the indicated GFP fusion proteins. Cells were fixed 20 min after treatment with 200 ng/ml SDF-1 α and stained for F-actin. Arrows indicate transfected cells; GFP signals and additional Nef mutants are shown in Figure S4D. Scale bar = 10 μ m.

(B) Frequency of the cells shown in (A) and Figure S4D that display membrane ruffling in response to treatment with SDF-1 α or a solvent control (ctrl). Depicted are mean values from four independent experiments \pm SD with at least 100 cells analyzed per condition. P values are calculated relative to the GFP control.

(C) Chemotaxis toward SDF-1 α . Jurkat T lymphocytes (Jurkat E6-1) expressing the indicated proteins were subjected to a transwell chemotaxis assay. Depicted is the percentage of GFP-positive cells that migrated toward 10 ng/ml SDF-1 α over 2 hr. Values are the mean with SEM from four experiments performed in triplicates. P values are calculated relative to the GFP control.

(D) Still images of the time-lapse Movies S3, S4, and S5. Jurkat T lymphocytes (Jurkat-CCR7) were cotransfected with RFP, WT, or F195A Nef.RFP and lifeact.GFP to reveal F-actin. Shown are maximum intensity projections of the GFP signal every 30 s. The first and the last panel show single confocal pictures of the RFP signal before and after acquisition of the movie.

(E) Kymographs from the white lines of the cells shown in (D).

(Nishita et al., 2005). Transient expression of WT Nef in Jurkat T lymphocytes caused a marked inhibition of SDF-1 α -induced actin rearrangement and membrane ruffling (see Figures 2A and S4D for analysis of fixed cells). The activity pattern of Nef mutants correlated well with the previous results in CHO cells, with the F195 residue being one essential determinant for this phenotype (Figure 2B). This was particularly apparent in real-time confocal analysis, which revealed dynamic protrusion and retraction of actin-rich lamellododia and filopodia in the presence of RFP or Nef F195A.RFP, while WT Nef.RFP-expressing cells failed to undergo such dynamic plasma membrane reorganiza-

tion (Figures 2D and 2E, Movies S3, S4, and S5). Moreover, Nef caused a marked reduction of T lymphocyte chemotaxis toward SDF-1 α (Figure 2C) (Choe et al., 2002). This inhibition in T lymphocyte chemotaxis was significantly impaired, but not entirely abrogated for the Nef F195A mutant. WT and F195A Nef proteins both induced comparable, moderate downregulation of the SDF-1 α receptor CXCR4 from the cell surface (Schindler et al., 2007 and data not shown) and associated to a similar extent with DOCK2-ELMO1 (Figure S5). Inhibition of SDF-1 α -induced membrane ruffling and chemotaxis was observed, albeit with varying efficiency, with different *nef* alleles from HIV-1, HIV-2,

and simian immunodeficiency virus (SIV), demonstrating that they represent conserved activities of lentiviral Nef proteins (Figures S6A–S6C). Notably, a strong correlation was observed between the ability of Nef variants and mutants to interfere with SDF-1 α -induced membrane ruffling and chemotaxis (Figures S4C and S6D). To extend these findings to the context of HIV-1 infection, primary human peripheral blood lymphocytes (PBLs) were infected with HIV-1 WT, HIV-1 Δ Nef lacking Nef expression, or an isogenic virus expressing the F195I Nef mutant and analyzed for their ability to undergo membrane ruffling and chemotaxis upon treatment with the CXCR4 ligand SDF-1 α or the CCR7 ligands CCL-19 or CCL-21, respectively (Figure 3). Infection with WT, but not Δ Nef HIV-1, potentially blocked the formation of large polarized membrane ruffles in the presence of any of the three chemokines and impaired lymphocyte chemotaxis (Figures 3A–3C and S7A, Movies S6 and S7). These Nef effects depended again on F195 and Nef effects on T lymphocyte chemotaxis and membrane ruffling correlated with each other.

Effects of Nef on SDF-1 α -Mediated Zebrafish Primordial Germ Cell Migration In Vivo

We sought to explore whether Nef can also affect migration of cells in the context of an intact organism at physiological SDF-1 α concentrations. The lack of an HIV-1-permissive small animal and limited transduction rates of primary mouse T lymphocytes prevented us from performing such experiments in mice in the context of HIV-1 infection or upon adoptive transfer of Nef-expressing T lymphocytes. To address functions of Nef in vivo, we studied primordial germ cell (PGC) migration in zebrafish embryos. Migration of the CXCR4b-expressing PGCs toward cells expressing SDF-1 α , a zebrafish ortholog of mammalian SDF-1 α , represents a well-established model for an SDF-1-guided migration process that typically culminates in clustering of PGCs at the site of gonad development in 24 hr old zebrafish embryos (Doitsidou et al., 2002) (Figure 4A, left panel). When PGCs expressed WT Nef.GFP, arrival of these cells at the target site in 24 hr old embryos was dramatically disrupted, such that 91% of the embryos showed PGCs to be distributed in ectopic positions throughout the embryo (average of 62% ectopic PGCs in 106 embryos) (Figure 4A). This severe migration phenotype was virtually reversed upon expression of the Nef mutant F195A protein fused to GFP: In the majority (80%, $n = 48$) of these embryos, PGCs arrived at the target site in a manner indistinguishable from that observed in control embryos (Figure 4A). To analyze the basis for the compromised ability of WT Nef-expressing PGCs to reach the target, cells expressing either WT or F195A Nef were monitored by time-lapse microscopy, and their tracks of migration were delineated. Similar to normal PGCs (Reichman-Fried et al., 2004), F195A-expressing cells displayed long and directional tracks (Figures 4B and 4C, Movie S8). Tracks of WT Nef-expressing PGCs, however, were significantly shorter and coiled, reflecting severe inhibition of motility (Figures 4B and 4C, Movie S9). Furthermore, direct examination of the frequency of motile cells in each experimental group revealed that while 75% of the F195A-expressing cells were motile and exhibited normal directed migration (211 cells analyzed in 16 embryos), the majority of cells expressing WT Nef (77%) were nonmotile and largely remained on the spot when compared to somatic cells (160 cells analyzed in 12 embryos) (Figure 4D,

Movies S8 and S9). Together, expression of WT Nef potentially inhibits PGC motility in vivo in a manner that is dependent on F195, the site that enables its association with Pak2.

Nef Inactivates Cofilin by Inducing Its Hyperphosphorylation via Association with Pak2 Activity

To address whether the association of Nef with Pak2 is instrumental for the inhibition of actin remodeling and cell motility by the viral protein, we tested if signaling events downstream of Pak2 were altered in the presence of Nef. Indeed, cofilin, a key regulator of actin depolymerization that is inactivated by phosphorylation of serine at position 3 downstream of p21-activated kinases Pak1 and Pak2 (Edwards et al., 1999; Misra et al., 2005), was markedly hyperphosphorylated in the presence of WT Nef in CHO cells directly or 4 hr after wounding (Figure 5A). In most experiments, a reduction in levels of phosphorylated cofilin (p-cofilin) 4 hr postwounding was observed in GFP control cells. In contrast, WT Nef-expressing cells never displayed a similar reduction in cofilin phosphorylation after scratch wounding. Phosphorylation of Src and Merlin was unaffected by Nef expression. Similar to the results obtained for cell migration and actin remodeling, the F195 residue and the PxxP motif of Nef were essential for cofilin phosphorylation (Figures 5B and 5C). Cofilin hyperphosphorylation in Nef-expressing cells was sustained for at least 24 hr after scratch wounding (Figure 5D). In contrast to the Pak effector cofilin, GTPase activity of the Rac1 and Cdc42 upstream regulators of Pak activity was unaffected in cells expressing WT or F195A Nef (Figure 5E). In addition to Pak-dependent pathways, cofilin phosphorylation can also be regulated via the Rho-ROCK pathway (Maekawa et al., 1999). Inhibition of ROCK activity by the specific inhibitor Y27632, however, did not reverse Nef-induced hyperphosphorylation of cofilin (Figure 5F). Cofilin inactivation was also observed in Jurkat T lymphocytes expressing WT Nef.GFP or HIV-1-infected PBLs (Figures 6A–6E, S7B, and S7C). Quantification on a single-cell level revealed that, even in the absence of any stimulation, significantly more Nef-expressing cells displayed elevated p-cofilin levels in comparison to the controls (Figures 6B and 6E). Based on pixel quantifications of confocal Z stacks of individual cells, Nef expression caused a more than 4-fold increase in levels of p-cofilin per cell (Figure 6C). To test the contribution of Pak2 to Nef's effects on cofilin deregulation directly, we used RNAi-mediated knockdown of Pak2 expression to analyze the role of the kinase for Nef's inhibitory effects in Jurkat T lymphocytes (Figures 6F–6I and S7D). We previously established that potent reduction of Pak2 protein levels in these cells causes a marked, but incomplete, decrease in Nef-associated Pak2 activity, by 35% (Rauch et al., 2008). Basal p-cofilin levels were not affected by Pak2 RNAi in the absence of Nef. In contrast, Pak2 knockdown significantly reduced the frequency and magnitude of cofilin hyperphosphorylation in the presence of Nef (see also Figure S8F). We conclude that Nef induces the accumulation of phosphorylated, inactive cofilin and that Pak2 is critical for this deregulation of cofilin.

Nef-Associated Pak2 Determines Inhibition of Cell Motility by Nef, Possibly by Direct Phosphorylation of Cofilin

We next determined the role of Pak2 for the effects of Nef on actin remodeling and cell motility. Analysis of F-actin

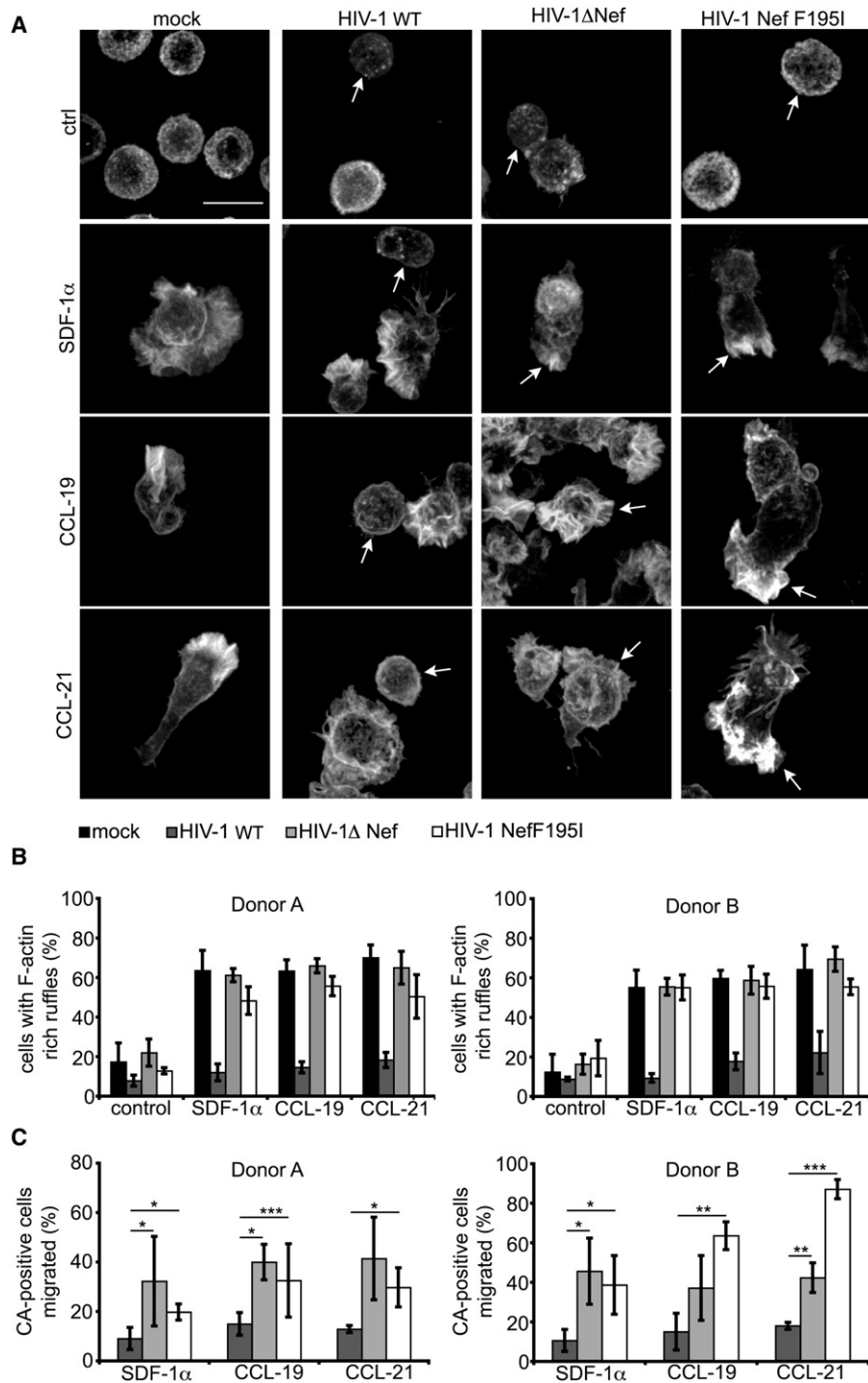


Figure 3. Nef Inhibits Chemokine-Induced Actin Remodeling and Chemotaxis in HIV-1-Infected Primary Human T Lymphocytes

(A) Representative maximum projections of confocal Z stacks of PBLs infected with WT HIV-1 (HIV-1 WT), its *nef*-deleted counterpart HIV-1ΔNef, or the isogenic virus HIV-1 Nef F195I. Cells were treated with 200 ng/ml SDF-1α, CCL-19, or CCL-21 for 20 min or left untreated (ctrl); fixed; and stained for intracellular p24CA and F-actin. Arrows indicate infected cells; p24CA signals are shown in Figure S7A. Scale bar = 10 μm.

(B) Frequency of the cells shown in (A) with membrane ruffling. Depicted are mean values from quadruplicate infections ± SD for two independent donors with at least 100 cells analyzed per condition.

(C) Chemotaxis toward SDF-1α, CCL-19, or CCL-21 of two independent donors. PBLs infected with the indicated viruses were subjected to a transwell chemotaxis assay. Depicted is the percentage of p24CA-positive cells that migrated toward 10 ng/ml SDF-1α or 25 ng/ml CCL-19 or CCL-21 over 2 hr. Values are the mean with SD from triplicate infections.

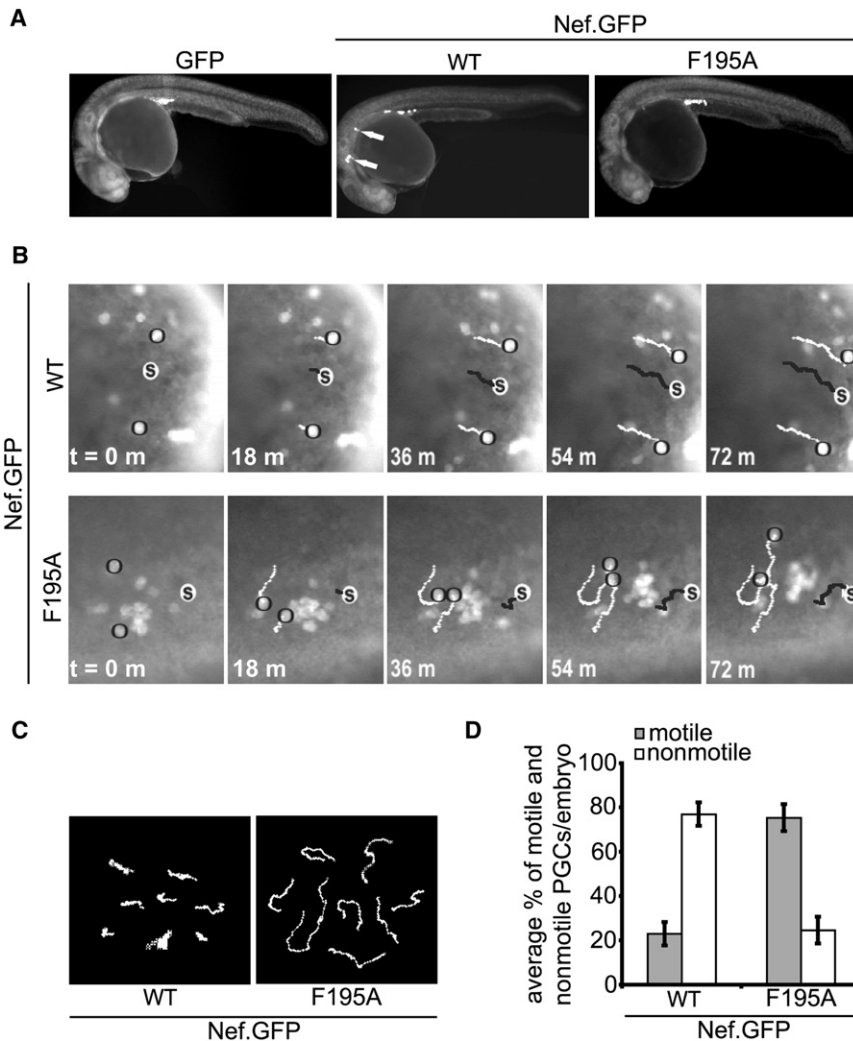


Figure 4. Nef Inhibits Motility of Zebrafish PGCs

(A) Images of representative zebrafish embryos, at 24 hr after fertilization, whose PGCs express GFP alone (left panel) or GFP fusion of either WT Nef (middle panel) or F195A Nef mutant (right panel). White arrows point at PGCs found at abnormal (ectopic) positions.

(B) Snapshots from the time-lapse Movies S8 and S9. The migration of PGCs expressing F195A or WT Nef.GFP was followed for 72 min. PGCs (circled in black) are tracked as indicated by the white line in comparison to a black track generated by a moving somatic cell (whitened cell marked with an "s").

(C) Examples for 72 min migration tracks of PGCs expressing F195A or WT Nef.GFP as indicated in (B). The migration of PGCs was followed in time-lapse movies and subtracted for somatic cell movement. Short tracks reflect inhibition of motility and are the basis for the inability of many PGCs to reach their target at 24 hr of development. (D) Average frequency of motile and nonmotile PGCs expressing F195A or WT Nef.GFP. The results are presented as average percentage of motile and nonmotile PGCs per embryo. Error bars represent SEM of at least 80 cells in eight embryos.

Pak2 targets cofilin, we failed to overcome the Nef-dependent inhibition of actin ruffle formation and cofilin deregulation in T lymphocytes by coexpression of dominant-negative variants of kinases (LIMK, TESK) or phosphatases (slingshot, chronophin) with known roles in cofilin regulation (Edwards et al., 1999; Huang et al., 2006; Misra et al., 2005; data not shown). This prompted us to test whether

reorganization revealed that treatment of cells with control or Pak2-specific RNAi had no effect on cell morphology prior to stimulation with SDF-1 α and did not affect membrane ruffle formation of GFP-expressing cells in response to the chemokine (Figures 7A, 7B, and S7E). Thus, Pak2 does not control actin remodeling, chemotaxis, and cofilin phosphorylation in our cells in the absence of Nef. In turn, knockdown of Pak2 markedly diminished Nef's ability to block actin remodeling. This rescue was partial, but correlated well with the 35% reduction in Nef-associated Pak2 activity observed under these conditions. Consistently, expression of a dominant-negative Pak significantly enhanced SDF-1 α -mediated membrane ruffling in the presence of Nef (Figure S9). Pak2 knockdown also significantly improved the migratory response of Nef-expressing cells toward SDF-1 α , however less efficiently than in the actin remodeling assay (Figure 7D). Similarly in CHO fibroblasts, Pak2 RNAi almost completely rescued Nef-mediated disruption of actin filament assembly without appreciable effects in the absence of Nef and partially released the block of wound closure and cofilin hyperphosphorylation imposed by the viral protein (Figure S8). In an attempt to define the mechanism by which Nef-associated

Pak2 might phosphorylate cofilin directly. Indeed, recombinant Pak2 was able to phosphorylate cofilin in vitro, a reaction that was not affected by the presence of Nef (Figures 7E and 7F). Importantly, cofilin also served as efficient substrate of Nef-Pak2 complexes isolated from T lymphocytes with WT, but not F195A Nef (Figure 7G). While these results do not exclude the involvement of other components of the Nef-Pak2 complex, they suggest that Nef-associated Pak2 itself mediates phosphorylation of cofilin. Nef may thus impair actin remodeling and directional cell motility by hijacking Pak2 via a physical association that retargets the biological activity of the kinase toward direct phosphorylation of cofilin.

DISCUSSION

This study reveals that the HIV-1 pathogenicity factor Nef interferes with cell motility by blocking chemoattractant-triggered actin remodeling. The effect of Nef on cell motility occurs independently of the cellular context *ex vivo* in Nef-expressing fibroblasts and HIV-1-infected primary T lymphocytes, as well as in zebrafish PGCs *in vivo*, and represents a conserved activity of

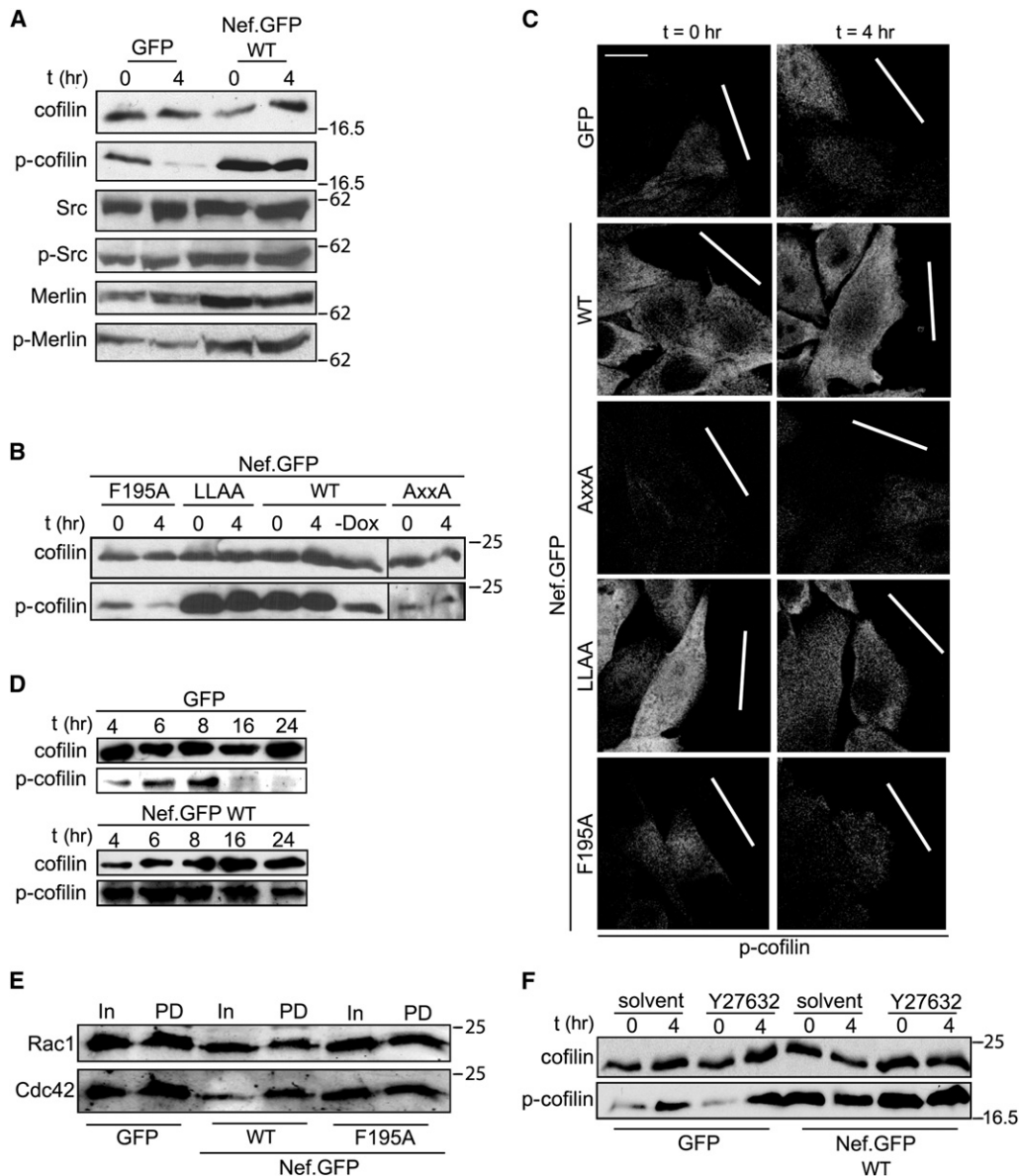


Figure 5. Nef Induces Cofilin Hyperphosphorylation

(A–D) Multiple wounds were introduced to confluent CHO cells expressing GFP or WT Nef.GFP (A and D) or the indicated Nef mutants (B). Cells were harvested at the indicated time points after wounding and analyzed by western blotting using the indicated antibodies. –Dox indicates that expression of Nef has not been induced. Note that quantification of the merlin/p-merlin ratio (A) from five independent experiments did not reveal statistically significant differences between GFP and Nef.GFP-expressing cells and that in (D), 3× more protein was loaded per lane for GFP than for Nef.GFP-expressing cells in order to detect a p-cofilin signal. Representative confocal micrographs of the cells analyzed in (A) and (B) following staining for p-cofilin are shown in (C). Bold white lines indicate the trajectory of the wound. Scale bar = 10 μm.

(E) Rac1 and Cdc42 activity levels of CHO cells expressing the indicated proteins determined by western blotting following pull-down by the GST-CRIB peptide of Pak1 (In, input; PD, pull-down).

(F) Levels of p-cofilin in CHO cells expressing GFP or WT Nef.GFP in the absence or presence of ROCK inhibitor Y27632.

Nef proteins from various HIV-1, HIV-2, and SIV strains. Mechanistic analyses demonstrate that inhibition of actin remodeling is mediated by Nef via its ability to associate with the cellular kinase Pak2, resulting in hyperphosphorylation and thereby inactivation of the evolutionary conserved actin depolymerization factor, cofilin. This is achieved by retargeting Pak2 toward cofilin, which can serve as direct Pak2 substrate in the presence of Nef. HIV,

thus, has evolved the viral factor Nef to hijack the host cell cytoskeleton for impairment of cell motility.

While alterations in actin organization in the presence of Nef were reported from several cell systems (Campbell et al., 2004; Haller et al., 2006; Lu et al., 2008; Quaranta et al., 2003), mechanism and functional consequence of this phenomenon have remained largely unclear. Addressing these issues by the

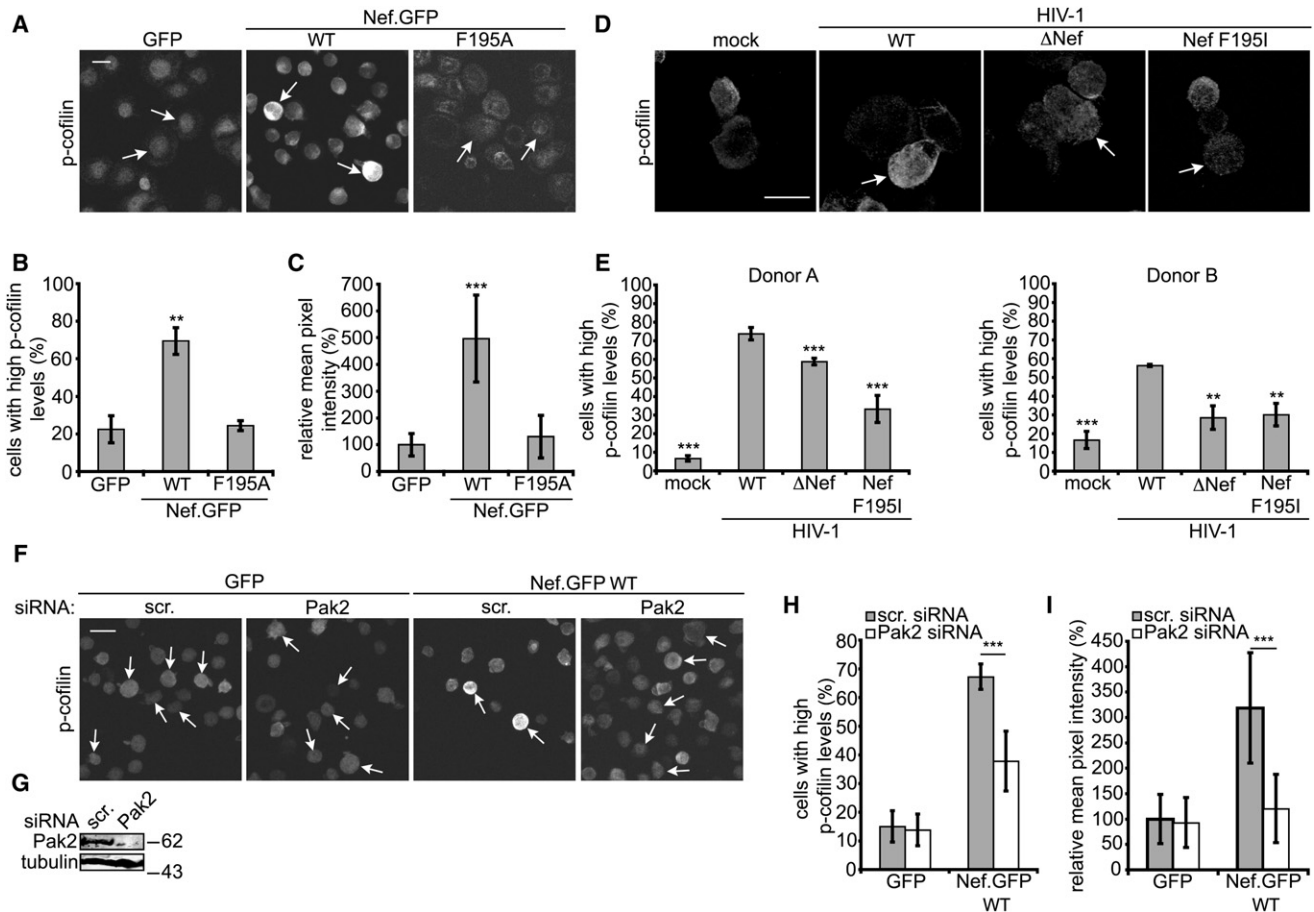


Figure 6. Nef-Induced Cofilin Hyperphosphorylation in Infected Primary Human T Lymphocytes Depends on Pak2

(A) Representative sum-intensity projections of confocal Z stacks of Jurkat T lymphocytes (Jurkat TAG) transiently expressing the indicated GFP fusion proteins. Cells were plated onto cover glasses, fixed, and stained for p-cofilin. Arrows indicate transfected cells; the GFP signal is shown in Figure S7B. Scale bar = 10 μ m.

(B) Frequency of the cells shown in (A) with high p-cofilin levels. Depicted are mean values \pm SD from three independent experiments with at least 100 cells analyzed per transfection, with cells scored as containing high p-cofilin levels when they were apparently brighter than untransfected neighboring cells. P values are calculated relative to the GFP-transfected cells.

(C) Relative mean pixel intensity of the cells in (A). Depicted are mean values \pm SD from at least ten representative cells. P values are calculated relative to the GFP-transfected cells.

(D) P-cofilin levels in PBLs infected with HIV-1 WT, HIV-1 Δ Nef, or HIV-1 Nef F195I. Cells were analyzed as in (A) with an additional stain for p24CA (shown in Figure S7C). Arrows indicated infected cells. Scale bar = 10 μ m.

(E) Frequency of the cells shown in (D) with high p-cofilin levels. Depicted are mean values \pm SD from quadruplicate infections of two independent donors with at least 100 cells analyzed per infection. P values are calculated relative to the WT HIV-1-infected cells.

(F) P-cofilin levels of Jurkat T lymphocytes (Jurkat TAG) transiently transfected with siRNA oligos specific for Pak2 or a nonspecific scrambled siRNA (scr.) together with an expression plasmid for GFP or Nef.GFP. Arrows indicate transfected cells; the GFP signal is shown in Figure S7D. Scale bar = 10 μ m.

(G) Western blot analysis of the cells used in (F).

(H) Frequency of the cells shown in (F) with high p-cofilin levels. Depicted are mean values \pm SD from three independent experiments with at least 100 cells analyzed per transfection.

(I) Relative mean pixel intensities of the cells in (F). Depicted are mean values \pm SD from at least ten representative cells per condition.

use of Nef mutants and Pak2-specific RNAi revealed, first, that the association of Nef with Pak2 activity is essential for the interference with chemoattractant-induced actin remodeling. Second, we identify cofilin as a downstream target of the Nef-Pak2 complex that causes a marked and sustained enrichment of the phosphorylated, inactive form of cofilin, even prior to migratory stimulation. Third, cofilin deregulation was demonstrated to be directly involved in Nef-mediated inhibition of actin remodeling and cell motility. This identification of cofilin as a target for the regulation of cell motility is consistent with cofilin's well-characterized role as master switch of actin remodeling in motile cells. Severing of actin filaments by active cofilin results in depolymerization of F-actin and generation of F-actin fragments that serve as substrate for nucleation of new filaments (Bamburg and Bernstein, 2008). This activity is essential for the directionality of cell movement during, e.g., lymphocyte chemotaxis or tumor cell invasion (Nishita et al., 2005; Wang et al., 2007). Cofilin is tightly regulated in migrating cells by phosphorylation of serine at position 3. It is therefore conceivable that Nef-induced inactivation of cofilin results in a net reduction of

lin's well-characterized role as master switch of actin remodeling in motile cells. Severing of actin filaments by active cofilin results in depolymerization of F-actin and generation of F-actin fragments that serve as substrate for nucleation of new filaments (Bamburg and Bernstein, 2008). This activity is essential for the directionality of cell movement during, e.g., lymphocyte chemotaxis or tumor cell invasion (Nishita et al., 2005; Wang et al., 2007). Cofilin is tightly regulated in migrating cells by phosphorylation of serine at position 3. It is therefore conceivable that Nef-induced inactivation of cofilin results in a net reduction of

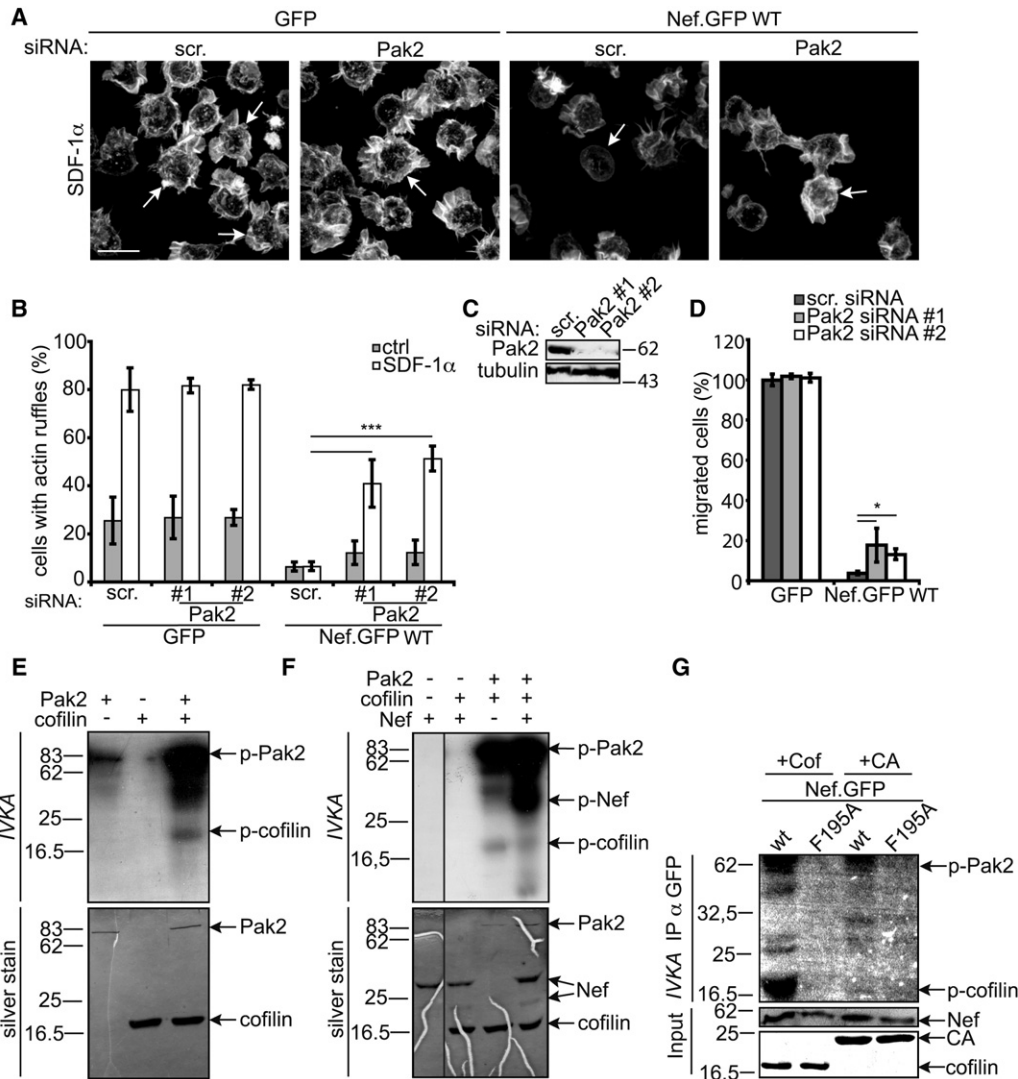


Figure 7. Nef-Associated Pak2 Is Involved in the Interference of Nef with Ruffle Formation and Chemotaxis in T Lymphocytes and Phosphorylates Cofilin

(A) Membrane ruffling analysis as in Figure 2A of Jurkat T lymphocytes (Jurkat CCR7) transfected with siRNA oligos specific for Pak2 or a nonspecific scrambled siRNA (scr.) together with an expression plasmid for GFP or WT Nef.GFP. Arrows indicate transfected cells; the GFP signal is shown in Figure S7E. Scale bar = 10 μ m.

(B) Frequency of the cells shown in (A) that display membrane ruffling. Depicted is the mean \pm SD of 3–8 independent experiments with at least 100 cells analyzed per condition.

(C) Western blot analysis of lysates of the cells used in (A).

(D) Chemotaxis toward SDF-1 α . Cells shown in (A) were subjected to a transwell chemotaxis assay. Depicted is the percentage of GFP-positive cells that migrated toward 10 ng/ml SDF-1 α over 2 hr. Values are the mean with SEM from four experiments performed in triplicates.

(E) Pak2 phosphorylates cofilin in vitro. Recombinant GST-Pak2 and cofilin were subjected to an in vitro kinase assay (IVKA), separated by SDS-PAGE, and analyzed by silver stain and autoradiography.

(F) Experiment as in (E) in the presence of recombinant myristoylated Nef. Pak2 phosphorylates cofilin in vitro in the presence of Nef.

(G) Nef-associated Pak2 phosphorylates cofilin. Jurkat TAg cells expressing WT or F195A Nef.GFP were subjected to anti-GFP immunoprecipitation and subsequent in vitro kinase assay (IVKA) in the presence of recombinant cofilin or HIV-1 CA as substrate. Phosphorylated Pak2 (p-PAK2) and p-cofilin present in the IVKA were detected by autoradiography. Nef in the input was detected by western blot; recombinant cofilin and p24CA by Coomassie stain.

actin turnover and subsequent cell motility. Interestingly, cofilin was also identified recently as regulator of HIV-1 entry (Yoder et al., 2008) and thus emerges as an important player in HIV-1's host cell interactions.

However, rescue of cofilin deregulation in Nef-expressing cells by Pak2-specific RNAi improved but did not fully restore their

motility. This reflects, at least in part, the presence of residual Nef-Pak2 association in the RNAi experiments due to incomplete knockdown of Pak2 expression (Rauch et al., 2008), but may also indicate the involvement of additional cytoskeleton regulation downstream of Nef-Pak2. However, the Nef F195A mutant, which lacks any detectable Pak2 kinase association and cofilin

deregulation, maintained some inhibitory activity despite normal actin remodeling. Thus, Nef likely exerts effects on cell motility via a second, actin-independent mechanism. With DOCK2-ELMO1 and Lck, Nef functionally interacts with at least two additional host cell factors implicated in cell motility control (Fukui et al., 2001; Janardhan et al., 2004; Okabe et al., 2005; Thoulouze et al., 2006). While both factors appear dispensable for effects on actin via Nef-Pak2 (Rauch et al., 2008) (Figures S5 and S10), their intrinsic requirement for cell motility precludes direct analysis of their contribution to cell motility restriction by Nef. In addition, Nef disturbs a variety of intracellular sorting processes (Roeth and Collins, 2006) and might affect cell motility via such mechanisms.

The results of this study provide important insight into the mechanism of cofilin deregulation by Nef. Notably, reduction of Pak2 expression had no major effects on actin remodeling, cofilin phosphorylation, and cell motility in the absence of Nef. Endogenous Pak2 therefore does not control these parameters in our cell systems. Our results are thus most consistent with a scenario in which Nef subverts intrinsic properties of Pak2. This might have included alterations in known pathways that govern cofilin phosphorylation; however, we failed to detect a role of such factors for Nef action (data not shown). Instead, we discovered that cofilin can be phosphorylated in the presence of Nef-Pak2 complexes, suggesting that the association with the viral protein alters the substrate specificities of Pak2 to retarget its activity toward cofilin. Consistent with such a scenario, the subcellular localization of phosphorylated Pak was altered by the presence of Nef in motile cells (Figure S11). The presence of another cofilin kinase in the Nef-associated protein complex, however, cannot be excluded. Efforts to unravel the molecular details of the retargeting mechanism, including attempts to determine the full composition of the labile and short-lived Nef-Pak2 complex, are currently ongoing.

We consider the introduction of zebrafish PGC migration as an experimental system for *in vivo* studies on Nef function to be an important aspect of this work. Zebrafish are readily accessible to specific expression of genes in germ cells and real-time imaging analyses. These features allowed us to quantify, in a physiological context, cell motility events analogous to T lymphocyte chemotaxis that are, upon transient expression of genes of interest, exceedingly difficult to assess in other *in vivo* experimental systems. Although limited to processes that are conserved between the natural target cells of a given pathogen and zebrafish germ cells, zebrafish PGC migration is likely to further serve as a useful model for the functional analysis of pathogen-host interactions in the case of HIV-1, but also other viral pathogens, such as Epstein-Barr virus (Ehlin-Henriksson et al., 2006) or human T lymphotropic virus type I (Arai et al., 1998).

For HIV-1 Nef, the high degree of evolutionary conservation of the mechanism by which HIV-1 hijacks an endogenous cellular pathway to affect host cell actin remodeling and motility implies that this provides the virus with significant benefits in the infected host. In newly infected individuals, HIV-1-loaded dendritic cells transport virus from mucosal surfaces to lymph nodes, where virus is efficiently transmitted to T lymphocytes (Wu and KewalRamani, 2006). Subsequent intra-lymph node

motility of productively infected T lymphocytes ensures mounting of an appropriate humoral immune response by providing B lymphocyte stimulation, induction of germinal centers for specialized production of high-affinity antibodies, and surveillance of overall architecture and *de novo* genesis of lymph nodes as well as tertiary lymphatic tissue (Friedl and Weigelin, 2008; Stein and Nombela-Arrieta, 2005). Lymph node homing and intra-lymph node motility of T lymphocytes rely on sensing of chemokine gradients and chemotaxis toward SDF-1 α , CCL-19, and CCL-21 (Wei et al., 2003). Thus, our results predict that Nef interferes with such motile events in infected individuals. Intriguingly, B lymphocyte dysfunction as consequence of disruption of germinal center formation is increasingly recognized as an important parameter in the symptom-complex AIDS (De Milito, 2004; Moir et al., 2008), a phenotype that is readily reflected in Nef-transgenic mice (Poudrier et al., 2001). Moreover, histological analysis of lymph nodes from macaques 2 weeks after infection with WT or Δ Nef SIV detected Δ Nef SIV-infected cells in germinal centers that were dramatically enlarged due to infiltration of infected cells. In stark contrast, WT SIV-infected cells were predominantly located in the paracortex, and B cell follicle displayed a normal architecture (Sugimoto et al., 2003). Together with the *in vivo* analyses presented here, these findings strongly suggest that Nef, by interfering with membrane ruffling and thus chemotaxis, prevents intra-lymph node migration of HIV-1/SIV-infected T lymphocytes to undermine the humoral immune response to virus infection. Simultaneously, reduced motility of HIV-1-infected T lymphocytes may result in the generation of microenvironments that are particularly prone to virus transmission to uninfected cells. Modulation of cell motility may thus emerge as an unexpected strategy to optimize immune evasion and replication of HIV-1 in the infected host.

EXPERIMENTAL PROCEDURES

Lymphocyte Ruffling and Chemotaxis Assay

Jurkat T lymphocytes (1×10^7) were electroporated (30–60 μ g of plasmid DNA; 960 μ F for Jurkat TAG, 850 μ F for Jurkat E6-1 and Jurkat CCR7, 250 V, Biorad Genepulser; Munich) with GFP or Nef.GFP expression plasmids. For microscopy, cover glasses were incubated for 30 min at 37°C with 0.01% poly-L-lysine, washed two times with water, and kept in PBS at 4°C until usage. Twenty-four hours after transfection, cells were seeded onto treated cover glasses for 5 min at 37°C and either fixed directly for staining of p-cofilin or incubated with 200 ng/ml SDF-1 α or solvent control for another 20 min at 37°C for the analysis of membrane ruffling before fixation. Chemotaxis assays were performed with three independent transfections per experiment. Twenty-four hours after transfection, cells were starved in medium containing 0.5% FCS and incubated for another 24 hr. Transwell inserts (5 μ m pores, 24-well plates, Costar3421, Corning; Kaiserslautern, Germany) were equilibrated overnight. The bottom chamber of the transwell was filled with 450 μ l starving medium containing 10 ng/ml or no SDF-1 α ; 1×10^6 transfected cells resuspended in 100 μ l starving medium were loaded to the upper side of each transwell. Total cell numbers and transfection efficiencies were determined from another 100 μ l aliquot of the identical cell suspension. Cells were allowed to chemotax for 2 hr at 37°C before cells in the lower chamber were collected and analyzed by FACS (FACScalibur, BD; Heidelberg, Germany) for 1 min monitoring GFP-expressing cells. In the absence of a stimulus, 1%–5% of the input cells migrated into the lower chamber of the transwell, whereas in the presence of SDF-1 α , typically 30%–60% of the cells chemotaxed. Percentage of GFP-positive cells migrated relative to transfection efficiency was calculated to address inhibitory effects.

Expression and Analysis of WT and F195A Nef in PGCs of Zebrafish Embryos

Directing expression of various genes specifically to PGCs is facilitated by fusing the gene of interest to the 3' untranslated region of *nanos-1* (*nos3*'UTR), a zebrafish germ cell-specific gene (Köprunner et al., 2001). Capped sense RNA of WT or F195A *nef* fused to *gfp* and to *nos3*'UTR or of *gfp* alone fused to *nos3*'UTR was synthesized with the MessageMachine kit (Ambion; Darmstadt, Germany) and microinjected into zebrafish embryos (450 pg per embryo) at one-cell stage. Fish used are of the AB background. Epifluorescence images of 24 hr embryos were captured with a 5× objective using the Axioplan2 microscope (Zeiss; Göttingen, Germany) controlled by MetaMorph software (Universal Imaging; Sunnyvale, CA). Time-lapse movies for track and motility analysis were generated with a 10× objective. Frames were captured at 1 min intervals, and for tracking of migrating germ cells, the "Track Objects" software module of MetaMorph was used. Tracks delineating active migration of PGCs were corrected for movement originating in the surrounding cells that passively drag PGCs along. For better visualization of PGCs in this analysis, *gfp-nos3*'UTR RNA was injected (150 pg per embryo) along with WT or F195A *nef* RNA.

Statistical Evaluation

Statistical significance was calculated by performing a Student's *t* test (***, *p* < 0.0005; **, *p* < 0.005; *, *p* < 0.05).

SUPPLEMENTAL DATA

Supplemental Data include Supplemental Experimental Procedures, Supplemental References, 12 figures, and nine movies and can be found online at [http://www.cell.com/cell-host-microbe/supplemental/S1931-3128\(09\)00216-9](http://www.cell.com/cell-host-microbe/supplemental/S1931-3128(09)00216-9).

ACKNOWLEDGMENTS

We are grateful to Walter Nickel, Scott R. Struthers, Michael Sixt, Vanda Bartonova, Hans-Georg Kräusslich, Matthias Geyer, and Felix Wieland for the kind gift of reagents; to Oliver Keppler for critical comments on the manuscript; to the FACS sorting facility of SFB638 and the Nikon Imaging Center (EXC81) for service; and to Nadine Tibroni for expert technical help. This project was supported financially by the Deutsche Forschungsgemeinschaft (SFB638, project A11 to O.T.F., GRK1188 fellowships to B.S. and S.H., Cellular Networks PhD fellowship to L.A., and GR 2111/1-3 to R.G.) O.T.F. and R.G. are members of the CellNetworks Cluster of Excellence EXC81.

Received: February 12, 2009

Revised: April 30, 2009

Accepted: June 1, 2009

Published: August 19, 2009

REFERENCES

Arai, M., Ohashi, T., Tsukahara, T., Murakami, T., Hori, T., Uchiyama, T., Yamamoto, N., Kannagi, M., and Fujii, M. (1998). Human T-cell leukemia virus type 1 Tax protein induces the expression of lymphocyte chemoattractant SDF-1/PBSF. *Virology* 241, 298–303.

Bamburg, J.R., and Bernstein, B.W. (2008). ADF/cofilin. *Curr. Biol.* 18, R273–R275.

Bokoch, G.M. (2003). Biology of the p21-activated kinases. *Annu. Rev. Biochem.* 72, 743–781.

Bukrinskaya, A., Brichacek, B., Mann, A., and Stevenson, M. (1998). Establishment of a functional human immunodeficiency virus type 1 (HIV-1) reverse transcription complex involves the cytoskeleton. *J. Exp. Med.* 188, 2113–2125.

Campbell, E.M., Nunez, R., and Hope, T.J. (2004). Disruption of the actin cytoskeleton can complement the ability of Nef to enhance human immunodeficiency virus type 1 infectivity. *J. Virol.* 78, 5745–5755.

Chhabra, E.S., and Higgs, H.N. (2007). The many faces of actin: matching assembly factors with cellular structures. *Nat. Cell Biol.* 9, 1110–1121.

Choe, E.Y., Schoenberger, E.S., Gropman, J.E., and Park, I.W. (2002). HIV Nef inhibits T cell migration. *J. Biol. Chem.* 277, 46079–46084.

Cook, T.A., Nagasaki, T., and Gundersen, G.G. (1998). Rho guanosine triphosphatase mediates the selective stabilization of microtubules induced by lysophosphatidic acid. *J. Cell Biol.* 141, 175–185.

De Milito, A. (2004). B lymphocyte dysfunctions in HIV infection. *Curr. HIV Res.* 2, 11–21.

Deacon, N.J., Tsykin, A., Solomon, A., Smith, K., Ludford-Menting, M., Hooker, D.J., McPhee, D.A., Greenway, A.L., Ellett, A., Chatfield, C., et al. (1995). Genomic structure of an attenuated quasi species of HIV-1 from a blood transfusion donor and recipients. *Science* 270, 988–991.

Doitsidou, M., Reichman-Fried, M., Stebler, J., Köprunner, M., Dorries, J., Meyer, D., Esguerra, C.V., Leung, T., and Raz, E. (2002). Guidance of primordial germ cell migration by the chemokine SDF-1. *Cell* 111, 647–659.

Edwards, D.C., Sanders, L.C., Bokoch, G.M., and Gill, G.N. (1999). Activation of LIM-kinase by Pak1 couples Rac/Cdc42 GTPase signalling to actin cytoskeletal dynamics. *Nat. Cell Biol.* 1, 253–259.

Ehlin-Henriksson, B., Mowafi, F., Klein, G., and Nilsson, A. (2006). Epstein-Barr virus infection negatively impacts the CXCR4-dependent migration of tonsillar B cells. *Immunology* 117, 379–385.

Fackler, O.T., and Grosse, R. (2008). Cell motility through plasma membrane blebbing. *J. Cell Biol.* 181, 879–884.

Fackler, O.T., Alcover, A., and Schwartz, O. (2007). Modulation of the immunological synapse: a key to HIV-1 pathogenesis? *Nat. Rev. Immunol.* 7, 310–317.

Friedl, P., and Weigelin, B. (2008). Interstitial leukocyte migration and immune function. *Nat. Immunol.* 9, 960–969.

Fukui, Y., Hashimoto, O., Sanui, T., Koga, H., Abe, M., Inayoshi, A., Noda, M., Oike, M., Shirai, T., and Sasazuki, T. (2001). Haematopoietic cell-specific CDM family protein DOCK2 is essential for lymphocyte migration. *Nature* 412, 826–831.

Geyer, M., Fackler, O.T., and Peterlin, B.M. (2001). Structure–function relationships in HIV-1 Nef. *EMBO Rep.* 2, 580–585.

Haller, C., Rauch, S., Michel, N., Hannemann, S., Lehmann, M.J., Keppler, O.T., and Fackler, O.T. (2006). The HIV-1 pathogenicity factor Nef interferes with maturation of stimulatory T-lymphocyte contacts by modulation of N-Wasp activity. *J. Biol. Chem.* 281, 19618–19630.

Hanna, Z., Kay, D.G., Rebai, N., Guimond, A., Jothy, S., and Jolicœur, P. (1998). Nef harbors a major determinant of pathogenicity for an AIDS-like disease induced by HIV-1 in transgenic mice. *Cell* 95, 163–175.

Huang, T.Y., DerMardirossian, C., and Bokoch, G.M. (2006). Cofilin phosphatases and regulation of actin dynamics. *Curr. Opin. Cell Biol.* 18, 26–31.

lafrate, A.J., Bronson, S., and Skowronski, J. (1997). Separable functions of Nef disrupt two aspects of T cell receptor machinery: CD4 expression and CD3 signaling. *EMBO J.* 16, 673–684.

Janardhan, A., Swigut, T., Hill, B., Myers, M.P., and Skowronski, J. (2004). HIV-1 Nef binds the DOCK2-ELMO1 complex to activate rac and inhibit lymphocyte chemotaxis. *PLoS Biol.* 2, E6.

Jiménez-Baranda, S., Gómez-Moutón, C., Rojas, A., Martínez-Prats, L., Mira, E., Ana Lacalle, R., Valencia, A., Dimitrov, D.S., Viola, A., Delgado, R., et al. (2007). Filamin-A regulates actin-dependent clustering of HIV receptors. *Nat. Cell Biol.* 9, 838–846.

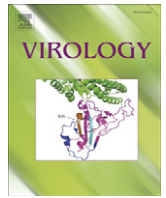
Keppler, O.T., Allespach, I., Schüller, L., Fenard, D., Greene, W.C., and Fackler, O.T. (2005). Rodent cells support key functions of the human immunodeficiency virus type 1 pathogenicity factor Nef. *J. Virol.* 79, 1655–1665.

Kestler, H.W., 3rd, Ringler, D.J., Mori, K., Panicali, D.L., Sehgal, P.K., Daniel, M.D., and Desrosiers, R.C. (1991). Importance of the nef gene for maintenance of high virus loads and for development of AIDS. *Cell* 65, 651–662.

Köprunner, M., Thisse, C., Thisse, B., and Raz, E. (2001). A zebrafish *nanos*-related gene is essential for the development of primordial germ cells. *Genes Dev.* 15, 2877–2885.

Lu, T.C., He, J.C., Wang, Z.H., Feng, X., Fukumi-Tominaga, T., Chen, N., Xu, J., lyengar, R., and Klotman, P.E. (2008). HIV-1 Nef disrupts the podocyte actin

- cytoskeleton by interacting with diaphanous interacting protein. *J. Biol. Chem.* 283, 8173–8182.
- Lu, X., Wu, X., Plemenitas, A., Yu, H., Sawai, E.T., Abo, A., and Peterlin, B.M. (1996). CDC42 and Rac1 are implicated in the activation of the Nef-associated kinase and replication of HIV-1. *Curr. Biol.* 6, 1677–1684.
- Maekawa, M., Ishizaki, T., Boku, S., Watanabe, N., Fujita, A., Iwamatsu, A., Obinata, T., Ohashi, K., Mizuno, K., and Narumiya, S. (1999). Signaling from Rho to the actin cytoskeleton through protein kinases ROCK and LIM-kinase. *Science* 285, 895–898.
- Malim, M.H., and Emerman, M. (2008). HIV-1 accessory proteins—ensuring viral survival in a hostile environment. *Cell Host Microbe* 3, 388–398.
- McDonald, D., Vodicka, M.A., Lucero, G., Svitkina, T.M., Borisy, G.G., Emerman, M., and Hope, T.J. (2002). Visualization of the intracellular behavior of HIV in living cells. *J. Cell Biol.* 159, 441–452.
- Misra, U.K., Deedwania, R., and Pizzo, S.V. (2005). Binding of activated alpha2-macroglobulin to its cell surface receptor GRP78 in 1-LN prostate cancer cells regulates PAK-2-dependent activation of LIMK. *J. Biol. Chem.* 280, 26278–26286.
- Moir, S., Ho, J., Malaspina, A., Wang, W., DiPoto, A.C., O’Shea, M.A., Roby, G., Kottlilil, S., Arthos, J., Proschan, M.A., et al. (2008). Evidence for HIV-associated B cell exhaustion in a dysfunctional memory B cell compartment in HIV-infected viremic individuals. *J. Exp. Med.* 205, 1797–1805.
- Nabi, I.R. (1999). The polarization of the motile cell. *J. Cell Sci.* 112, 1803–1811.
- Nishita, M., Tomizawa, C., Yamamoto, M., Horita, Y., Ohashi, K., and Mizuno, K. (2005). Spatial and temporal regulation of cofilin activity by LIM kinase and Slingshot is critical for directional cell migration. *J. Cell Biol.* 171, 349–359.
- Nunn, M.F., and Marsh, J.W. (1996). Human immunodeficiency virus type 1 Nef associates with a member of the p21-activated kinase family. *J. Virol.* 70, 6157–6161.
- O’Neill, E., Kuo, L.S., Krisko, J.F., Tomchick, D.R., Garcia, J.V., and Foster, J.L. (2006). Dynamic evolution of the human immunodeficiency virus type 1 pathogenic factor, Nef. *J. Virol.* 80, 1311–1320.
- Okabe, S., Fukuda, S., Kim, Y.J., Niki, M., Pelus, L.M., Ohyashiki, K., Pandolfi, P.P., and Broxmeyer, H.E. (2005). Stromal cell-derived factor-1alpha/CXCL12-induced chemotaxis of T cells involves activation of the RasGAP-associated docking protein p62Dok-1. *Blood* 105, 474–480.
- Pollard, T.D., and Borisy, G.G. (2003). Cellular motility driven by assembly and disassembly of actin filaments. *Cell* 112, 453–465.
- Poudrier, J., Weng, X., Kay, D.G., Paré, G., Calvo, E.L., Hanna, Z., Kosco-Vilbois, M.H., and Jolicoeur, P. (2001). The AIDS disease of CD4C/HIV transgenic mice shows impaired germinal centers and autoantibodies and develops in the absence of IFN-gamma and IL-6. *Immunity* 15, 173–185.
- Quaranta, M.G., Mattioli, B., Spadaro, F., Straface, E., Giordani, L., Ramoni, C., Malorni, W., and Viora, M. (2003). HIV-1 Nef triggers Vav-mediated signaling pathway leading to functional and morphological differentiation of dendritic cells. *FASEB J.* 17, 2025–2036.
- Rafelski, S.M., and Theriot, J.A. (2004). Crawling toward a unified model of cell motility: spatial and temporal regulation of actin dynamics. *Annu. Rev. Biochem.* 73, 209–239.
- Rauch, S., Pulkkinen, K., Saksela, K., and Fackler, O.T. (2008). Human immunodeficiency virus type 1 Nef recruits the guanine exchange factor Vav1 via an unexpected interface into plasma membrane microdomains for association with p21-activated kinase 2 activity. *J. Virol.* 82, 2918–2929.
- Reichman-Fried, M., Minina, S., and Raz, E. (2004). Autonomous modes of behavior in primordial germ cell migration. *Dev. Cell* 6, 589–596.
- Renkema, G.H., Manninen, A., Mann, D.A., Harris, M., and Saksela, K. (1999). Identification of the Nef-associated kinase as p21-activated kinase 2. *Curr. Biol.* 9, 1407–1410.
- Roeth, J.F., and Collins, K.L. (2006). Human immunodeficiency virus type 1 Nef: adapting to intracellular trafficking pathways. *Microbiol. Mol. Biol. Rev.* 70, 548–563.
- Schindler, M., Münch, J., Kutsch, O., Li, H., Santiago, M.L., Bibollet-Ruche, F., Müller-Trutwin, M.C., Novembre, F.J., Peeters, M., Courgnaud, V., et al. (2006). Nef-mediated suppression of T cell activation was lost in a lentiviral lineage that gave rise to HIV-1. *Cell* 125, 1055–1067.
- Schindler, M., Rajan, D., Specht, A., Ritter, C., Pulkkinen, K., Saksela, K., and Kirchhoff, F. (2007). Association of Nef with p21-activated kinase 2 is dispensable for efficient human immunodeficiency virus type 1 replication and cytopathicity in ex vivo-infected human lymphoid tissue. *J. Virol.* 81, 13005–13014.
- Schrager, J.A., and Marsh, J.W. (1999). HIV-1 Nef increases T cell activation in a stimulus-dependent manner. *Proc. Natl. Acad. Sci. USA* 96, 8167–8172.
- Stein, J.V., and Nombela-Arrieta, C. (2005). Chemokine control of lymphocyte trafficking: a general overview. *Immunology* 116, 1–12.
- Sugimoto, C., Tadakuma, K., Otani, I., Moritoyo, T., Akari, H., Ono, F., Yoshikawa, Y., Sata, T., Izumo, S., and Mori, K. (2003). nef gene is required for robust productive infection by simian immunodeficiency virus of T-cell-rich paracortex in lymph nodes. *J. Virol.* 77, 4169–4180.
- Thoulouze, M.I., Sol-Foulon, N., Blanchet, F., Dautry-Varsat, A., Schwartz, O., and Alcover, A. (2006). Human immunodeficiency virus type-1 infection impairs the formation of the immunological synapse. *Immunity* 24, 547–561.
- Wang, W., Eddy, R., and Condeelis, J. (2007). The cofilin pathway in breast cancer invasion and metastasis. *Nat. Rev. Cancer* 7, 429–440.
- Wei, S.H., Parker, I., Miller, M.J., and Cahalan, M.D. (2003). A stochastic view of lymphocyte motility and trafficking within the lymph node. *Immunol. Rev.* 195, 136–159.
- Witte, V., Laffert, B., Rosorius, O., Lischka, P., Blume, K., Galler, G., Stilper, A., Willbold, D., D’Aloja, P., Sixt, M., et al. (2004). HIV-1 Nef mimics an integrin receptor signal that recruits the polycomb group protein Eed to the plasma membrane. *Mol. Cell* 13, 179–190.
- Wolf, D., Witte, V., Laffert, B., Blume, K., Stromer, E., Trapp, S., d’Aloja, P., Schürmann, A., and Baur, A.S. (2001). HIV-1 Nef associated PAK and PI3-kinases stimulate Akt-independent Bad-phosphorylation to induce anti-apoptotic signals. *Nat. Med.* 7, 1217–1224.
- Wu, L., and KewalRamani, V.N. (2006). Dendritic-cell interactions with HIV: infection and viral dissemination. *Nat. Rev. Immunol.* 6, 859–868.
- Yoder, A., Yu, D., Dong, L., Iyer, S.R., Xu, X., Kelly, J., Liu, J., Wang, W., Vorster, P.J., Agulto, L., et al. (2008). HIV envelope-CXCR4 signaling activates cofilin to overcome cortical actin restriction in resting CD4 T cells. *Cell* 134, 782–792.



RIG-I is cleaved during picornavirus infection

Paola M. Barral^a, Devanand Sarkar^{a,b,c}, Paul B. Fisher^{a,b,c}, Vincent R. Racaniello^{d,*}

^a Department of Human and Molecular Genetics, Virginia Commonwealth University School of Medicine, 1101 East Marshall Street, Sanger Hall Building, Room 11-015, Richmond, VA 23298-0033, USA

^b VCU Institute of Molecular Medicine, Virginia Commonwealth University School of Medicine, 1101 East Marshall Street, Sanger Hall Building, Room 11-015, Richmond, VA 23298-0033, USA

^c Massey Cancer Center, Virginia Commonwealth University School of Medicine, 1101 East Marshall Street, Sanger Hall Building, Room 11-015, Richmond, VA 23298-0033, USA

^d Department of Microbiology, Columbia University Medical Center, College of Physicians and Surgeons, 701 W. 168th St., New York, NY 10032, USA

ARTICLE INFO

Article history:

Received 28 October 2008

Returned to author for revision

18 November 2008

Accepted 25 June 2009

Available online 22 July 2009

Keywords:

Poliovirus

Picornavirus

Innate immunity

Interferon

Pathogenesis

ABSTRACT

The innate immune system senses RNA virus infections through membrane-bound Toll-like receptors or the cytoplasmic proteins RIG-I and MDA-5. RIG-I is believed to recognize the 5'-triphosphate present on many viral RNAs, and hence is important for sensing infections by paramyxoviruses, influenza viruses, rhabdoviruses, and flaviviruses. MDA-5 recognizes dsRNA, and senses infection with picornaviruses, whose RNA 5'-ends are linked to a viral protein, VPg, not a 5'-triphosphate. We previously showed that MDA-5 is degraded in cells infected with different picornaviruses, and suggested that such cleavage might be a mechanism to antagonize production of type I IFN in response to viral infection. Here we examined the state of RIG-I during picornavirus infection. RIG-I is degraded in cells infected with poliovirus, rhinoviruses, echovirus, and encephalomyocarditis virus. In contrast to MDA-5, cleavage of RIG-I is not accomplished by cellular caspases or the proteasome. Rather, the viral proteinase 3C^{pro} cleaves RIG-I, both in vitro and in cells. Cleavage of RIG-I during picornavirus infection may constitute another mechanism for attenuating the innate response to viral infection.

© 2009 Elsevier Inc. All rights reserved.

Introduction

When viruses infect cells, intrinsic defensive actions are initiated almost immediately. These defenses include the innate immune system, which provides cytokines to halt virus infection, and modulate the adaptive immune response should the infection proceed unchecked (Janeway and Medzhitov, 2002). The innate immune system is activated when microbial products, such as lipopolysaccharide or viral nucleic acids, are detected. RNA viruses are recognized as foreign by cellular sensors that are activated by viral proteins or nucleic acids, leading to the production of the critical antiviral type I interferons.

Sensing of RNA virus infection by the innate immune system is carried out by membrane-bound Toll-like receptors, or by cytoplasmic sensors such as PKR, RIG-I, and MDA-5 (reviewed in Kato et al., 2005; Yoneyama and Fujita, 2007; Yoneyama et al., 2004). RIG-I and MDA-5 proteins comprise an amino-terminal caspase recruitment domain (CARD) and an RNA helicase domain (Kang et al., 2002). Results of a recent study on the evolution of RIG-I and MDA-5 indicate that the unique protein domain arrangement evolved independently by domain grafting and not by a simple gene duplication event of the entire four-domain arrangement, which may have been initiated by differential sensitivity of these proteins to viral infection (Sarkar et al., 2008). Additionally, MDA-5, but not RIG-I, orthologs are found in fish

indicating that MDA-5 might have evolved before RIG-I (Sarkar et al., 2008). After binding viral RNA, these sensors interact with a CARD-containing adaptor protein, IPS-1, located in the outer membrane of mitochondria (Kawai et al., 2005; Meylan et al., 2005; Seth et al., 2005; Xu et al., 2005). This interaction mediates recruitment and activation of protein kinases that phosphorylate the transcription protein IFN-regulatory factor 3, leading to synthesis of type I IFN.

An important question is how RIG-I and MDA-5 distinguish viral from cellular RNAs. It was originally believed that these proteins recognize dsRNA, which is rarely found in the cytoplasm of cells but is abundant in virus-infected cells (Yoneyama et al., 2004). More recently it has become clear that RIG-I recognizes RNA with a 5'-triphosphate (Hornung et al., 2006; Pichlmair et al., 2006). Because most cellular cytoplasmic RNAs bear a 5'-cap structure, this observation seems to explain the ability of RIG-I to discriminate between host and viral RNA. This substrate specificity is supported by observations that suggest that RIG-I and MDA-5 specialize in recognition of different viruses. Infection of mice lacking the gene encoding either protein reveals that RIG-I is essential for detecting infection by rhabdoviruses, influenza viruses, paramyxoviruses, and flaviviruses (Kato et al., 2006). Replication of these viruses leads to production of RNAs with a 5'-triphosphate. In contrast, MDA-5 senses infection with picornaviruses, whose RNA 5'-ends are linked to a viral protein, VPg, not a 5'-triphosphate (Gitlin et al., 2006; Kato et al., 2006). It has been suggested that dsRNAs produced during picornavirus replication are the substrates for MDA-5 recognition.

* Corresponding author. Fax: +1 212 305 5106.

E-mail address: vrr1@columbia.edu (V.R. Racaniello).

Despite these elegant innate mechanisms, virus infections still occur because their genomes encode proteins that antagonize this and every other step of host defense. Examples include inhibition of RIG-I function by binding of the influenza virus NS1 protein (Guo et al., 2007; Mibayashi et al., 2007; Opitz et al., 2007), and cleavage of IPS-1 by proteases encoded in the genomes of picornaviruses and hepatitis C virus (Li et al., 2005, 2006) (J. Drahos and V. Racaniello, unpublished data). We previously showed that MDA-5 is degraded in cells infected with different picornaviruses, and suggested that such cleavage might be a mechanism to antagonize production of type I IFN in response to viral infection (Barral et al., 2007). Here we examine the state of RIG-I during picornavirus infection. We found that RIG-I is degraded in cells infected with poliovirus, rhinoviruses, echovirus, and encephalomyocarditis virus. In contrast to MDA-5, cleavage of RIG-I is not accomplished by cellular caspases or the proteasome (Barral et al., 2007). Rather, the viral proteinase 3C^{pro} cleaves RIG-I, both in vitro and in cells. Cleavage of RIG-I during picornavirus infection may constitute another mechanism for attenuating the innate response to viral infection.

Results

Cleavage of RIG-I in cells infected with picornaviruses

Consistent with the suggestion that picornavirus infections are detected by MDA-5 (Kato et al., 2006) is the observation that this protein is degraded during infection with poliovirus, rhinovirus type 1a, and EMCV (Barral et al., 2007). It was therefore of interest to determine the state of RIG-I during picornavirus infection. HeLa cells were infected with poliovirus, and at different times after infection, RIG-I protein was examined by western blot analysis. Beginning at 4 h post-infection, levels of RIG-I protein declined, and a protein of ~70 kDa appeared which might be a cleavage product (Fig. 1A). Cleavage of RIG-I protein was also observed during poliovirus infection of the neuroblastoma cell line SH-SY-5Y (Fig. 1B).

Cleavage of RIG-I was also observed in cells infected with other picornaviruses. In cells infected with echovirus type 1 (Fig. 1C) or

EMCV (Fig. 1F), an ~70 kDa putative cleavage product was first detected at 6 h post-infection. When cells were infected with rhinovirus type 16 at 33 °C, a temperature at which viral replication is more efficient, only the ~70 kDa protein was observed at 14 h post-infection and later (Fig. 1D). Slight cleavage of RIG-I was detected in cells infected with rhinovirus type 1A at 37 °C (Fig. 1E).

Effect of proteasome and caspase inhibitors on poliovirus-induced cleavage of RIG-I

Poliovirus-induced cleavage of MDA-5 is carried out by the proteasome and caspases (Barral et al., 2007). The effect of inhibitors of the proteasome (MG132) and caspases (Z-VAD) on RIG-I cleavage was therefore determined. HeLa cells were infected with poliovirus, and culture medium was added with or without inhibitor. The level of RIG-I at different times after infection was determined by western blot analysis. In the absence of inhibitor, cleavage of RIG-I was observed beginning at 4 h post-infection and was complete by 8 h (Fig. 2A). In the presence of Z-VAD or MG132, degradation of RIG-I was first observed at 6 h post-infection, and was complete by 8 h post-infection (Figs. 2B, C). In contrast, poliovirus-induced degradation of MDA-5 is completely inhibited by MG132 and Z-VAD, even though neither drug impairs viral yields (Barral et al., 2007). These results indicate that, in contrast to poliovirus-induced degradation of MDA-5, cleavage of RIG-I during poliovirus infection occurs by a process that is independent of caspases and the cellular proteasome.

Effect of amino acid changes in poliovirus proteinases on cleavage of RIG-I

The two polioviral proteinases, 2A^{pro} and 3C^{pro}, not only process the viral polyprotein to produce the functional viral proteins, but also degrade cellular proteins such as eIF4G (Krausslich et al., 1987) and cellular transcription proteins (Weidman et al., 2003). Polioviruses with single amino acid changes in either 2A^{pro} or 3C^{pro} have been isolated which prevent cleavage of cellular proteins. These viral mutants were used to determine whether either viral proteinase plays a role in poliovirus-induced cleavage of RIG-I. Poliovirus mutant

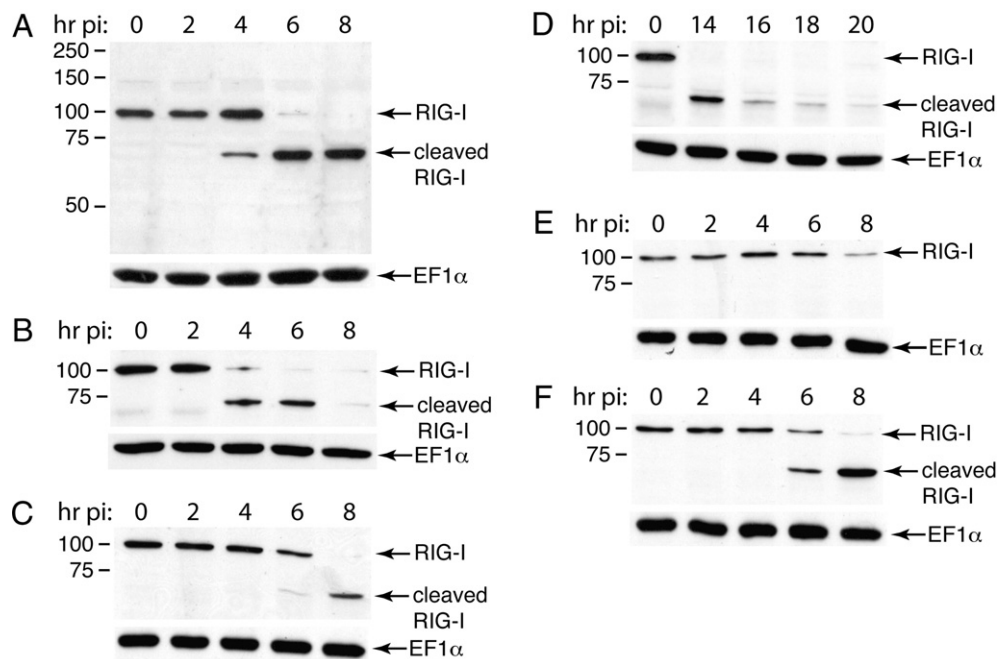


Fig. 1. Degradation of RIG-I during picornavirus infection. Monolayers of HeLa cells (A, C–F) or SH-SY-5Y cells (B) were infected (MOI 10) with poliovirus (A, B), echovirus (C), rhinovirus type 16 (D), rhinovirus type 1A (E) or EMCV (F). At the indicated times after infection, cell extracts were prepared, fractionated by SDS-PAGE, and RIG-I was detected by western blot analysis. Positions of RIG-I and a putative cleavage product are indicated. Separate bottom panels show detection of EF1α to ensure that equal amounts of protein were applied to each lane.

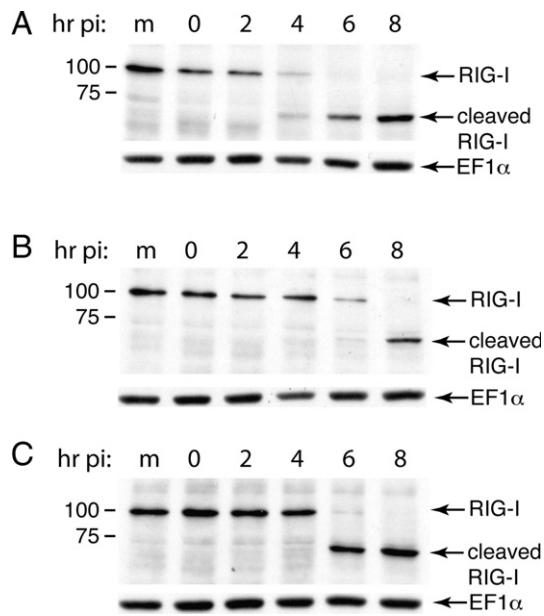


Fig. 2. Effect of protease inhibitors on poliovirus-induced cleavage of RIG-I. Monolayers of HeLa cells were infected with poliovirus (MOI 10) in the absence (A) or presence of Z-VAD-FMK (100 μM) (B) or MG132 (20 μM) (C). At the indicated times after infection, cell extracts were prepared, fractionated by SDS-PAGE, and RIG-I was detected by western blot analysis. Positions of RIG-I and a putative cleavage product are indicated. Separate bottom panels show detection of EF1α to ensure that equal amounts of protein were applied to each lane.

2A^{pro} Y88L contains a single amino acid change in 2A^{pro} that abolishes cleavage of eIF4G, but does not affect cleavage of the viral polyprotein (Yu et al., 1995). Poliovirus mutant Se1-3C-02 contains a single amino acid change in 3C^{pro} that has been reported to block cleavage of host cell transcription proteins, but not processing of the viral polyprotein (Clark et al., 1991; Dewalt and Semler, 1987). RIG-I cleavage was observed starting at 6 h post-infection in cells infected with either 2A^{pro} Y88L or Se1-3C-02 (Figs. 3B, C). The delay in cleavage is likely a consequence of the slower replication kinetics of these viruses (unpublished data).

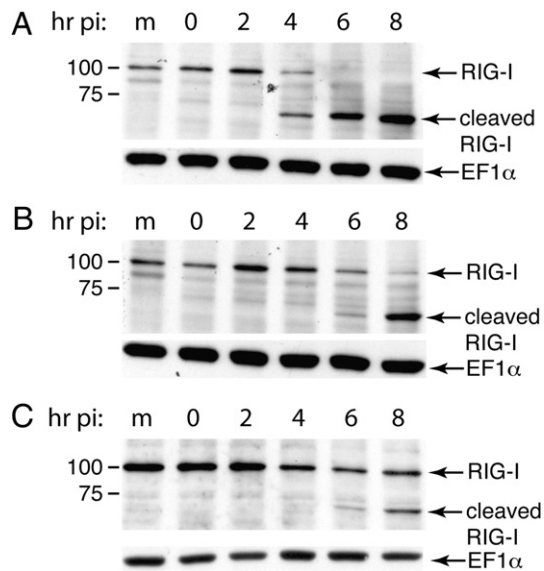


Fig. 3. Effect of amino acid changes in polioviral proteinases 2A^{pro} and 3C^{pro} on cleavage of RIG-I. Monolayers of HeLa cells were infected with wild-type poliovirus (A), mutant 2A^{pro}Y88L (B) or mutant Se1-3C-02 (C) (MOI 10). At the indicated times after infection, cell extracts were prepared, fractionated by SDS-PAGE, and RIG-I was detected by western blot analysis. Positions of RIG-I and a putative cleavage product are indicated. Separate bottom panels show detection of EF1α to ensure that equal amounts of protein were applied to each lane.

Cleavage of RIG-I by 3C^{pro} in a cell extract

To further explore the identity of the viral proteinase that cleaves RIG-I, we determined whether RIG-I could be directly cleaved in vitro by either viral proteinase. Purified Poliovirus 3CD^{pro} or coxsackievirus B3 2A^{pro} was added to a cytoplasmic extract produced from HeLa cells, and after incubation, RIG-I protein was detected by western blot analysis. Coxsackievirus B3 2A^{pro} was used in these experiments because it has not been possible to purify Poliovirus 2A^{pro}. Poliovirus 3CD^{pro} is the precursor to 3C^{pro} and is believed to carry out the majority of protein processing during infection. Degradation of RIG-I and production of the putative ~70 kDa cleavage product was observed after incubation with 3CD^{pro}, but not with 2A^{pro} (Fig. 4A) or incubation without enzyme (unpublished data). Proteinase activity of 2A^{pro} was confirmed by demonstrating cleavage of the known substrates PABP (Fig. 4B) and eIF4G1 (Fig. 4C). Although PABP is known to be cleaved by 3CD^{pro}, for unknown reasons the protein remained intact in this assay (Fig. 5B).

Cleavage of RIG-I by 3C^{pro} in cultured cells

To determine whether either poliovirus proteinase cleaves RIG-I in cells, plasmids encoding these proteins linked to a FLAG epitope were introduced into 293A cells by DNA-mediated transformation. Twenty-four hours later, cell extracts were prepared and RIG-I was detected by western blot analysis. Cleavage of RIG-I and production of the ~70 kDa protein was observed in cells transformed with plasmids encoding 3C^{pro}, but not 2A^{pro} (Fig. 5). Synthesis of both proteinases in 293A cells was verified by western blot analysis using anti-FLAG antibody. Furthermore, activity of 2A^{pro} was confirmed by observation of cleavage of its known substrate, eIF4G1. We conclude that 3C^{pro} is the poliovirus proteinase responsible for cleavage of RIG-I during infection.

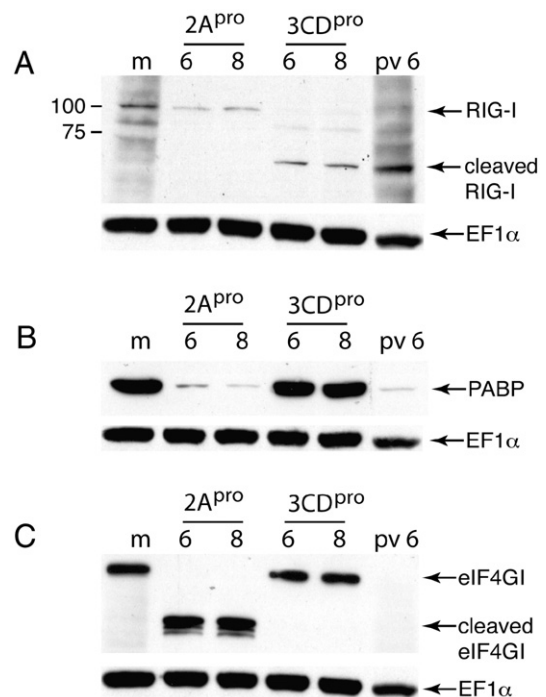


Fig. 4. Effect of 2A^{pro} and 3CD^{pro} on RIG-I in vitro. A cytoplasmic extract from HeLa cells was incubated with purified 2A^{pro} or 3CD^{pro} for 6 or 8 h, fractionated by SDS-PAGE, and RIG-I was detected by western blot analysis. Cytoplasmic extracts from mock-infected HeLa cells (m) and from cells 6 h after poliovirus infection (pv 6) were included to show the location of uncleaved and cleaved RIG-I, respectively. eIF4G1 and PABP (to confirm enzyme activity of 2A^{pro} and 3CD^{pro}) and EF1α (loading control) were detected by western blot analysis.

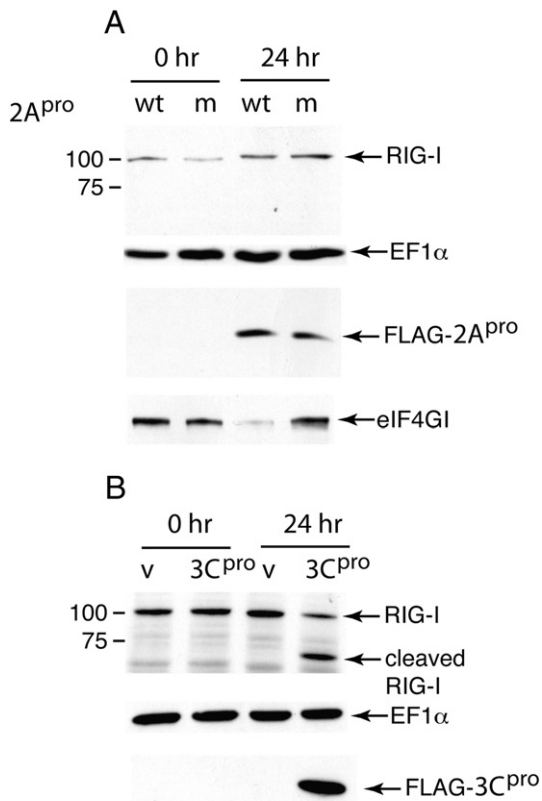


Fig. 5. Effect of 2A^{pro} and 3C^{pro} on RIG-I in vivo. Plasmids encoding poliovirus 2A^{pro} or 3C^{pro} (each with an N-terminal FLAG epitope) or vector alone (v) were introduced into HeLa cells by transformation. At 0 and 24 after DNA-mediated transformation, cell extracts were prepared, fractionated by SDS-PAGE, and RIG-I was detected by western blot analysis. Production of each viral proteinase was confirmed by western analysis using anti-FLAG antibody. eIF4GI (to confirm enzyme activity of 2A^{pro}) and EF1α (loading control) were detected by western blot analysis.

Discussion

Cleavage of RIG-I was observed in cells infected with all picornaviruses examined, including poliovirus, rhinovirus types 1a and 16, echovirus type 1, and encephalomyocarditis virus. We previously showed that another cytoplasmic RNA sensor, MDA-5, is degraded during picornavirus infection in a proteasome- and caspase-dependent manner (Barral et al., 2007). However, inhibitors of these cellular proteases had no effect on poliovirus-induced cleavage of RIG-I. The results of in vitro cleavage assays, and expression of DNAs encoding viral proteinases in cultured cells, showed that RIG-I is cleaved by poliovirus 3C^{pro}. The 3C^{pro} proteinase of the other picornaviruses examined is also likely to cleave RIG-I. The second enterovirus proteinase, 2A^{pro}, is not encoded by the genome of encephalomyocarditis virus and therefore could not explain the cleavage of RIG-I observed in these experiments.

Although the kinetics of cleavage induced by different picornaviruses varied, an ~70 kDa putative cleavage product was always observed. This cleavage product represents the carboxy-terminal portion of RIG-I, because the antibody used to detect it by western blot analysis is directed against a peptide from the last 17 amino acids of the protein. It was therefore possible to predict 3C^{pro} cleavage sites in RIG-I that would yield the ~70 kDa cleavage product. We introduced amino acid changes at 12 of these cleavage sites, but none altered processing of RIG-I during poliovirus infection (unpublished data). Therefore either the correct 3C^{pro} cleavage site has not yet been identified, or the amino acid changes made were not sufficient to block cleavage.

It is believed that MDA-5, not RIG-I, is crucial for sensing infections with picornaviruses. Mice lacking the gene encoding MDA-5 are more susceptible to infection with encephalomyocarditis virus, and produce less IFN after infection compared with wild-type littermates (Gitlin et al., 2006; Kato et al., 2006). Mice lacking the gene encoding RIG-I were no more susceptible to infection with encephalomyocarditis virus and showed no difference in IFN production (Kato et al., 2006). The cleavage of MDA-5 during picornavirus infection is consistent with a role for this protein in detecting infection with members of this virus family (Barral et al., 2007). It is not clear why RIG-I would be cleaved during picornavirus infection if this sensor plays no role in innate responses against these viruses. RIG-I is known to be activated by short (~1 kb) stretches of dsRNA (Hornung et al., 2006; Pichlmair et al., 2006) that are certainly found in picornavirus infected cells. A U-rich sequence in the genome of hepatitis C virus has been shown to activate RIG-I (Saito et al., 2008). Similar sequences are present in the genomes of picornaviruses and might serve as substrates for RIG-I. Perhaps the results obtained by infecting *rig-I*^{-/-} mice with encephalomyocarditis virus are not representative of all picornaviruses. Understanding the role of RIG-I cleavage during enterovirus infection will require synthesis in cell cultures and in mice of non-cleavable forms of the protein.

IPS-1 is also cleaved during infection with poliovirus and rhinovirus (J. Drahas and V. Racaniello, unpublished data) as well as hepatitis A virus (Yang et al., 2007). Therefore, infection with certain picornaviruses leads to cleavage of not only both cytoplasmic RNA sensors, but also the mitochondrial membrane protein that is crucial in transmitting the signal from RIG-I and MDA-5 that leads to induction of IFN transcription. It seems unlikely that the cleavage of three members of this sensing pathway is coincidental. It is possible that these cleavages target unknown functions of RIG-I, MDA-5, and IPS-1 unrelated to sensing RNA. Further experiments are clearly required to understand why these components of the innate RNA sensing pathway are cleaved during picornavirus infection.

Materials and methods

Cells and viruses

S3 HeLa and SH-SY5Y cells were grown in Dulbecco's modified Eagle medium (Invitrogen, Carlsbad, California USA), 10% bovine calf serum (Hyclone, Logan, Utah USA), and 1% penicillin/streptomycin (Invitrogen). For plaque assays HeLa cells were grown in Dulbecco's modified Eagle medium (Specialty Media, Phillipsburg, New Jersey, USA), 0.2% NaHCO₃, 5% bovine calf serum, 1% penicillin/streptomycin, and 0.9% bacto-agar (Difco, Franklin Lakes, New Jersey, USA).

Stocks of poliovirus strain P1/Mahoney, rhinovirus type 16, and encephalomyocarditis virus (EMCV) were produced by transfecting HeLa cells with RNA transcripts derived by in vitro transcription of plasmids harboring complete DNA copies of the viral genomes (Duke and Palmenberg, 1989; Lee et al., 1995; Racaniello and Baltimore, 1981a). Stocks of echovirus type 1 and rhinovirus type 1a were obtained from the American Type Culture Collection, Manassas, VA, and were propagated in HeLa cells. poliovirus mutant Se1-3C-02, which contains the single amino acid change V54A in 3C^{pro} (Dewalt and Semler, 1987), was obtained from B. Semler, University of California, Irvine. A poliovirus mutant with a single amino acid change, Y88L (Yu et al., 1995), in 2A^{pro} was constructed by site-directed mutagenesis of a full length DNA copy of the genome of poliovirus strain P1/Mahoney.

In vitro cleavage reaction

A cytoplasmic extract was prepared from HeLa cells as described (Todd, Towner, and Semler, 1997). Briefly, 1 × 10⁸ HeLa cells were centrifuged, washed with phosphate-buffered saline, resuspended in

hypotonic buffer (20 mM Hepes KOH pH 7.4, 10 mM KCl, 1.5 mM MgOAc, 1 mM dithiothreitol), and lysed with a Dounce homogenizer. The extract was then centrifuged at 10,000 ×g and the supernatant was stored. For proteinase cleavage, 25 µl of cytoplasmic extract was incubated for 6 h with 0.5 µg purified 2A^{pro} or 3CD^{pro} (gift of Bert Semler, University of California, Irvine) in a 100 µl reaction containing 50 mM NaCl, 5 mM MgCl₂. Cleavage of RIG-I was assessed by western blot analysis as described below.

Synthesis of 2A^{pro} and 3C^{pro} in cells

Primers were designed to place a FLAG epitope at the amino terminus of 2A^{pro} and 3C^{pro}, using a DNA copy of the genome of poliovirus type 1 Mahoney as the template (Racaniello and Baltimore, 1981b). DNAs encoding the proteinases were cloned in the vector pcDNA3 (Invitrogen). DNA-mediated transformation of 293A cells was done using Lipofectamine reagent (Invitrogen) according to the manufacturer's protocol. Cell extracts were prepared 24 h later as described below for western blot analysis.

Reagents

Rabbit antibody against a peptide comprising amino acids 909–925 of RIG-I was purchased from Abgent, Inc., San Diego, CA. Mouse monoclonal anti-EF1α was purchased from Upstate USA Inc., Chicago, IL. Mouse monoclonal anti-PABP was purchased from Abcam, Cambridge, MA. The proteasome inhibitor MG132 was purchased from Calbiochem, San Diego, CA. The general caspase inhibitor benzyloxycarbonyl-Val-Ala-Asp-(OMe) fluoromethylketone (Z-VAD-FMK) was purchased from R&D Systems, Minneapolis, MN. Purified poliovirus proteinase 3C^{pro} and purified coxsackievirus B3 2A^{pro} were gifts of Richard Lloyd, Baylor College of Medicine (Joachims et al., 1999).

Western blot analysis

Cells were harvested into the culture medium with a plastic scraper, collected by centrifugation, washed with phosphate-buffered saline (PBS, 136.9 mM NaCl, 2.68 mM KCl, 8.1 mM Na₂HPO₄, 1.47 mM KH₂PO₄), and lysed in radio-immunoprecipitation buffer (RIPA, PBS containing 1% NP40, 0.5% sodium deoxycholate, and 0.1% sodium dodecyl sulfate). Aliquots containing 50 µg total protein were fractionated by 10% SDS-PAGE. Proteins were transferred electrophoretically to a nitrocellulose membrane, which was then incubated with antibody in PBS containing 5% nonfat milk for 2 h at room temperature. The membrane was washed in PBS containing 0.1% Tween, followed by addition of the appropriate secondary antibody. Proteins were visualized using the ECL chemiluminescence system (Amersham BioSciences, Piscataway, NJ).

Acknowledgments

This study was supported in part by Public Health Service Grants AI50754 and T32AI07161 from the National Institute of Allergy and Infectious Diseases, and by NIGMS grant GM068448. DS is the Harrison Endowed Scholar in Cancer Research at the Massey Cancer Center. PBF holds the Thelma Newmeyer Corman Chair in Cancer Research at the Massey Cancer Center and is a Samuel Waxman Cancer Research Foundation (SWCRF) Investigator. We thank Richard Lloyd and Bert Semler for gifts of 2A^{pro} and 3CD^{pro} viral proteinases, respectively, and Bert Semler for the gift of poliovirus mutant Se1-3C-02.

References

Barral, P.M., Morrison, J.M., Drahos, J., Gupta, P., Sarkar, D., Fisher, P.B., Racaniello, V.R., 2007. MDA-5 is cleaved in poliovirus-infected cells. *J. Virol.* 81 (8), 3677–3684.

Clark, M.E., Hämmerle, T., Wimmer, E., Dasgupta, A., 1991. Poliovirus proteinase 3C converts an active form of transcription factor IIC to an inactive form: a mechanism for inhibition of host cell polymerase III transcription by poliovirus. *EMBO J.* 10, 2941–2947.

Dewalt, P.G., Semler, B.L., 1987. Site-directed mutagenesis of proteinase 3C results in a poliovirus deficient in synthesis of viral RNA polymerase. *J. Virol.* 61, 2162–2170.

Duke, G.M., Palmenberg, A.C., 1989. Cloning and synthesis of infectious *Cardiovirus* RNAs containing short, discrete poly(C) tracts. *J. Virol.* 63, 1822–1826.

Gitlin, L., Barchet, W., Gilfillan, S., Cella, M., Beutler, B., Flavell, R.A., Diamond, M.S., Colonna, M., 2006. Essential role of mda-5 in type I IFN responses to polyriboinosinic:polyribocytidylic acid and encephalomyocarditis picornavirus. *Proc. Natl. Acad. Sci. U. S. A.* 103 (22), 8459–8464.

Guo, Z., Chen, L.M., Zeng, H., Gomez, J.A., Plowden, J., Fujita, T., Katz, J.M., Donis, R.O., Sambhara, S., 2007. NS1 protein of *Influenza A virus* inhibits the function of intracytoplasmic pathogen sensor, RIG-I. *Am. J. Respir. Cell Mol. Biol.* 36 (3), 263–269.

Hornung, V., Ellegast, J., Kim, S., Brzozka, K., Jung, A., Kato, H., Poeck, H., Akira, S., Conzelmann, K.K., Schlee, M., Endres, S., Hartmann, G., 2006. 5'-Triphosphate RNA is the ligand for RIG-I. *Science* 314 (5801), 994–997.

Janeway Jr., C.A., Medzhitov, R., 2002. Innate immune recognition. *Annu. Rev. Immunol.* 20, 197–216.

Joachims, M., Van Breugel, P.C., Lloyd, R.E., 1999. Cleavage of poly(A)-binding protein by *Enterovirus* proteases concurrent with inhibition of translation in vitro. *J. Virol.* 73 (1), 718–727.

Kang, D.C., Gopalkrishnan, R.V., Wu, Q., Jankowsky, E., Pyle, A.M., Fisher, P.B., 2002. mda-5: an interferon-inducible putative RNA helicase with double-stranded RNA-dependent ATPase activity and melanoma growth-suppressive properties. *Proc. Natl. Acad. Sci. U. S. A.* 99 (2), 637–642.

Kato, H., Sato, S., Yoneyama, M., Yamamoto, M., Uematsu, S., Matsui, K., Tsujimura, T., Takeda, K., Fujita, T., Takeuchi, O., Akira, S., 2005. Cell type-specific involvement of RIG-I in antiviral response. *Immunity* 23 (1), 19–28.

Kato, H., Takeuchi, O., Sato, S., Yoneyama, M., Yamamoto, M., Matsui, K., Uematsu, S., Jung, A., Kawai, T., Ishii, K.J., Yamaguchi, O., Otsu, K., Tsujimura, T., Koh, C.S., Reis e Sousa, C., Matsuura, Y., Fujita, T., Akira, S., 2006. Differential roles of MDA5 and RIG-I helicases in the recognition of RNA viruses. *Nature* 441 (7089), 101–105.

Kawai, T., Takahashi, K., Sato, S., Coban, C., Kumar, H., Kato, H., Ishii, K.J., Takeuchi, O., Akira, S., 2005. IPS-1, an adaptor triggering RIG-I- and Mda5-mediated type I interferon induction. *Nat. Immunol.* 6 (10), 981–988.

Krausslich, H.G., Nicklin, M.J.H., Toyoda, H., Etchison, D., Wimmer, E., 1987. Poliovirus proteinase 2A induces cleavage of eukaryotic initiation factor 4F polypeptide p220. *J. Virol.* 61, 2711–2718.

Lee, W.M., Wang, W., Rueckert, R.R., 1995. Complete sequence of the RNA genome of human rhinovirus 16, a clinically useful common cold virus belonging to the ICAM-1 receptor group. *Virus Genes* 9 (2), 177–181.

Li, X.D., Sun, L., Seth, R.B., Pineda, G., Chen, Z.J., 2005. Hepatitis C virus protease NS3/4A cleaves mitochondrial antiviral signaling protein off the mitochondria to evade innate immunity. *Proc. Natl. Acad. Sci. U. S. A.* 102 (49), 17717–17722.

Lin, R., Lacoste, J., Nakhaei, P., Sun, Q., Yang, L., Paz, S., Wilkinson, P., Julkunen, I., Vitour, D., Meurs, E., Hiscott, J., 2006. Dissociation of a MAVS/IPS-1/VISA/Cardif-1Kepsilon molecular complex from the mitochondrial outer membrane by hepatitis C virus NS3-4A proteolytic cleavage. *J. Virol.* 80 (12), 6072–6083.

Meylan, E., Curran, J., Hofmann, K., Moradpour, D., Binder, M., Bartenschlager, R., Tschopp, J., 2005. Cardif is an adaptor protein in the RIG-I antiviral pathway and is targeted by hepatitis C virus. *Nature* 437 (7062), 1167–1172.

Mibayashi, M., Martinez-Sobrido, L., Loo, Y.M., Cardenas, W.B., Gale Jr., M., Garcia-Sastre, A., 2007. Inhibition of retinoic acid-inducible gene I-mediated induction of beta interferon by the NS1 protein of *Influenza A virus*. *J. Virol.* 81 (2), 514–524.

Opitz, B., Rejaibi, A., Dauber, B., Eckhard, J., Vinzing, M., Schmeck, B., Hippenstiel, S., Suttrop, N., Wolff, T., 2007. IFNbeta induction by *Influenza A virus* is mediated by RIG-I which is regulated by the viral NS1 protein. *Cell. Microbiol.* 9 (4), 930–938.

Pichlmair, A., Schulz, O., Tan, C.P., Naslund, T.I., Liljestrom, P., Weber, F., Reis e Sousa, C., 2006. RIG-I-mediated antiviral responses to single-stranded RNA bearing 5'-phosphates. *Science* 314 (5801), 997–1001.

Racaniello, V.R., Baltimore, D., 1981a. Cloned poliovirus complementary DNA is infectious in mammalian cells. *Science* 214, 916–919.

Racaniello, V.R., Baltimore, D., 1981b. Molecular cloning of poliovirus cDNA and determination of the complete nucleotide sequence of the viral genome. *Proc. Natl. Acad. Sci. U. S. A.* 78, 4887–4891.

Saito, T., Owen, D.M., Jiang, F., Marcotrigiano, J., Gale Jr., M., 2008. Innate immunity induced by composition-dependent RIG-I recognition of hepatitis C virus RNA. *Nature* 454 (7203), 523–527.

Sarkar, D., Boukerche, H., Su, Z.Z., Fisher, P.B., 2008. mda-9/Syntenin: more than just a simple adapter protein when it comes to cancer metastasis. *Cancer Res.* 68 (9), 3087–3093.

Seth, R.B., Sun, L., Ea, C.K., Chen, Z.J., 2005. Identification and characterization of MAVS, a mitochondrial antiviral signaling protein that activates NF-kappaB and IRF 3. *Cell* 122 (5), 669–682.

Todd, S., Towner, J.S., Semler, B.L., 1997. Translation and replication properties of the human rhinovirus genome in vivo and in vitro. *Virology* 229 (1), 90–97.

Weidman, M.K., Sharma, R., Raychaudhuri, S., Kundu, P., Tsai, W., Dasgupta, A., 2003. The interaction of cytoplasmic RNA viruses with the nucleus. *Virus Res.* 95 (1–2), 75–85.

Xu, L.G., Wang, Y.Y., Han, K.J., Li, L.Y., Zhai, Z., Shu, H.B., 2005. VISA is an adapter protein required for virus-triggered IFN-beta signaling. *Mol. Cell* 19 (6), 727–740.

- Yang, Y., Liang, Y., Qu, L., Chen, Z., Yi, M., Li, K., Lemon, S.M., 2007. Disruption of innate immunity due to mitochondrial targeting of a picornaviral protease precursor. *Proc. Natl. Acad. Sci. U. S. A.* 104 (17), 7253–7258.
- Yoneyama, M., Fujita, T., 2007. RIG-I family RNA helicases: cytoplasmic sensor for antiviral innate immunity. *Cytokine Growth Factor Rev.* 18 (5–6), 545–551.
- Yoneyama, M., Kikuchi, M., Natsukawa, T., Shinobu, N., Imaizumi, T., Miyagishi, M., Taira, K., Akira, S., Fujita, T., 2004. The RNA helicase RIG-I has an essential function in double-stranded RNA-induced innate antiviral responses. *Nat. Immunol.* 5 (7), 730–737.
- Yu, S.F., Benton, P., Bovee, M., Sessions, J., Lloyd, R.E., 1995. Defective RNA replication by poliovirus mutants deficient in 2A protease cleavage activity. *J. Virol.* 69 (1), 247–252.



Contents lists available at ScienceDirect

Virology

journal homepage: www.elsevier.com/locate/yviro

The viral RNA recognition sensor RIG-I is degraded during encephalomyocarditis virus (EMCV) infection

Laura Papon^{a,b,c}, Alexandra Oteiza^{a,b,c}, Tadaatsu Imaizumi^d, Hiroki Kato^e, Emiliana Brocchi^f, T. Glen Lawson^g, Shizuo Akira^e, Nadir Mechti^{a,b,c,*}

^a Université Montpellier 1, Centre d'études d'agents Pathogènes et Biotechnologies pour la Santé (CPBS)

^b CNRS, UMR 5236, CPBS, 4 Bd Henri IV, CS 69033, F-34965 Montpellier, France

^c Université Montpellier 2, CPBS, F-34095 Montpellier, France

^d Department of Vascular Biology, Hirosaki University Graduate School of Medicine, Hirosaki, 035-8562, Japan

^e Research Institute for Microbial Diseases, Osaka University, Osaka, Japan

^f Istituto zooprofilattico sperimentale della lombardia e dell'emilia, Via A. Bianchi, 7-25124 Brescia, Italy

^g Department of Chemistry, Bates College, Lewiston, ME 04240, USA

ARTICLE INFO

Article history:

Received 24 June 2009

Returned to author for revision 10 July 2009

Accepted 4 August 2009

Available online xxx

Keywords:

RIG-I

Encephalomyocarditis virus

3C protease

Viral subversion

ABSTRACT

RNA helicase-like receptors MDA-5 but not RIG-I has been shown to be essential for triggering innate immune responses against picornaviruses. However, virus–host co-evolution has selected for viruses capable of replicating despite host cells antiviral defences. In this report, we demonstrate that RIG-I is degraded during encephalomyocarditis virus (EMCV) infection. This effect is mediated by both the viral-encoded 3C protease and caspase proteinase. In addition, we show that RIG-I overexpression confers IFN- β promoter activation during EMCV infection, in MDA-5 knockout (MDA-5^{-/-}) mouse embryo fibroblasts. This induction is followed by a strong inhibition reflecting the ability of EMCV to disrupt RIG-I signalling. Taken together, our data strongly suggest that during evolution RIG-I has been involved for triggering innate immune response to picornavirus infections.

© 2009 Elsevier Inc. All rights reserved.

Introduction

Viral infections lead to the activation of the innate immune signalling pathway critical for an effective antiviral immune response (Iwasaki and Medzhitov, 2004; Krishnan et al., 2007; Loo et al., 2008; Loo and Gale, 2007; Medzhitov, 2007; Noppert et al., 2007). The cytoplasmic DEx(D/H) box RNA helicase-like receptors RIG-I (retinoic-acid-inducible protein I, also known as Ddx58) and MDA-5 (melanoma-differentiation-associated gene 5) act as sensors in coupling recognition of RNA virus infections to the type I interferon (IFN) gene induction (Andrejeva et al., 2004; Takeuchi and Akira, 2007; Yoneyama and Fujita, 2007; Yoneyama et al., 2005). Experiments with RIG-I-null mice have revealed that this molecule is required for the recognition of a subset of ssRNA viruses, including flaviviruses, paramyxoviruses, orthomyxoviruses and rhabdoviruses (Kato et al., 2005, 2006). MDA-5-null mice have been used to show that MDA-5 is critical for the recognition of picornavirus infections (Gitlin et al., 2006; Kato et al., 2006). However, these studies did not address the ability of viruses to circumvent the innate antiviral defences. Indeed, the disruption of retinoic acid-inducible gene I (RIG-I) signalling by

the viral NS3/4A protease and HCV non-structural proteins NS4B provides evidences to the ability of viruses to control innate antiviral defences (Breiman et al., 2005; Foy et al., 2005; Tasaka et al., 2007).

Several reports point to the involvement of the picornavirus-encoded 3C protease (3C^{PRO}) in circumventing fundamental cellular processes and inhibiting effector proteins, playing a key role in innate antiviral mechanisms (Chen and Gerlier, 2006; Ehrenfeld, 1982; Yalamanchili et al., 1996, 1997a, 1997b). For example, poliovirus 3C^{PRO} has been shown to cleave several transcription factors including, TBP (Yalamanchili et al., 1996), Oct-1 (Yalamanchili et al., 1997b), CREB (Yalamanchili et al., 1997a) and TFIIC (Shen et al., 1996), signifying the involvement of this viral protein in the inhibition of host transcription machinery. The cleavage of poly(A)-binding protein (PABP) by 3C^{PRO} causes severe translation inhibition of endogenous mRNAs in poliovirus-infected cells (Ehrenfeld, 1982; Kuyumcu-Martinez et al., 2004). In addition, 3C^{PRO} can promote virus dissemination by altering host sensing pathways critical for an effective innate antiviral immune response (Barral et al., 2007; Neznanov et al., 2005). Indeed, in the later stage of both poliovirus and rhinovirus infection, inactivation of NF- κ B function by proteolytic cleavage of p65-RelA was proposed as a common mechanism by which picornaviruses suppress the innate immune response (Neznanov et al., 2005). In hepatitis A virus-infected cells,

* Corresponding author. CNRS UMR 5236 - UM1-UM2, 15, Avenue Charles Flahault BP 14 491, 34 093 MONTPELLIER Cedex 5, France. Fax: +33 4 67 66 81 87.

E-mail address: nadir.mechti@univ-montp1.fr (N. Mechti).

the mitochondrial signalling protein IPS-1 involved in the MDA5 pathway that induces protective IFN responses, is cleaved by the 3C^{PRO} activity of the 3ABC precursor viral protein, resulting in the disruption of the MDA5-mediated innate immunity (Yang et al., 2007). Recently, the caspase-dependent cleavage of MDA5 was reported in response to some picornavirus infections (Barral et al., 2007). These data prompted us to analyze the ability of encephalomyocarditis virus (EMCV), the prototype of the cardiomyovirus subgroup of picornaviruses, to disrupt RIG-I-mediated antiviral immune response.

In this report, we demonstrate that RIG-I is degraded during EMCV infection. This effect is mediated, at least in part, by the viral-encoded 3C^{PRO} and caspase proteinase. In addition, we show that RIG-I overexpression confers EMCV-mediated induction of IFN- β promoter activity followed by a strong inhibition. As virus–host co-evolution has selected for viruses capable of replicating despite host cells antiviral defences, our data strongly suggest that RIG-I has been involved for triggering innate immune response to picornavirus infection.

Results

RIG-I expression is down-regulated during EMCV infection

It has been suggested that picornavirus infections are detected by MDA-5 and not RIG-I (Gitlin et al., 2006; Kato et al., 2006). However, the reported picornavirus-mediated degradation of the innate immune response effectors led us to evaluate whether virus-mediated degradation of RIG-I could explain why RIG-I fails to detect picornavirus infections. To this end, HeLa cells were infected with EMCV at a multiplicity of infection (MOI) of 10. Various times after infection, cell extracts were prepared and analyzed by Western blotting for the presence of RIG-I, using rabbit polyclonal anti-RIG-I

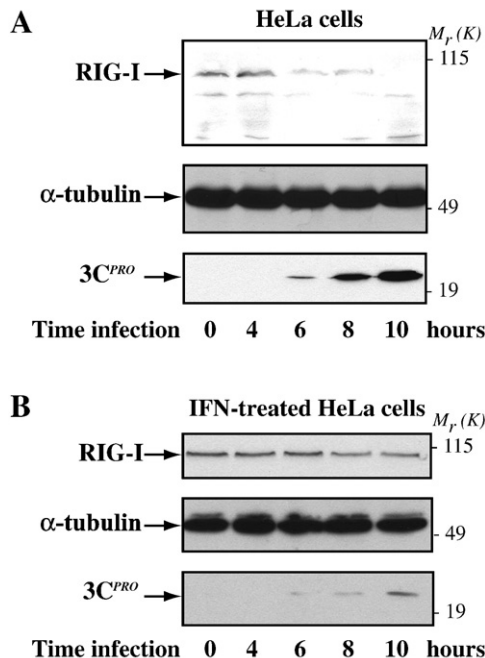


Fig. 1. RIG-I expression is down-regulated during EMCV infection. (A) HeLa cells were infected with EMCV at 10 MOI. Various times after infection, whole cell extracts were prepared and analyzed by Western blotting (WB) for the presence of endogenous RIG-I, using rabbit anti-RIG-I antibodies (Imaizumi et al., 2004b). EMCV protein expression was monitored by detection of EMCV 3C^{PRO} protein accumulations, using anti-3C^{PRO} antibodies (Lawson et al., 1994). Detection of α -tubulin was used to ensure that equal amounts of protein were loaded to each lane. (B) HeLa cells were treated with 1000 U/ml of IFN- α , prior EMCV infection. Then, the cells were analyzed for RIG-I expression, as described above.

antibodies (Imaizumi et al., 2004a). As shown Fig. 1A, the level of RIG-I expression was unchanged during the first 4 h of infection and decreased 6 h post-infection to remain barely detectable up to 10 h. Viral protein expression was monitored using antibodies directed against the viral protease 3C^{PRO} (Lawson et al., 1994). Interestingly, the decrease of RIG-I expression was concomitant with 3C^{PRO} accumulation suggesting that RIG-I down-regulation could result, at least, in part from 3C^{PRO} activity. To determine whether a functional EMCV viral life cycle is required for RIG-I down-regulation, HeLa cells were treated for 16 h with IFN- α before infection, conditions that are known to induce strong antiviral effects against EMCV (Hassel et al., 1993). As expected, in these experimental conditions the level of RIG-I protein is more elevated in IFN- α -treated cells (Imaizumi et al., 2004b), and EMCV protein expression was strongly reduced (Fig. 1B). Concomitantly, the inhibition of RIG-I expression appeared to be more

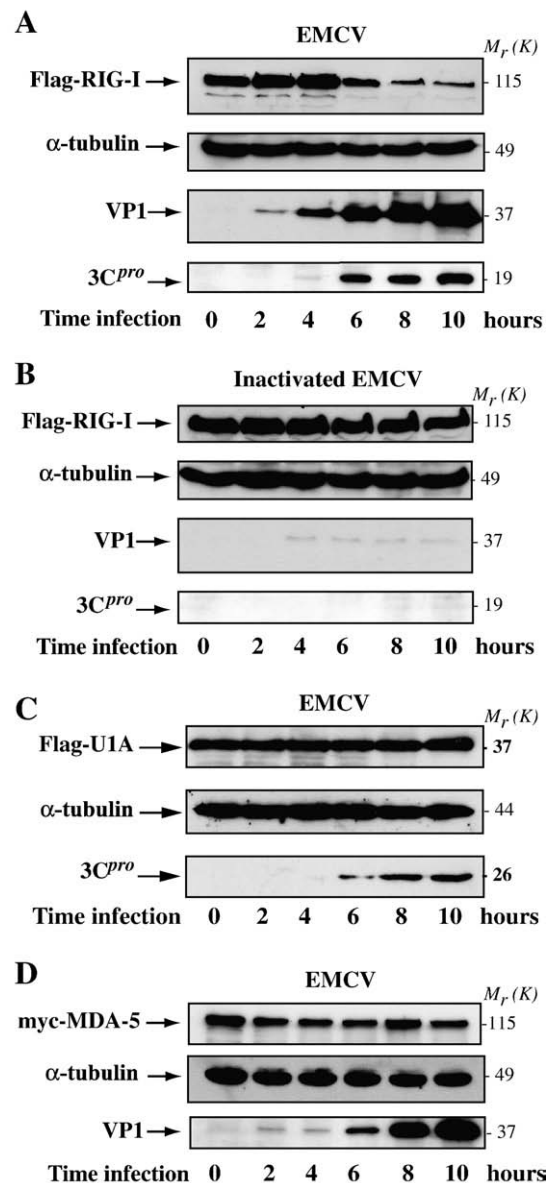


Fig. 2. Flag-RIG-I is degraded during EMCV infection. Flag-RIG-I (A and B), Flag-U1A (C) and myc-MDA-5 (D)-expressing HeLa cells were infected with EMCV at 10 MOI (A, C and D) or with heat-inactivated EMCV (B). Various times after infection, whole cell extracts were prepared and analyzed by Western blotting (WB) for the presence of Flag-RIG-I, Flag-U1A or myc-MDA-5, using anti-Flag or anti-myc antibodies, respectively. EMCV protein expressions were monitored by detection of EMCV VP1 capsid or 3C^{PRO} protein accumulations, using anti-VP1 and anti-3C^{PRO} antibodies. Detection of α -tubulin was used to ensure that equal amounts of protein were loaded to each lane.

modest indicating that viral protein expression was required for RIG-I down regulation.

Because very long time exposures of Western Blot have been necessary to detect the very low level of endogenous RIG-I protein in HeLa cells, we wanted to exclude the possibility that the observed variations in the level of RIG-I expression could result from the detection procedure. To this end, we conducted experiments in HeLa cells overexpressing Flag-RIG-I fusion protein under the control of the constitutive cytomegalovirus (CMV) promoter. Subsequently, the cells were infected with EMCV at 10 MOI. Various times after infection, cell extracts were prepared and analyzed by Western blotting for the presence of RIG-I using anti-Flag antibodies. The viral replication was monitored using antibodies directed against EMCV capsid protein VP1 (Borrego et al., 2002) and $3C^{PRO}$. The results of a typical experiment are presented in Fig. 2A. Consistent with our previous observations, the level of Flag-RIG-I expression was roughly reduced 6 h post-infection and correlated with the appearance of the viral protease. No modulation of Flag-RIG-I expression was observed with a heat-inactivated EMCV confirming that viral protein expression is essential for EMCV-mediated RIG-I regulation (Fig. 2B). Furthermore, EMCV infection had no effect on Flag-U1A fusion protein expression driven by the CMV promoter (Fig. 2C) demonstrating that EMCV did not affect CMV promoter expression. For comparison, the effect of EMCV infection on MDA-5 expression was conducted in the same experimental conditions in HeLa cells overexpressing myc-MDA-5 fusion protein (Fig. 2D). Altogether, these data demonstrate that RIG-I expression is repressed during EMCV infection presumably, at a post-transcriptional level thought degradation by viral proteases and/or by cellular proteinases.

RIG-I is a substrate for $3C^{PRO}$ activity *in vitro*

To evaluate whether RIG-I down-regulation resulted from its specific cleavage by the EMCV $3C^{PRO}$, whole cell extracts from Flag-RIG-I-expressing HeLa cells or Flag-RIG-I expressed in HeLa cells and subsequently immobilized on anti-Flag magnetic beads were incubated with purified bacterially-expressed $3C^{PRO}$ (Lawson et al., 1994). The resulting reaction mixtures were analyzed by Western blotting. Consistent with our hypothesis, a fragment of approximately 49-kDa was generated from Flag-RIG-I when cleavage reactions were realized both with whole cell extracts from Flag-RIG-I-expressing HeLa cells (Fig. 3A) or with immuno-purified Flag-RIG-I (Fig. 3B). Incubations with increasing concentrations of recombinant $3C^{PRO}$ resulted in a dose-dependent cleavage of Flag-RIG-I demonstrating the specificity of the reaction (Fig. 3C). In addition, the generation of cleavage product was not observed when extracts were incubated with an inactive $3C^{PRO}$ mutant, in which the cysteine 159 was mutated to alanine (C159A- $3C^{PRO}$), demonstrating that RIG-I cleavage is dependent upon functional $3C^{PRO}$ activity (Fig. 3D). These data demonstrate that RIG-I is a potential substrate for $3C^{PRO}$ -mediated degradation. However, the level of RIG-I cleavage appeared modest in our *in vitro* assay and could not account for the significant loss of RIG-I observed in infected cells suggesting that cellular protein degradation pathways were required for efficient RIG-I degradation. Accordingly, no specific RIG-I cleavage products were observed in infected cells, probably due to rapid degradations by cellular proteinases.

The transient association of proteases with potential recognition sites on their target proteins is a prerequisite for the cleavage reaction to be initiated. To verify whether $3C^{PRO}$ interacted with RIG-I, whole

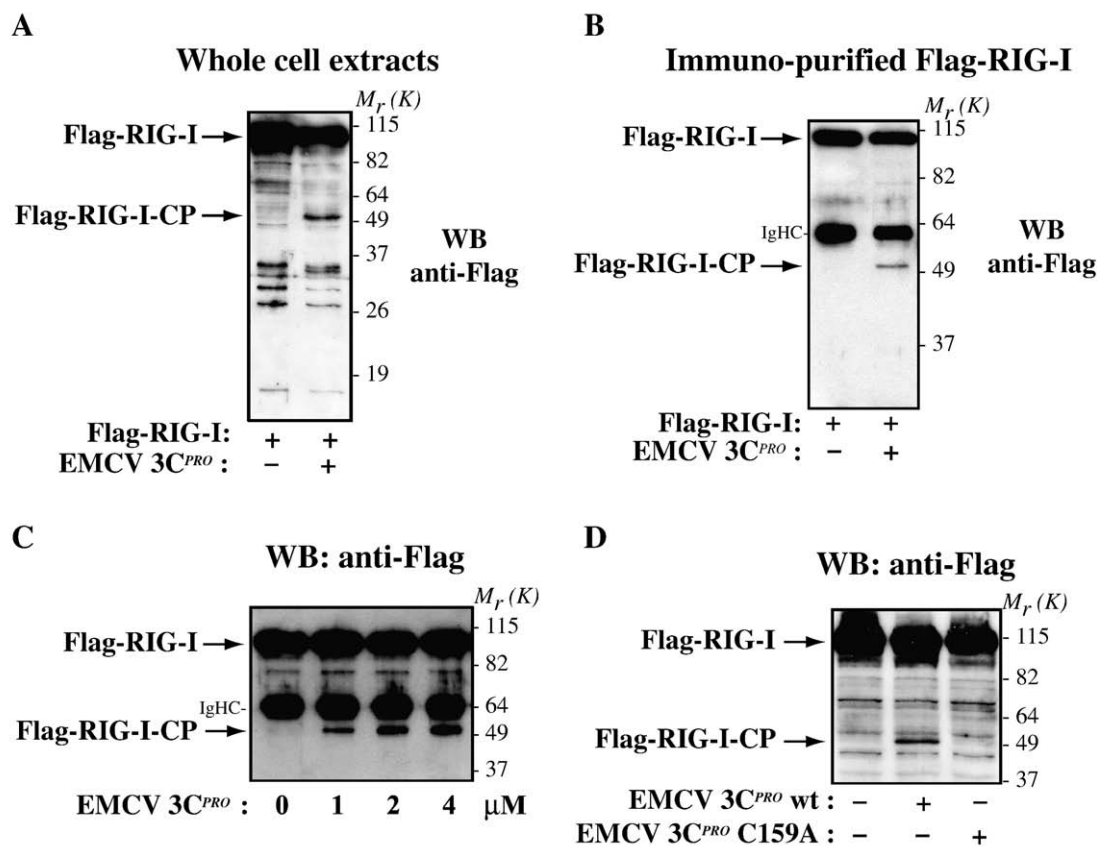


Fig. 3. RIG-I is cleaved by EMCV $3C^{PRO}$ *in vitro*. Whole cell extracts from HeLa cells expressing Flag-RIG-I (A) or immuno-purified Flag-RIG-I on anti-Flag magnetic beads (B) were submitted to an *in vitro* cleavage assay with recombinant EMCV $3C^{PRO}$ as described in Materials and methods. After 2 h of incubation, the reaction products were analyzed by Western blotting (WB) for the presence of Flag-RIG-I using anti-Flag monoclonal antibodies. The locations of the full length Flag-RIG-I and the 49-kDa cleavage product fragment of Flag-RIG-I (Flag-RIG-I-CP) are indicated. The same experiment was performed from immuno-purified Flag-RIG-I with increasing concentration of recombinant EMCV $3C^{PRO}$ (C). *In vitro* cleavage assays were performed from whole cell extracts of Flag-RIG-I-expressing HeLa cells and either recombinant wild type EMCV $3C^{PRO}$ or an EMCV $3C^{PRO}$ inactive mutant (C159A) (D).

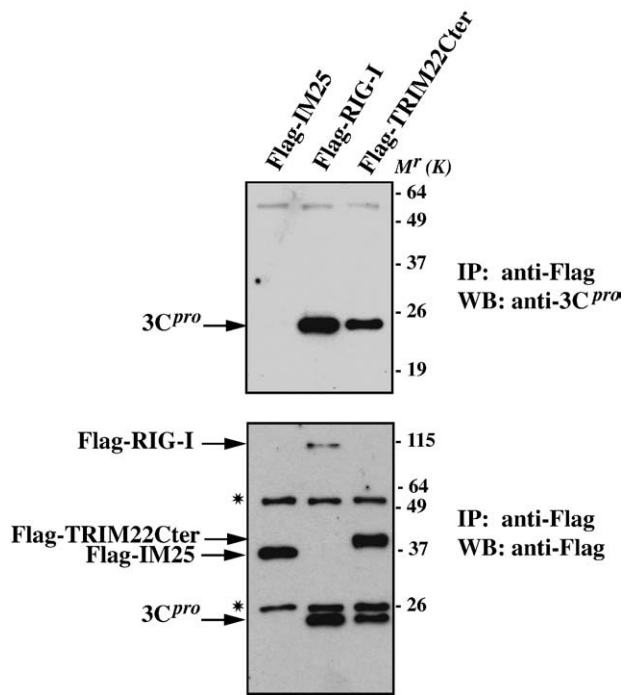


Fig. 4. RIG-I interacts with EMCV $3C^{PRO}$. Whole cell extracts from Flag-RIG-I-expressing HeLa cells were incubated with $1 \mu\text{M}$ of purified bacterially-expressed $3C^{PRO}$. The resulting reaction mixtures were subjected to immunoprecipitations using monoclonal anti-Flag antibodies and the immunoprecipitates were analyzed by Western blotting for the presence of $3C^{PRO}$ using anti- $3C^{PRO}$ polyclonal antibodies. Extract from HeLa cells expressing the human pre-mRNA cleavage factor IM25 (Flag-IM25), a non- $3C^{PRO}$ substrate protein, was used as negative control. Extract from HeLa cells expressing the C-terminal domain of the ubiquitin ligase TRIM22 (Flag-TRIM22Cter), previously shown to tightly interact with $3C^{PRO}$ (Eldin et al., 2009), was used for comparison. The blot was reprobed with anti-Flag antibodies to verify Flag-RIG-I, Flag-IM25 and Flag-TRIM22Cter expressions. (*) indicate the immunoglobulin chains.

cell extracts from Flag-RIG-I-expressing HeLa cells were incubated with $1 \mu\text{M}$ of purified bacterially expressed $3C^{PRO}$. The resulting reaction mixtures were subjected to immunoprecipitations using monoclonal anti-Flag antibodies and the immunoprecipitates were analyzed by Western blotting for the presence of $3C^{PRO}$. Extracts from HeLa cells expressing the human pre-mRNA cleavage factor IM25 (Flag-IM25), a non- $3C^{PRO}$ substrate protein, were used as negative control. As shown Fig. 4, $3C^{PRO}$ was strongly co-precipitated with Flag-RIG-I. No co-precipitation was detectable when immunoprecipitations were performed with either extracts from Flag-IM25-expressing HeLa cells (Fig. 4) or extracts from cells transfected with the p3XFlag empty vector (data not shown). The C-terminal domain of the ubiquitin ligase TRIM22, previously shown to tightly interact with $3C^{PRO}$ (Eldin et al., 2009), was used for comparison. These data clearly demonstrate that $3C^{PRO}$ can bind RIG-I and strengthen our findings that RIG-I could be a target for $3C^{PRO}$ -mediated degradation.

RIG-I degradation during EMCV infection requires caspase proteinase

Recently, degradation of MDA-5 in poliovirus-infected cells has been reported to occur in a viral protease-independent pathway involving both caspases and the cellular proteasome (Barral et al., 2007). Interestingly, stimulation of cells with poly(I:C), a synthetic dsRNA that mimics intracellular dsRNA infection, was reported to promote RIG-I degradation through a proteasome-independent pathway, demonstrating the susceptibility of RIG-I to the degradation by others cellular proteinases (Kim et al., 2008). As the *in vitro* RIG-I cleavage by $3C^{PRO}$ could not account for the level of its degradation in infected cells, we next evaluated whether caspases or proteasome might be involved in this process. First, to test the susceptibility of

RIG-I to caspase-mediated degradation, Flag-RIG-I-expressing HeLa cells were treated with puromycin, a known caspase-dependent inducer of apoptosis. As shown Fig. 5A, puromycin treatment led to a diminution of Flag-RIG-I expression that remain undetectable after 8 h. The down-regulation of Flag-RIG-I expression in response to poly(I:C) was also observed (Fig. 5B), as previously described (Kim et al., 2008). These results indicated that RIG-I is a potential substrate for cellular proteinase degradation. To evaluate whether caspase-mediated degradation of RIG-I occurred during EMCV infection, Flag-RIG-I-expressing HeLa cells were infected with EMCV at a multiplicity of infection (MOI) of 10, in the presence of $50 \mu\text{M}$ of Z-VAD, a general caspase inhibitor that has been reported to not affect picornavirus infection (Barral et al., 2007). Various times after infection, cell extracts were prepared and analyzed by Western blotting for the presence of Flag-RIG-I. As shown Figs. 5C–D, the degradation of Flag-RIG-I by EMCV was abolished in cells treated with Z-VAD. Unfortunately, we were unable to evaluate the impact of proteasome pathway on RIG-I degradation because, in our hands, proteasome inhibitor such as MG132 strongly inhibited EMCV replication. Altogether, our findings demonstrate that in addition to $3C^{PRO}$ cleavage, a caspase-

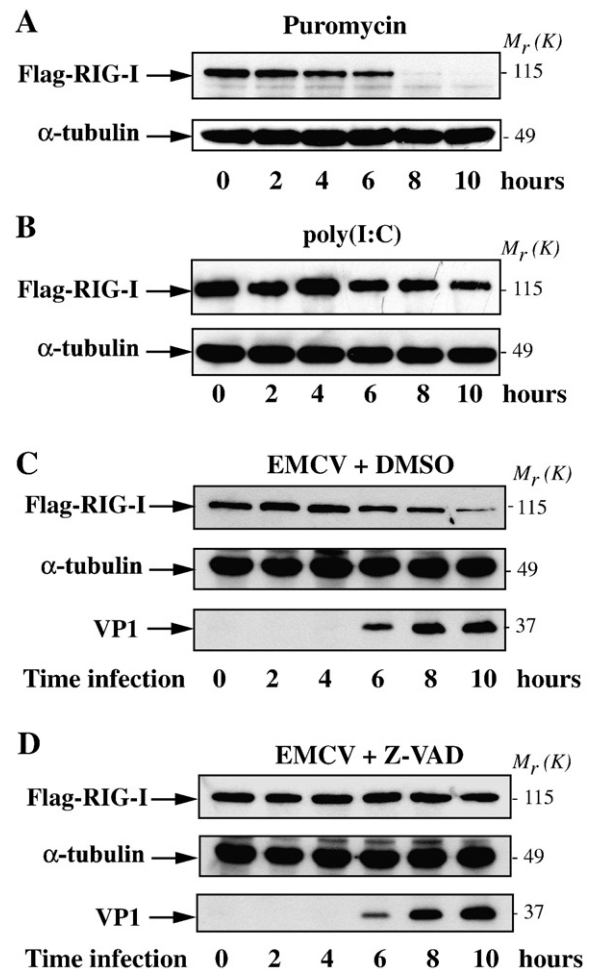


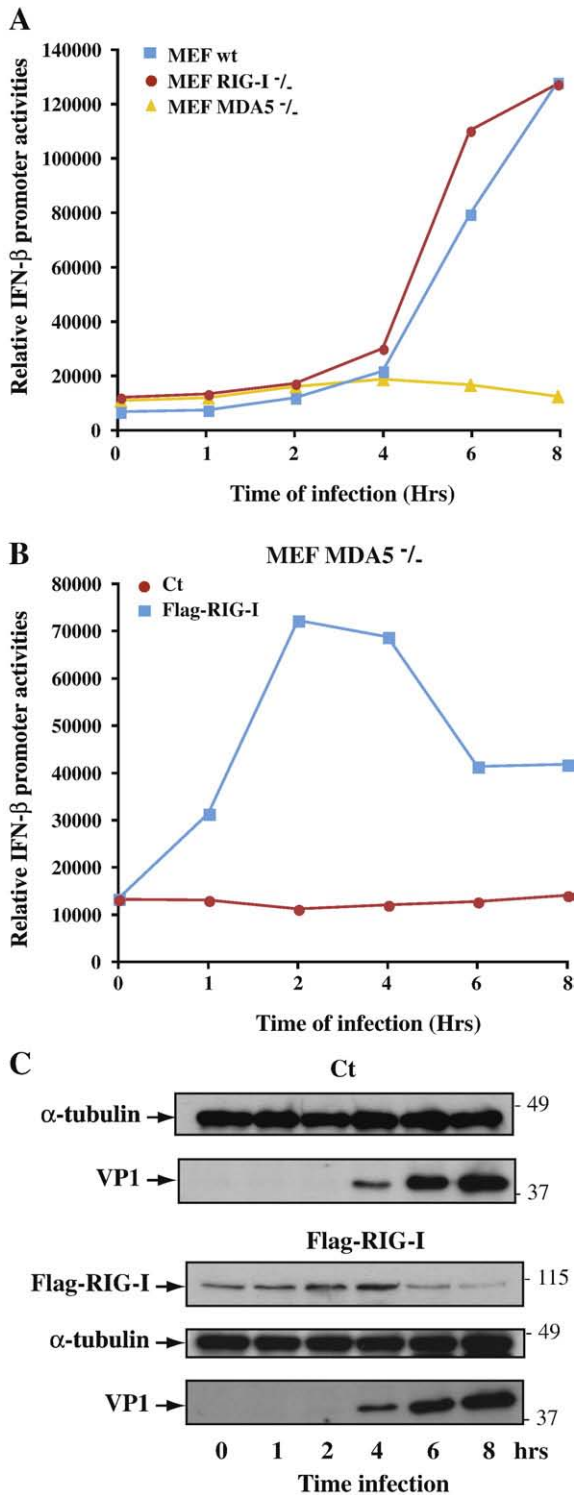
Fig. 5. RIG-I degradation during EMCV infection requires caspase proteinase. Flag-RIG-I-expressing HeLa cells were treated various times with $0.5 \mu\text{g/ml}$ of puromycin (A) or $20 \mu\text{g/ml}$ of poly(I:C) (B). Whole cell extracts were prepared and analyzed by Western blotting for the presence of Flag-RIG-I, using anti-Flag antibodies. In parallel, Flag-RIG-I-expressing HeLa cells were infected with EMCV at 10 MOI, in the presence of 0.1 % DMSO (C) or $50 \mu\text{M}$ of Z-VAD solubilized in DMSO (D). Various times after infection, whole cell extracts were prepared and analyzed by Western blotting for the presence of Flag-RIG-I. EMCV protein expressions were monitored by detection of EMCV VP1 capsid protein accumulations, using anti-VP1 antibodies. Detection of α -tubulin was used to ensure that equal amounts of protein were loaded to each lane.

dependent process could in part mediate RIG-I degradation, in EMCV infected cells.

RIG-I expression confers transient IFN- β promoter activation during EMCV infection

MDA-5 but not RIG-I has been shown essential for triggering innate immune responses against picornaviruses (Kato et al., 2005, 2006). Although these studies are convincing, the cleavage of RIG-I during EMCV infection demonstrates the ability of viruses to

efficiently disrupt innate immune signalling and throws new light on the role of RIG-I as potential sensor for picornavirus infections. These observations prompted us to analyze the contribution of RIG-I in innate immune IFN- β signalling in response to EMCV infection, in MDA-5 knockout (MDA-5^{-/-}), RIG-I knockout (RIG-I^{-/-}) and in their corresponding wild-type (wt) mouse embryo fibroblasts (MEF). The cells were transfected with an IFN- β -promoter-luciferase construct for 24 h and then infected with EMCV at an MOI of 10. Various times after infection, IFN- β -promoter activities were monitored. EMCV infections of wt and RIG-I^{-/-} MEF triggered similar strong induction of IFN- β -promoter activities whereas no significant modulation was observed in MDA-5^{-/-} (Fig. 6A). This is consistent with studies from knockout mice showing that MDA-5 is involved in the innate immune response to picornaviruses (Kato et al., 2005, 2006). However, our findings on the degradation of RIG-I could explain why EMCV fails to induce IFN- β -promoter in infected-MDA-5^{-/-} cells. To examine this possibility, Flag-RIG-I was overexpressed in IFN- β -promoter-luciferase-expressing MDA-5^{-/-} cells. Cells transfected with the p3XFlag empty vector were used as negative control. After infection with EMCV at an MOI of 10, IFN- β -promoter activities were monitored as previously described and viral protein expressions were verified with EMCV capsid protein VP1. As shown Fig. 6B, Flag-RIG-I expression conferred a strong induction of IFN- β -promoter activity in the first hours of EMCV infection. This induction was transient and followed by a repression after 4 h of infection. Consistent with our previous observation on HeLa cells, Flag-RIG-I expression was strongly reduced 6 h post-infection suggesting that a rapid feedback regulation of RIG-I activity occurs during EMCV infection in MDA-5^{-/-} cells (Fig. 6C). These results indicate that RIG-I is efficient for triggering rapid and transient innate immune signalling against EMCV and suggest that it represents a new sensor for signalling picornaviruses infection.



Discussion

Virus infections are detected by sensor molecules, generally referred as “pattern recognition receptor” (PRR). PRR play a central function in innate immunity by detecting pathogen components leading to production and secretion of type I IFN, critical for virus dissemination (Abreu et al., 2005; Akira et al., 2006; Medzhitov, 2007). In particular, the cytoplasmic RNA helicase-like receptors RIG-I and MDA-5 can detect intracellular viral RNAs to signal type I IFN production through interaction with the IPS-1 (MAVS/VISA/CARDIF) mitochondrial adaptor (Kawai et al., 2005; Meylan et al., 2005; Seth et al., 2005; Xu et al., 2005). Although RIG-I and MDA-5 share similar structural and functional features (Yoneyama et al., 2005), the two helicases have been reported to discriminate among different ligands to trigger an innate immune response to RNA viruses. In particular, picornavirus infections have been reported to be essentially detected by MDA-5 (Gitlin et al., 2006; Kato et al., 2006).

Here, we report that RIG-I is down regulated during EMCV infection. The level of RIG-I protein declines after 6 h of infection concomitantly with the expression of the EMCV 3C^{PRO}, suggesting that

Fig. 6. RIG-I expression confers transient IFN- β promoter activation in EMCV-infected MDA-5^{-/-} mouse embryo fibroblasts. (A) IFN- β -promoter-luciferase constructs was transfected in MDA-5^{-/-}, RIG-I^{-/-} and in their corresponding wild-type (wt) mouse embryo fibroblasts (MEF). Subsequently, the cells were infected with EMCV at an MOI of 10. IFN- β -promoter activities were monitored various times after infection by measuring the luciferase activities. (B) Flag-RIG-I-expressing vector or p3XFlag empty vector were co-transfected with IFN- β -promoter-luciferase constructs in MDA-5^{-/-} cells. Subsequently, the cells were infected with EMCV at 1 MOI. Various times after infection IFN- β -promoter activities were monitored as described above. Results of a typical experiment are presented. Similar results were obtained in several independent experiments. (C) Whole cell extracts Flag-RIG-I-expressing MDA-5^{-/-} cells were prepared and analyzed by Western blotting (WB) for the presence of Flag-RIG-I, using anti-Flag antibodies. EMCV protein expressions were monitored by detection of EMCV VP1 capsid protein accumulation, using anti-VP1 antibodies. Detection of α -tubulin was used to ensure that equal amounts of protein were loaded to each lane.

the disappearance of RIG-I protein results, at least in part, from its cleavage by the viral protease. Accordingly, using *in vitro* 3C^{PRO} cleavage assays, we show that Flag-RIG-I is specifically cleaved by purified recombinant EMCV 3C^{PRO} leading to an approximately 49-kDa cleavage product. However, the weak part of Flag-RIG-I cleaved by recombinant 3C^{PRO} in these experiments did not reflect the strong degradation observed in infected cells. In addition, we failed to detect the 49-kDa cleavage fragment during EMCV infections suggesting that RIG-I and RIG-I cleavage products could be substrate for cellular proteinase degradations. Interestingly, the degradation of RIG-I in poly(I:C) treated cells were reported to occur through a proteasome-independent pathway, providing evidences that RIG-I can be sensitive to caspase degradation pathways (Kim et al., 2008). Similarly, we show that treatment of HeLa cells with puromycin, a known caspase-dependent inducer of apoptosis, leads to RIG-I down regulation. Using the general caspase inhibitor Z-VAD, we demonstrate that RIG-I degradation in EMCV infected cells is in part mediated through a caspase-dependent process. Recently, cleavage of MDA-5 during poliovirus infection was described to occur both in a proteasome- and caspase-dependent manner (Barral et al., 2007), therefore we cannot exclude the contribution of proteasome pathway in EMCV-mediated RIG-I degradation. Unfortunately, because proteasome inhibitor impairs EMCV replication, we were unable to test this hypothesis.

According to our data, pending submission of our manuscript, RIG-I has been reported to be cleaved during picornavirus infection with a more pronounced effect with poliovirus than other picornaviruses (Barral et al., 2009). Using recombinant poliovirus 3CD^{PRO} precursor, the authors showed that cleavage of RIG-I occurs in a 3CD^{PRO}-dependent process. Accordingly, we demonstrated that recombinant EMCV 3C^{PRO} binds and cleaves RIG-I in an *in vitro* cleavage assay. In addition, Barral et al described that cleavage of RIG-I resulted in the generation of an approximately 70-kDa carboxy-terminal cleavage product detected in Western blotting with an anti-RIG-I antibody directed against the C-terminal end of protein (amino acids 909–925). Using anti-Flag antibodies we observed that, in our *in vitro* assay, an approximately 49-kDa NH2-terminal fragment was generated by 3C^{PRO} from a N-ter-tagged Flag-RIG-I fusion protein. Interestingly, the sum of the molecular weight of the N-ter (49) and C-ter (70) observed in the two studies are consistent with the 115-kDa molecular weight of the full length RIG-I protein suggesting that the cleavage of RIG-I by the different viral proteases occurred at a unique and identical site. Contrary to Barral et al., we failed to detect a cleavage product in HeLa cells suggesting that N-ter fragment is more sensitive to cellular protease degradation than the C-ter. In addition, the fact that RIG-I appeared to be more efficiently cleaved during poliovirus infection than EMCV infection (Barral et al., 2009) can explain why the authors observed only a partial inhibition of RIG-I cleavage by Z-VAD during poliovirus infection. Altogether, these data strongly strengthen our finding on a potential role of RIG-I in signalling picornavirus infection.

It has been reported that several picornavirus polyprotein precursor sustain functional 3C^{PRO} activity involved in viral polyprotein maturation and cleavage of cellular factors (Whitton et al., 2005). For example, during hepatitis A infection, the mitochondrial signalling protein IPS-1 is cleaved by the 3C^{PRO} activity contained in the 3ABC polyprotein precursor viral protein but not by the 3C^{PRO} itself (Yang et al., 2007). Thus, it is conceivable that functionally described 3C^{PRO}-containing 3ABC, 3ABCD, 3BCD or 3CD polyprotein precursors (Aminev et al., 2003; Hall and Palmenberg, 1996) can be in the EMCV-infected cells the major source of protease activity for RIG-I cleavage. Accordingly, Barral et al reported that RIG-I cleavage by poliovirus 3CD is detectable in an *in vitro* assay (Barral et al., 2009). Furthermore, in addition to 3C^{PRO} activity, the viral 2A protease (2A^{PRO}) is responsible for maturation and degradation of viral and cellular proteins (Blom et al., 1996). Interestingly, both the cleavage by viral 2A protease (2A^{PRO}) and by 3C^{PRO} of eukaryotic translation

initiation factor 4GI (eIF4GI) was required to cause severe translation inhibition in poliovirus-infected cells (Borman et al., 1997; Joachims et al., 1999; Kempf and Barton, 2008; Kuyumcu-Martinez et al., 2004; Ziegler et al., 1995). As these two proteases can trigger degradation of common substrates, it will be very interesting to test whether such cooperation occurs in RIG-I degradation during EMCV infection, although, poliovirus 2A^{PRO} did not seem able to cleave RIG-I *in vitro* (Barral et al., 2009). Additional experiments using recombinant 3C^{PRO}-containing polyproteins and 2A^{PRO} will be required to evaluate these different hypothesis. Finally, according to previous publications (Lawson et al., 1994), the fact that recombinant 3C^{PRO} needs to be refolded after purification leading to only a weak part of functional protease could explained, in part, the incomplete cleavage and the low level of *in vitro* cleavage activity observed. Although we demonstrate that 3C^{PRO} directly interacts with RIG-I, we cannot strictly exclude the possibility that 3C^{PRO} can act indirectly to produce the RIG-I cleavage product.

The caspase-dependent cleavage of MDA5 in poliovirus-infected cells was recently reported in response to some picornavirus infections (Barral et al., 2007). No evidence of MDA-5 cleavage was described with rhinovirus type 16 or echovirus type 1 whereas a weak effect was observed for EMCV infections suggesting that MDA-5 signalling is more critical for poliovirus than other picornaviruses (Barral et al., 2007). These data are very important because they provide evidences that different pathways can trigger the antiviral response against members of the same virus family. In this context, our findings point to a role of RIG-I, beside MDA-5, as a critical mediator for innate antiviral immunity against picornaviruses, such as EMCV. Because evolution has selected viruses for growth despite antiviral defences, it is not surprising that some viral-encoded proteins can target and inhibit cellular effectors proteins playing a key role in innate antiviral mechanisms (Chen and Gerlier, 2006; Hiscott et al., 2006; Loo and Gale, 2007; Weber et al., 2004). The preferential degradation of RIG-I in EMCV-infected cells strongly suggests that RIG-I expression is more detrimental for EMCV dissemination than MDA-5 expression. Consistent with this hypothesis, we show that the overexpression of Flag-RIG-I sustains a strong and transient activation of IFN- β signalling in MDA-5^{-/-} mouse embryo fibroblasts. Interestingly, in these experimental conditions, IFN- β promoter activities were strongly diminished after 4 h of infection suggesting that EMCV can efficiently inhibit RIG-I signalling. However, it seems probable that other mechanism of viral subversion of RIG-I signalling occur during EMCV infection leading to an efficient inhibition. Indeed, the fact that MDA-5-null mice failed to produce type I IFN when infected with EMCV, and have been shown more susceptible to infection (Gitlin et al., 2006; Kato et al., 2006) probably reflects the complete disruption of RIG-I signalling by EMCV in the animal model.

The huge diversity of virus families and the fact that viruses have developed strategies to circumvent innate antiviral immunity imply that mammalian cells use various sensor molecules to efficiently trigger IFN β signalling in response to a given family of viruses. However it is still unclear what specific features of picornavirus are required for activating RIG-I or MDA-5 pathway. It is conceivable that additional cellular co-factors may be required for efficient pathogen recognition, depending of the cellular context. In addition, it will be important to evaluate the susceptibility of both RIG-I and MDA-5 inhibition during infection by other picornaviruses to better understand how RIG-I and MDA-5 can discriminate among these viruses. By playing a role in innate signalling during picornavirus infection, RIG-I represent an attractive target for virus control of host defences and viral strategies to disrupt RIG-I function can provide effective means of evading the innate immune response. Importantly, because several picornaviral 3C^{PRO} share sequence homology and have similar substrate specificities, antagonized RIG-I signalling could be a general picornaviral-mediated mechanism of innate immune

system subversion. The identification of the precise 3C^{PRO}-cleavage site on RIG-I and generation of a RIG-I mutant resistant to virus-induced degradation will be necessary to rule definitively on this point. Altogether, our findings provide the first evidence that RIG-I signalling activation may play a role in the antiviral innate immune response against picornavirus infection.

Materials and methods

Cell culture, transfection and virus stocks

Human HeLa cells, MDA-5 knockout (MDA-5^{-/-}), RIG-I knockout (RIG-I^{-/-}) and in their corresponding wild-type (wt) mouse embryo fibroblasts (MEF) were cultured at 37 °C in DMEM medium supplemented with 10% FBS. Transient transfection experiments were performed in 6-well plates by the Lipofectamine Plus Reagent method (Invitrogen, France). Twenty-four hours after transfection, cells were washed twice in phosphate-buffered-saline (PBS) and infected with EMCV at an MOI of 10 in DMEM medium supplemented with 10% FBS. EMCV stocks were prepared from supernatants of virus-infected L929 cells.

Plasmid constructs

The Flag-RIG-I expression vector was obtained from Dr. E. Meurs. The IFN- β -promoter-luciferase reporter construct was a gift from Dr. J. Hiscott. The myc-MDA-5 expression vector was obtained from Dr. S. Akira.

Antibodies

Polyclonal anti-EMCV-3C^{PRO} antibodies were prepared and purified as previously described (Lawson et al., 1994). Mouse monoclonal antibodies directed against EMCV capsid protein VP1 were prepared as described (Borrego et al., 2002). Anti-Flag monoclonal and polyclonal antibodies, anti-myc antibody, anti- α -tubulin monoclonal antibody, peroxidase-conjugated anti-mouse and anti-rabbit IgGs (whole molecule) secondary antibodies were purchased from Sigma Aldrich (France).

Immunoprecipitation and protein analysis

The cells were resuspended in a lysis buffer consisting of PBS buffer containing 1% NP40, 1 mM DTT, 100 mM phenylmethylsulphonyl fluoride (PMSF), protease inhibitor cocktail (1 tablet/10 ml, Roche Diagnostics). 10,000-g supernatant was prepared and used for immunoprecipitation. The extracts were incubated for 1 h at 4 °C with specific antibodies bound to sheep anti-mouse or anti-rabbit IgG-coupled magnetic beads (Dynabeads, Invitrogen). The beads were washed 5 times in the lysis buffer. The immunoprecipitated proteins were resuspended in 20 μ l of loading buffer (10 mM Tris-HCl pH 6.8, 1% SDS, 5 mM EDTA, and 50% glycerol), incubated 5 min at 95 °C, fractionated by SDS-PAGE and transferred onto PVDF membranes. After a blocking step, the membranes were incubated with the appropriate antibody and then developed using a chemiluminescent detection system (ECL+Plus, Amersham Pharmacia Biotech).

In vitro 3C^{PRO} cleavage assays

Whole cell extracts from Flag-RIG-I-expressing HeLa cells were used as substrate of the 3C^{PRO}. Wild type recombinant EMCV 3C^{PRO} or an inactive 3C^{PRO} mutant (3C^{PRO} C159A) were produced in *Escherichia coli* and purified as previously described (Lawson et al., 1994). The reactions were performed in a 50- μ l final volume containing: 12.5 μ l of extract, 25 μ l of a 2 \times reaction buffer (consisting of 20 mM Tris-HCl pH 8.0, 2 mM EDTA, 20 mM DTT) and various concentrations of

recombinant 3C^{PRO}. The mixtures were incubated 2 h at 37 °C. The reactions were stopped by the addition of 16.5 μ l of a 4 \times concentrated gel loading buffer and analyzed by Western blotting.

Acknowledgments

We thank Patrick Eldin for technical assistance. This work was supported by grants from the Association pour la Recherche contre le Cancer (ARC), the National Science Foundation MCB-0210188 and the Centre National de la Recherche Scientifique (CNRS).

References

- Abreu, M.T., Fukata, M., Arditi, M., 2005. TLR signaling in the gut in health and disease. *J. Immunol.* 174 (8), 4453–4460.
- Akira, S., Uematsu, S., Takeuchi, O., 2006. Pathogen recognition and innate immunity. *Cell* 124 (4), 783–801.
- Aminev, A.G., Amineva, S.P., Palmenberg, A.C., 2003. Encephalomyocarditis virus (EMCV) proteins 2A and 3BCD localize to nuclei and inhibit cellular mRNA transcription but not rRNA transcription. *Virus Res.* 95 (1–2), 59–73.
- Andrejeva, J., Childs, K.S., Young, D.F., Carlos, T.S., Stock, N., Goodbourn, S., Randall, R.E., 2004. The V proteins of paramyxoviruses bind the IFN-inducible RNA helicase, mda-5, and inhibit its activation of the IFN-beta promoter. *Proc. Natl. Acad. Sci. U. S. A.* 101 (49), 17264–17269.
- Barral, P.M., Morrison, J.M., Drahos, J., Gupta, P., Sarkar, D., Fisher, P.B., Racaniello, V.R., 2007. MDA-5 is cleaved in poliovirus-infected cells. *J. Virol.* 81 (8), 3677–3684.
- Barral, P.M., Sarkar, D., Fisher, P.B., Racaniello, V.R., 2009. RIG-I is cleaved during picornavirus infection. *Virology* 391 (2), 171–176.
- Blom, N., Hansen, J., Blaas, D., Brunak, S., 1996. Cleavage site analysis in picornaviral polyproteins: discovering cellular targets by neural networks. *Protein Sci.* 5 (11), 2203–2216.
- Borman, A.M., Kirchwegger, R., Ziegler, E., Rhoads, R.E., Skern, T., Kean, K.M., 1997. eIF4G and its proteolytic cleavage products: effect on initiation of protein synthesis from capped, uncapped, and IRES-containing mRNAs. *Rna* 3 (2), 186–196.
- Borrego, B., Garcia-Ranea, J.A., Douglas, A., Brocchi, E., 2002. Mapping of linear epitopes on the capsid proteins of swine vesicular disease virus using monoclonal antibodies. *J. Gen. Virol.* 83 (Pt 6), 1387–1395.
- Breiman, A., Grandvaux, N., Lin, R., Ottone, C., Akira, S., Yoneyama, M., Fujita, T., Hiscott, J., Meurs, E.F., 2005. Inhibition of RIG-I-dependent signaling to the interferon pathway during hepatitis C virus expression and restoration of signaling by IKKepsilon. *J. Virol.* 79 (7), 3969–3978.
- Chen, M., Gerlier, D., 2006. Viral hijacking of cellular ubiquitination pathways as an anti-innate immunity strategy. *Viral Immunol.* 19 (3), 349–362.
- Ehrenfeld, E., 1982. Poliovirus-induced inhibition of host-cell protein synthesis. *Cell* 28 (3), 435–436.
- Eldin, P., Papon, L., Oteiza, A., Brocchi, E., Lawson, T.G., Mechetti, N., 2009. TRIM22 E3 ubiquitin ligase activity is required to mediate antiviral activity against encephalomyocarditis virus. *J. Gen. Virol.* 90 (Pt 3), 536–545.
- Foy, E., Li, K., Sumpter Jr., R., Loo, Y.M., Johnson, C.L., Wang, C., Fish, P.M., Yoneyama, M., Fujita, T., Lemon, S.M., Gale Jr., M., 2005. Control of antiviral defenses through hepatitis C virus disruption of retinoic acid-inducible gene-1 signaling. *Proc. Natl. Acad. Sci. U. S. A.* 102 (8), 2986–2991.
- Gitlin, L., Barchet, W., Gilfillan, S., Cella, M., Beutler, B., Flavell, R.A., Diamond, M.S., Colonna, M., 2006. Essential role of mda-5 in type I IFN responses to polyriboinosinic:polyribocytidylic acid and encephalomyocarditis picornavirus. *Proc. Natl. Acad. Sci. U. S. A.* 103 (22), 8459–8464.
- Hall, D.J., Palmenberg, A.C., 1996. Mengo virus 3C proteinase: recombinant expression, intergenus substrate cleavage and localization in vivo. *Virus Genes* 13 (2), 99–110.
- Hassel, B.A., Zhou, A., Sotomayor, C., Maran, A., Silverman, R.H., 1993. A dominant negative mutant of 2-5A-dependent RNase suppresses antiproliferative and antiviral effects of interferon. *EMBO J.* 12 (8), 3297–3304.
- Hiscott, J., Nguyen, T.L., Arguello, M., Nakhaei, P., Paz, S., 2006. Manipulation of the nuclear factor-kappaB pathway and the innate immune response by viruses. *Oncogene* 25 (51), 6844–6867.
- Imaizumi, T., Hatakeyama, M., Yamashita, K., Yoshida, H., Ishikawa, A., Taima, K., Satoh, K., Mori, F., Wakabayashi, K., 2004a. Interferon-gamma induces retinoic acid-inducible gene-1 in endothelial cells. *Endothelium* 11 (3–4), 169–173.
- Imaizumi, T., Yagihashi, N., Hatakeyama, M., Yamashita, K., Ishikawa, A., Taima, K., Yoshida, H., Inoue, I., Fujita, T., Yagihashi, S., Satoh, K., 2004b. Expression of retinoic acid-inducible gene-1 in vascular smooth muscle cells stimulated with interferon-gamma. *Life Sci.* 75 (10), 1171–1180.
- Iwasaki, A., Medzhitov, R., 2004. Toll-like receptor control of the adaptive immune responses. *Nat. Immunol.* 5 (10), 987–995.
- Joachims, M., Van Bruegel, P.C., Lloyd, R.E., 1999. Cleavage of poly(A)-binding protein by enterovirus proteases concurrent with inhibition of translation in vitro. *J. Virol.* 73 (1), 718–727.
- Kato, H., Sato, S., Yoneyama, M., Yamamoto, M., Uematsu, S., Matsui, K., Tsujimura, T., Takeda, K., Fujita, T., Takeuchi, O., Akira, S., 2005. Cell type-specific involvement of RIG-I in antiviral response. *Immunity* 23 (1), 19–28.
- Kato, H., Takeuchi, O., Sato, S., Yoneyama, M., Yamamoto, M., Matsui, K., Uematsu, S., Jung, A., Kawai, T., Ishii, K.J., Yamaguchi, O., Otsu, K., Tsujimura, T., Koh, C.S., Reis

- Sousa, C., Matsuura, Y., Fujita, T., Akira, S., 2006. Differential roles of MDA5 and RIG-I helicases in the recognition of RNA viruses. *Nature* 441 (7089), 101–105.
- Kawai, T., Takahashi, K., Sato, S., Coban, C., Kumar, H., Kato, H., Ishii, K.J., Takeuchi, O., Akira, S., 2005. IPS-1, an adaptor triggering RIG-I- and Mda5-mediated type I interferon induction. *Nat. Immunol.* 6 (10), 981–988.
- Kempf, B.J., Barton, D.J., 2008. Poliovirus 2APro increased viral mRNA and polysome stability coordinately in time with cleavage of eIF4G. *J. Virol.* 82 (12), 5847–5859.
- Kim, M.J., Hwang, S.Y., Imaizumi, T., Yoo, J.Y., 2008. Negative feedback regulation of RIG-I-mediated antiviral signaling by interferon-induced ISG15 conjugation. *J. Virol.* 82 (3), 1474–1483.
- Krishnan, J., Selvarajoo, K., Tsuchiya, M., Lee, G., Choi, S., 2007. Toll-like receptor signal transduction. *Exp. Mol. Med.* 39 (4), 421–438.
- Kuyumcu-Martinez, N.M., Van Eden, M.E., Younan, P., Lloyd, R.E., 2004. Cleavage of poly (A)-binding protein by poliovirus 3C protease inhibits host cell translation: a novel mechanism for host translation shutoff. *Mol. Cell Biol.* 24 (4), 1779–1790.
- Lawson, T.G., Gronros, D.L., Werner, J.A., Wey, A.C., DiGeorge, A.M., Lockhart, J.L., Wilson, J.W., Wintrobe, P.L., 1994. The encephalomyocarditis virus 3C protease is a substrate for the ubiquitin-mediated proteolytic system. *J. Biol. Chem.* 269 (45), 28429–28435.
- Loo, Y.M., Gale Jr, M., 2007. Viral regulation and evasion of the host response. *Curr. Top. Microbiol. Immunol.* 316, 295–313.
- Loo, Y.M., Fornek, J., Crochet, N., Bajwa, G., Perwitasari, O., Martinez-Sobrido, L., Akira, S., Gill, M.A., Garcia-Sastre, A., Katze, M.G., Gale Jr, M., 2008. Distinct RIG-I and MDA5 signaling by RNA viruses in innate immunity. *J. Virol.* 82 (1), 335–345.
- Medzhitov, R., 2007. Recognition of microorganisms and activation of the immune response. *Nature* 449 (7164), 819–826.
- Meylan, E., Curran, J., Hofmann, K., Moradpour, D., Binder, M., Bartenschlager, R., Tschoop, J., 2005. Cardif is an adaptor protein in the RIG-I antiviral pathway and is targeted by hepatitis C virus. *Nature* 437 (7062), 1167–1172.
- Neznanov, N., Chumakov, K.M., Neznanova, L., Almasan, A., Banerjee, A.K., Gudkov, A.V., 2005. Proteolytic cleavage of the p65-RelA subunit of NF-kappaB during poliovirus infection. *J. Biol. Chem.* 280 (25), 24153–24158.
- Noppert, S.J., Fitzgerald, K.A., Hertzog, P.J., 2007. The role of type I interferons in TLR responses. *Immunol. Cell Biol.* 85 (6), 446–457.
- Seth, R.B., Sun, L., Ea, C.K., Chen, Z.J., 2005. Identification and characterization of MAVS, a mitochondrial antiviral signaling protein that activates NF-kappaB and IRF 3. *Cell* 122 (5), 669–682.
- Shen, Y., Igo, M., Yalamanchili, P., Berk, A.J., Dasgupta, A., 1996. DNA binding domain and subunit interactions of transcription factor IIIC revealed by dissection with poliovirus 3C protease. *Mol. Cell Biol.* 16 (8), 4163–4171.
- Takeuchi, O., Akira, S., 2007. Recognition of viruses by innate immunity. *Immunol. Rev.* 220, 214–224.
- Tasaka, M., Sakamoto, N., Itakura, Y., Nakagawa, M., Itsui, Y., Sekine-Osajima, Y., Nishimura-Sakurai, Y., Chen, C.H., Yoneyama, M., Fujita, T., Wakita, T., Maekawa, S., Enomoto, N., Watanabe, M., 2007. Hepatitis C virus non-structural proteins responsible for suppression of the RIG-I/Cardif-induced interferon response. *J. Gen. Virol.* 88 (Pt 12), 3323–3333.
- Weber, F., Kochs, G., Haller, O., 2004. Inverse interference: how viruses fight the interferon system. *Viral Immunol.* 17 (4), 498–515.
- Whitton, J.L., Cornell, C.T., Feuer, R., 2005. Host and virus determinants of picornavirus pathogenesis and tropism. *Nat. Rev. Microbiol.* 3 (10), 765–776.
- Xu, L.G., Wang, Y.Y., Han, K.J., Li, L.Y., Zhai, Z., Shu, H.B., 2005. VISA is an adapter protein required for virus-triggered IFN-beta signaling. *Mol. Cell* 19 (6), 727–740.
- Yalamanchili, P., Harris, K., Wimmer, E., Dasgupta, A., 1996. Inhibition of basal transcription by poliovirus: a virus-encoded protease (3Cpro) inhibits formation of TBP-TATA box complex in vitro. *J. Virol.* 70 (5), 2922–2929.
- Yalamanchili, P., Datta, U., Dasgupta, A., 1997a. Inhibition of host cell transcription by poliovirus: cleavage of transcription factor CREB by poliovirus-encoded protease 3Cpro. *J. Virol.* 71 (2), 1220–1226.
- Yalamanchili, P., Weidman, K., Dasgupta, A., 1997b. Cleavage of transcriptional activator Oct-1 by poliovirus encoded protease 3Cpro. *Virology* 239 (1), 176–185.
- Yang, Y., Liang, Y., Qu, L., Chen, Z., Yi, M., Li, K., Lemon, S.M., 2007. Disruption of innate immunity due to mitochondrial targeting of a picornaviral protease precursor. *Proc. Natl. Acad. Sci. U. S. A.* 104 (17), 7253–7258.
- Yoneyama, M., Fujita, T., 2007. RIG-I family RNA helicases: cytoplasmic sensor for antiviral innate immunity. *Cytokine Growth Factor Rev.* 18 (5-6), 545–551.
- Yoneyama, M., Kikuchi, M., Matsumoto, K., Imaizumi, T., Miyagishi, M., Taira, K., Foy, E., Loo, Y.M., Gale Jr, M., Akira, S., Yonehara, S., Kato, A., Fujita, T., 2005. Shared and unique functions of the DEXD/H-box helicases RIG-I, MDA5, and LGP2 in antiviral innate immunity. *J. Immunol.* 175 (5), 2851–2858.
- Ziegler, E., Borman, A.M., Deliat, F.G., Liebig, H.D., Jugovic, D., Kean, K.M., Skern, T., Kuechler, E., 1995. Picornavirus 2A proteinase-mediated stimulation of internal initiation of translation is dependent on enzymatic activity and the cleavage products of cellular proteins. *Virology* 213 (2), 549–557.